AtMRP5/AtABCC5 - An Inositolhexa*kis*phosphate Transporter Interacts with Hookless 1, a Protein Involved in Ethylene Signaling

---

Dissertation

zur

Erlangung der naturwissenschaftlichen Doktorwürde
(Dr. sc. nat.)

vorgelegt der

Mathematisch-naturwissenschaftlichen Fakultät

der Universität Zürich

von
Hanne Grob

von
Zürich ZH

Promotionskomitee

Prof. Dr. Enrico Martionia (Vorsitz und Leitung der Dissertation)

Prof. Dr. Leo Eberl

Prof. Dr. Stefan Hörtensteiner

Zürich 2014

Table of Contents **2**

Summary **5**

Zusammenfassung **7**

1 General introduction **9**

1.1 ABC Transporter 10

1.1.1 Structural classification of ABC-transporters 11

1.1.2 Directly energized transport process of ABC transporters 12

1.1.2.1 MDR1: A P-glycoprotein in Human 12

1.1.2.2 Sav1866/ ModBC-A: Two bacterial ABC transporters 13

1.1.3 ABC transporters: subfamily C 15

1.1.3.1 MRP transporters in animals 16

1.1.3.2 MRP transporters in yeast 17

1.1.3.3 MRP/ABCC transporters in plants 17

1.1.4 *At*MRP5 (AtABCC5), a MRP transporter protein in *Arabidopsis thaliana* 19

1.2 Regulation of plant transpiration through stomata 21

1.2.1 Role of the stomata complex 21

1.2.2 Physical features of transpiration 22

1.2.3 Guard cells 24

1.2.4 Stomata opening 25

1.2.5 Stomatal closure 28

2 Aim of the work **33**

3 The ATP binding cassette transporter *At*MRP5 (ABCC5) is a high affinity inositol hexakisphosphate transporter involved in signaling and phytate storage **34**

3.1 Main text J. Biol.Chem 284, 33614 - 33622 34

3.2 Supplementary Materials 43

4 *At*MRP5/*At*ABCC5 - An Inositolhexa*kis*phosphate transporter interacts with Hookless 1, a protein involved in ethylene signaling **52**

4.1 Introduction 53

4.2 Material and Methods 56

4.2.1 AtMRP5 interaction partner search using the conventional Yeast Two Hybrid System 56

4.2.2 Creating the bait constructs pLexA_kan-NBD1 and pLexA_kan-NBD2 and transformation of the Saccharomyces cervisiae strain LH40 56

4.2.3 Crude yeast cytosolic protein extraction and Western blot analysis 57

4.2.4 High efficiency transformation of cDNA library (prey) Into yeast containing the bait constructs 57

4.2.5 Yeast Two Hybrid Screen 57

4.2.6 X-Gal assay and yeast plasmid extraction/verification of positive prey clones 58

4.2.7 Phenotypical analysis of potential interaction partners of *At*MRP5 59

4.2.7.1 Plant growth conditions 59

4.2.7.2 Screen for altered stomatal aperture 59

4.2.8 Stomata aperture experiments with mutant plants displaying altered stomata movements in the screen 60

4.2.9 Drought stress experiments with Col-0 and *hls-1* plants in the dark 60

4.3 Results 61

4.3.1 Identification of possible interacting partner of *At*MRP5/ *At*ABCC5 using a yeast two hybrid screen and the nucleotide binding domain 1 of *At*MRP5 as a bait 61

4.3.2 Basic light/dark stomatal aperture screen 61

4.3.3 Verification of the full length HLS1 as interacting partner 62

4.3.4 Stomatal apertures are altered in the loss-of-function mutant 64

4.4 Discussion 69

4.4.1 Yeast two hybrid screen using the nucleotide binding domain 1 of *At*MRP5 as bait 69

4.4.2 Basic light/dark stomatal aperture screen 69

4.4.3 Stomatal aperture changes of the loss-of-function mutant *hls1* towards the phytohormone ABA and the ethylene synthesis blocker AVG in the light 70

4.4.4 Drought stress experiments performed with whole plants of *hls1* loss-of-function mutants and corresponding wild type (Col-0) in the dark 71

4.5 Conclusion 72

4.6 Supplementary Data 78

4.6.1 Results 78
4.6.1.1 *At*MRP5 interaction partner search using the conventional yeast two hybrid system 78
4.6.1.1.1 Crude yeast cytosolic protein extraction and Western blot analysis 78
4.6.1.1.2 X-Gal assay and yeast plasmid extraction/verification of positive prey clones 78
4.6.1.1.3 Co-immunoprecipitation of potential interaction partners of AtMRP5 87
4.6.1.1.4 Screen for altered Stomatal Aperture 88
4.6.1.2 Material and Methods 89
4.6.1.2.1 *At*MRP5 interaction partner search using the conventional yeast two hybrid System 89
4.6.1.2.2 Transformation of the bait constructs into competent cells of the yeast strain LH40 89
4.6.1.2.3 Crude Yeast Cytosolic Protein Extraction and Western Blot Analysis 90
4.6.1.2.4 Defining the amount of 3-Amino-1,2,4-triazole in screening plates to reduce false-positive clones 91
4.6.1.2.5 High efficiency transformation of a cDNA library (prey) into yeast containing the bait constructs 91
4.6.1.2.6 X-Gal assay of grown yeast colonies on screening SD plates 92
4.6.1.2.7 Yeast plasmid extraction and verification of positive prey clones 92
4.6.1.2.8 Co-immunoprecipitation of potential interaction partners of *At*MRP5 93
4.6.1.2.9 Screen for altered Stomatal Aperture 94
4.6.1.2.10 Verification of Homozygous Mutant Plants 95
4.6.1.2.11 Localization of *At*MRP5 98
4.7 References 100
5 Final Discussion and Conclusion 114
5.1 References 120
6 Appendix 122
7 Acknowledgements 134
8 Curriculum vitae 136

Summary

ATP-binding cassette (ABC) transporters form a family of membrane proteins, which are able to actively transport solutes against a concentration gradient by utilizing the free energy of ATP hydrolysis. One subfamily of ABC transporters is the ABCC subfamily, known to be crucial for detoxification processes and multidrug resistance. In humans, beside of the detoxifying abilities, ABCC transporters have been shown to regulate directly or indirectly ion channels, like potassium channels. Investigations of stomata movements in plants revealed, that ABCC transporters are also involved in guard cell regulation. This work sets a focus on *At*ABCC5 (*At*MRP5), an ABCC transporter of *Arabidopsis thaliana*, mainly expressed in guard cells and seeds.

The first chapter of this thesis gives an answer to the question about the substrates transported by *At*MRP5. Transport experiments with radioactive labelled inositolhexa*kis*phosphate ($InsP_6$) and microsomes isolated from yeasts expressing *At*MRP5, revealed that *At*MRP5 is an $InsP_6$ transporter, localized to the vacuolare membrane. Besides being a signaling compound, $InsP_6$ is the main storage form of phosphate in the vacuole of seed cells. Indeed, seeds of *atmrp5* plants are smaller and measurements of $InsP_6$ in wild type and *atmrp5* seeds showed, that mutant seeds contain highly reduced $InsP_6$ levels.

The second chapter focuses on the regulatory abilities of *At*MRP5 as a membrane protein. *atmrp5* knock out plants exhibit an increased water use efficiency phenotype due to altered stomata aperture size. Stomata of mutant plants show as well impaired responses towards different plant hormones such as, absiscic acid (ABA), auxin (IAA) and ethylene. Since it has been shown that *At*MRP5 is not a ion transporter, it is likely that the effect on guard cell regulation of the *atabcc5* mutant are either due only to the impaired $InsP_6$ transport capacity or/and to additional regulatory properties. A Yeast Two Hybrid screen revealed Hookless 1 (*At*HLS1) as an interaction partner of *At*MRP5, a protein involved in ethylene signalling. Furthermore *athls1* have stomata, which are slightly more open than the corresponding wild type. Based on these findings further stomata experiments were performed, including light/dark cycles and hormone treatments. The collected data show that *hls1* guard cells are also impaired in hormone perception, similarly to those of *abcc5*. These results support the hypothesis, that

*At*MRP5 interacts with *At*HLS1 and thereby blocks an increase of ethylene. Together with the ability of *At*MRP5 to transport $InsP_6$, which is one of the main signalling molecules in ABA signal cascade, *At*MRP5 is an important player in stomata regulation and phosphate storage management in seeds of *Arabidopsis thaliana*.

Zusammenfassung

ATP-binding cassette (ABC) Transporter bilden eine Gruppe von Membranproteinen, welche durch die freiwerdende Energie der ATP Hydrolyse aktiv Substrate gegen einen Konzentrationsgradienten transportieren. Eine Subfamilie der ABC Proteine ist die der ABCC Transporter, die dafür bekannt ist, für Entgiftungsprozesse und multiple Drogenresistenzen unerlässlich zu sein. Neben der Rolle in den Entgiftungs-mechanismen spielen ABCC Transporter im Menschen die Rolle von Ionenkanälen oder Regulatoren von Ionenkanälen. In Pflanzen zeigten Untersuchungen, dass neben ihrer Funktion in der Entgiftung ABCC Transporter auch in der Regulation der Spaltöffnungsbewegungen eine wichtige Rolle spielen. In dieser Arbeit wird ABCC5 (*At*MRP5), ein ABCC Transporter aus *Arabidopsis thaliana*, welcher vor allem in den Schliesszellen der Spaltöffnungen und in den Samen exprimiert wird, weiter untersucht.

Das erste Kapitel behandelt die Frage, welche Substrate spezifisch von *At*MRP5 transportiert werden. Transport Experimente mit radioaktiv markiertem Inositolhexa*kis*phosphat ($InsP_6$) und Mikrosomen, die aus Hefe isoliert wurden, die *At*ABCC5 exprimieren, zeigten, dass *At*MRP5 ein Inositolhexa*kis*phosphat ($InsP_6$) Transporter ist, der sich in der Vakuolenmembran befindet. Deshalb ist *At*MRP5 auch für die Akkumulation und Einlagerung von $InsP_6$, dem Hauptspeicher für Phosphat, in die Vakuole von Arabidopsis Samen verantwortlich. Tatsächlich sind die Samen von *atmrp5* Pflanzen kleiner, und $InsP_6$ Messungen in Wildtyp und mutanten Samen zeigten, dass in mutanten Samen kaum mehr $InsP_6$ vorhanden ist.

Das zweite Kapitel setzt den Fokus auf die Regulationsfähigkeiten von *At*MRP5 als Membranprotein. *At*MRP5 knock out Pflanzen zeigten gegenüber den Wildpflanzen eine bessere Wasser-Verbrauch Effizienz auf. Dies auf Grund einer geringeren Spaltöffnung. Des Weiteren zeigen Spaltöffnungen von *atmrp5* eine stark verringerte Reaktion gegenüber Abszisinsäure (ABA), Auxin (IAA) und Ethylene. Seit gezeigt wurde, dass *At*MRP5 selbst kein Ionentransporter/-kanal ist, muss angenommen werden, dass entweder der fehlende $InsP_6$ Transport für die gestörte Schliesszellenregulation verantwortlich ist, oder *At*MRP5 noch weitere regulierende Fähigkeiten hat. Untersuchungen mit dem Yeast Two Hybrid System zeigten, dass *At*MRP5 mit Hookless1 (*At*HLS1) interagiert, einem Protein das in der Ethylen Signalisationskaskade

involviert ist. Auch die Spaltöffnungen von *athls1* Pflanzen zeigten veränderte Öffnungsweiten, die aber in diesem Fall grösser waren als in Schliesszellen der Wildpflanze. Hingegen zeigte sich, dass die gestörte Reaktion auf Hormone die gleiche ist, wie bei der *abcc5* Mutante. Dies deutet darauf hin, dass die beiden Proteine in der Tat in der gleichen Signaltransduktionskette wirken und möglicherweise ihr Zusammenwirken der Erhöhung der Ethylenkonzentration engegenwirkt.

1 General Introduction

1.1 ABC transporters

The **A**TP-**B**inding-**C**assette (ABC)-transporter superfamily is a very large protein family that can be found in all organisms from bacteria to plants and humans (Henikoff *et al.*, 1997). Transport catalyzed by members of this family is, in most cases, directly energized by ATP hydrolysis. A functional ABC transporter is constituted by two transmembrane domains (TMDs), which may contain each four to six α-helices and two cytosolic domains, also called nuclear binding folds (NBDs). Within the NBDs three typical motifs are present in a region of about 215 amino acids (Higgins *et al.*, 1992). These are the Walker A and the Walker B motifs, which are required for ATP binding and hydrolysis, and between them the ABC signature (Schneider and Hunke, 1998).

In eukaryots, ABC transporters are implicated in the transport of a multitude of compounds, such as alkaloids, organic anions and heavy metals (Rea *et al.*, 2007), as well as lipids, glutathione, glucuronated and sulphated conjugates and phytohormones (Kang *et al.*, 2011, Sharom, 2011). Moreover, certain ABC transporters may exhibit or modulate ion channel activity. Two prominent examples for ion channel modulating ABC transporters are the human cystic fibrosis conductance regulator (CFTR) and the human sulfonylurea receptor (SUR1).

Some human ABC transporters, if defective, are the cause for several inherited genetic diseases, like cystic fibrosis (defective in CFTR), familial hyperinsulinism (defective in SUR1), the Dubin-Johnson syndrom or the Tangier disease. Additionally, it was found that ABC transporters could confer resistance towards certain chemotherapeutica due to their detoxifying ability.

Compared to other eukaryots the number of ABC transporters present in plants is exceptionally high. From the full genomic sequence of *Arabidopsis thaliana* it can be deduced that *Arabidopsis* contains 129 genes coding for ABC-type proteins (Sanchez-Fernández *et al.*, 2001, Verrier *et al.*, 2008). Among these, 53 genes code for full-size transporters, hence proteins where the two TMDs and NBDs are fused and constitute one protein. Nevertheless, just a few were described until now and the functions of most members are still unknown. The high number of ABC transporters present in plants and our limited knowledge about their function indicates that it is important to focus on elucidating the roles of these transporters in plants.

1.1.1 Structural classification of ABC-transporters

The ABC superfamily includes membrane-bound transporters as well as soluble proteins involved in a large range of processes in many different organisms. Since, ABC proteins transport a broad variety of substrates, a structural classification of ABC transporters may help to predict the function of ABC transporters of closely related species. In plants the nomenclature of ABC transporters was recently revised and a more universal nomenclature was defined. In the table below, the new names of the ABC subfamilies, as well as the old nomenclature are listed (Verrier *et al.*, 2008).

Subfamilies	**New systematic name**	**Name according to Sanchez-Fernández *et al.*, 2001**
Subfamily A	*At*ABCA1 - 12	AOH, ATH
Subfamily B	*At*ABCB1 - 29	MDR (PGP), ATM, TAP, DPL
Subfamily C	*At*ABCC1 - 15	MRP
Subfamily D	*At*ABCD1 - 2	PMP, FAE
Subfamily E	*At*ABCE1 - 3	RLI
Subfamily F	*At*ABCF1 - 5	GCN, ART
Subfamily G	*At*ABCG1 - 43	WBC, PDR
Subfamily H	No members in plants	-
Subfamily I	*At*ABCI1 - 21	CCM, NAP

Table I. Displayed are the new nomenclature for *Arabidopsis thaliana* ABC transporter subfamilies according to Verrier *et al.* (2008) and the former nomenclature according to Sánchez-Fernández *et al.* (2001). The classification is unified to ABC transporters from all kingdoms.

In this work not all subfamilies are considered. The main focus is on the subfamily C, since my work focused on *At*ABCC5 (formerly known as *At*MRP5), a member of this family. In this work, the ABC transporters are mainly referred to with their old names, thus using the names commonly used in the corresponding publications.

1.1.2 Directly energized transport process of ABC transporters

In contrast to the prevailing chemiosmotic model for energy-dependent transport in plants, ABC-protein-mediated transport is directly energized by MgATP and not by a transmembrane H^+-electrochemical potential difference established by the action of H^+-ATPases and/or H^+-pyrophosphatases (Lu *et al.*, 1998). The energy released by the hydrolysis of ATP is used to directly pump organic molecules across a membrane.
Diverse models for different ABC transporters were postulated and two possible mechanisms were discussed. The recent identification of ABC protein structures gave a deeper insight in the transport mechanism.

1.1.2.1 MDR1: A P-glycoprotein in Human

Human MDR1 P-glycoprotein (PGP) has been investigated most intensively among the ABC transporters and serves as a model for the so called “vacuum cleaner model“. *Hm*MDR1 exports a wide variety of structurally unrelated hydrophobic drugs, natural products and peptides from cells. Concentration gradients by a factor of 5 to 20 fold across the membrane have been reported, depending on the substrate. The catalytic pathway of MDR and other ABC transporters are thought to include the following steps: nucleotide and substrate binding, ATP hydrolysis, release of Pi, and release of ADP (Holland *et al.*, 2003).
Most PGP substrates are hydrophobic or amphiphilic, indicating that they are more soluble in the lipid bilayer than in the cytosol. This suggests that the binding of the substrate occurs, at least partially, within the lipid bilayer. The idea that MDRs may function as a ‘hydrophobic vacuum cleaner’ or flippase that extract substrate molecules out of the bilayer was first presented by Higgins and Gottesman (1992). It was shown, that in MDR1-over-expressing mammalian cells the movement of fluorescent rhodamine 123, a MDR substrate, was located within the membrane and did not accumulate in the cytosol. A two-step recognition process was proposed, consisting first of partitioning of the drug into the lipid bilayer, followed by the interaction with a relatively nonselective substrate-binding site within the protein (Higgins and Gottesman, 1992).
In contrast, other fluorescent substrates showed an accumulation of the dye in the cytosol (Kessel, 1989). This may be due to the fact that esterases rapidly cleave these

substrates producing the highly fluorescent free acid form of the dye, which is not a substrate of MDR1, and therefore is trapped in the cytosol (Homolya *et al.*, 1993). Nevertheless, in MDR1-over-expressing mammalian cells the intensity of fluorescence of the free dye in the cytosol is very low compared to what has been observed in low-expressing cells, indicating that the acetoxymethyl ester, rhodamine 123, is resorbed from the membrane by the MDR transporter, and in fact, never reaches the cytosol (Holland *et al.*, 2003).

1.1.2.2 Sav1866/ ModBC-A: Two bacterial ABC transporters

Structures for ABC importers and exporters have been presented and have shown to differ (Zolnerciks *et al.,* 2011). Type I ABC importer such as ModBC-A, a MoO_4/WO_4 importer from *A. fulgidus* (Hollenstein *et al.*, 2007a) has been described only in bacteria. Therefore in this brief overview I will focus on exporters, which can be found in bacteria as well as in eukaryotes. For these proteins, mechanisms were proposed, based on crystal structures of several ABC proteins. The first structure allowing comparison and modelling with the eukaryotic MDR/ABCB-type transporters was presented for Sav1866 from *S. aureus* (Locher *et al.*, 2006). Sav1866 is a half-size ABC transporter of the ABCB family and functions as a homodimer. In *Staphylococcus aureus* Sav1866 was shown to act as a detoxifier transporting various drugs such as Hoechst33342, vinblastine and verapamil (Velamakanni *et al.,* 2008).

Locher *et al.* (2006) determined the structure of Sav 1866 at a 3.0 Å resolution. They could show that this ABC transporter consists of two transmembrane domains (TMDs) that form a translocation pathway, and two nucleotide-binding domains (NBDs), which are exposed to the cytosol. These domains are able tobind and hydrolyze ATP. The two subunits are not aligned in parallel, but exhibit a twist, embracing each other. These results in a tight interaction of the two TMDs and NBDs.The interface of NBDs TMDs form a cavity, which is thought to bind the substrates. ATP is bound at the two Walker A and B motives located in the NBDs of a functional ABC transporter. It is thought that the first step of the transport cycle consists in substrate binding in the substrate-binding pocket. This favors the binding of the ATP molecules at the NBDs. This binding induces a conformational change leading to a dimerization of the NBDs, which are now in contact. Concomitantly the substrate-binding pocket faces now the outside and the

substrate can be released. In order to accomplish the transport cycle, ATP is hydrolyzed and consequently the stability of the interaction between the two NBDs is weakened and ADP and P_i released. This allows getting back to the original confirmation allowing a new transport cycle.

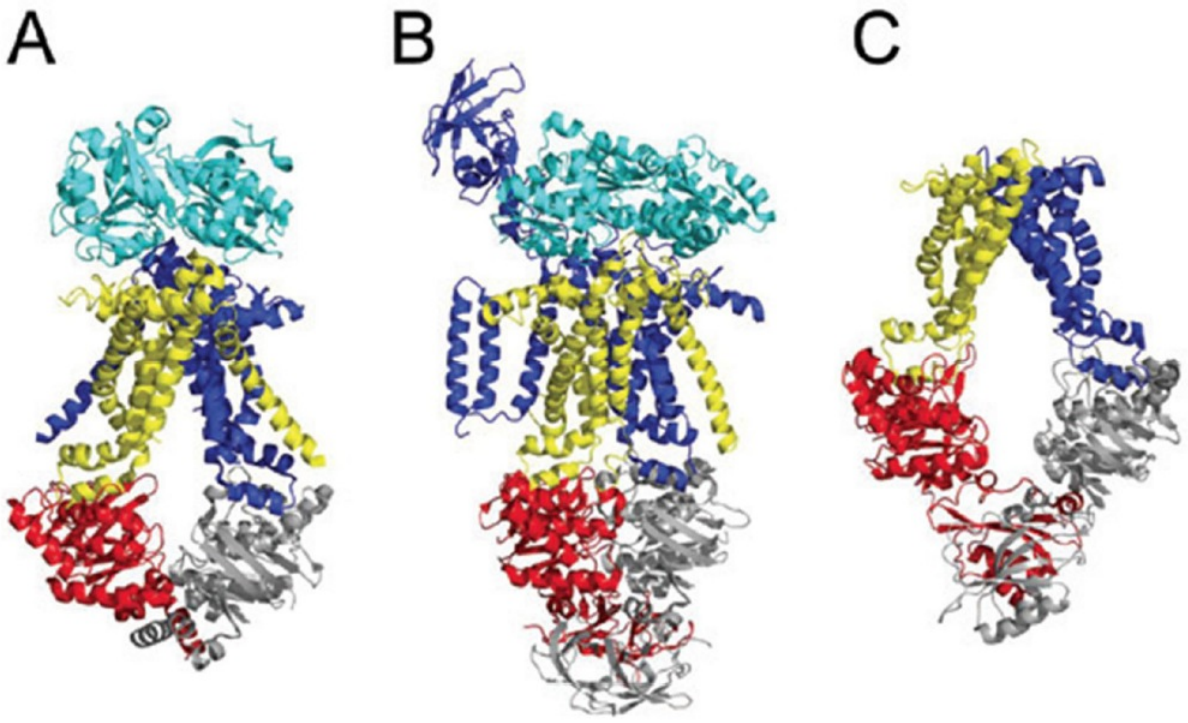

Figure 1 Structures of ABC exporters

All Protein structures are shown as Ribbon diagrams. TMDs are displayed in yellow and blue, NBDs in red and grey and SBPs are coloured cyan. (**A**) Sav1866 (PDB code 2HYD). (**B**) MsbA (PDB code 3B60). (**C**) Abcb I a (PDB code 3G5U).
(Figure source: Zolnerciks *et al.,* 2011)

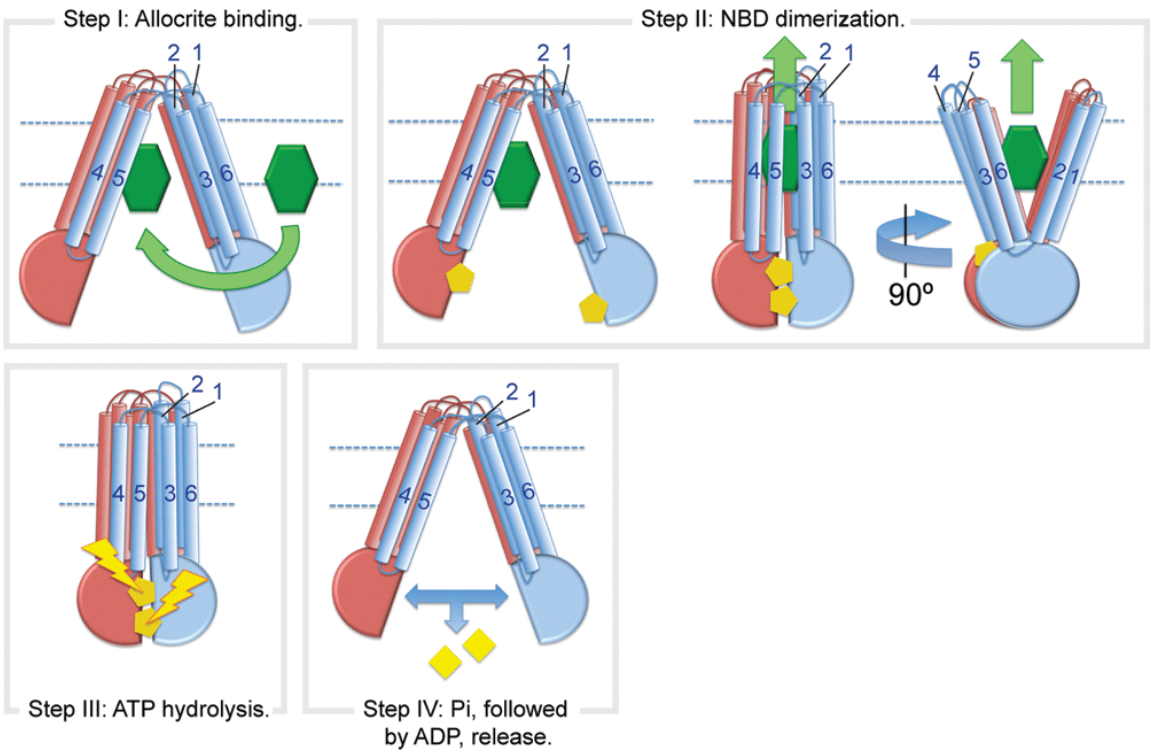

Figure 2 The transport cycle of an ABC transporter: The ATP-switch model

Cylinders spanning the membrane display the TMDs, whereas the NBDs are shown as semi-circles. (Figure source: Zolnerciks *et al.,* 2011)

1.1.3 ABC transporters: Subfamily C

The subfamily C of ABC transporters were formerly known as the MRP (multidrug resistance associated protein) subfamily. This group is functionally and structurally closely related to the MDR (multidrug resistance protein) subfamily, now known as subfamily B (ABCB). MDRs consist of about 1200 amino acids and have the following structure: N-terminus – TMD1 – NBD1 – TMD2 – NBD2 – C-terminus. In contrast, most members of the MRP family contain an additional N-terminally-located hydrophobic domain that consists of about 200amino acids. The following examples demonstrate some functions and mechanisms of members of the ABCC family and give a basic idea of the work performed in this thesis.

1.1.3.1 MRP transporters in animals

The substrate spectrum for MRP transporters can be clearly distinguished from that of PGPs. Substrates for ABCCs/MRPs described in animals are mostly organic anions such as GS-Xs (glutathione forming a complex with a compound X), bile acids or glucuronide conjugates. Conjugation of glutathione can be either purely chemical or mediated by a glutathione transferase (GST) (Kreuz *et al.*, 1996).

*Hs*MRP1 (Cole *et al.*, 1992) was the first protein characterized as a functional GS-X pump (Leier *et al.*, 1994; Müller *et al.*, 1994). It was shown subsequently that *Hs*MRP2 and 3 also exhibit GS-X transport activity. In addition to GS-X, these transporters accept other organic anions such as glucuronide conjugates or sulfated substances. The different MRPs exhibit distinct kinetics for their substrates. Furthermore, they are localized in different tissues and/or different membranes (in polar epithelia), suggesting specific functions for different isoforms (König *et al.*, 1999, Slot *et al.*, 2011).

*Hs*MRP2 (ABCC2) is involved in the unidirectional transport of anionic conjugates, such as bilirubin glucuronides and leukotriene C4 (LTC4), across the apical membrane of polarized cells. It plays an important role in the elimination and detoxification of endogenous and xenobiotic substances across the canalicular membrane of liver hepatocytes (Büchler *et al.*, 1996; Cui *et al.*, 1999; Evers *et al.*, 1998; Paulusma *et al.*, 1996; Taniguchi *et al.*, 1996). *Hs*MRP2 is therefore responsible for the excretion of catabolites and potentially toxic substances into the bile fluid in the liver. A naturally occurring mutation in *Hs*MRP2 is responsible for the Dubin-Johnson syndrome in humans. The liver of Dubin-Johnson patients appears dark blue or black, due to the deposition of a dark pigment in the pericanalicular area (Bosma *et al.*, 1994). Absence of a functional MRP2 protein leads to insufficient transport of anionic conjugates, including monoglucuronosyl bilirubin, from hepatocytes into the bile (Kartenbeck *et al.*, 1996; Keppler and Kartenbeck, 1996; Paulusma *et al.*, 1997; Tsujii *et al.*, 1999). Beside the nine typical MRPs/ABCCs two members of this family fulfil different tasks. CFTR/ABCC7 CFTR is a cAMP-regulated chloride channel itself (Anderson *et al.*, 1991), but it is also a cAMP-dependent regulator of sodium channels (Stutts *et al.*, 1995). Mutations in this channel have been associated with lung diseases. In pancreatic cells, SUR1/ABCC8 pairs with a $K_{IR}6.2$ subunit and four of these pairs form the complex $(SUR1/K_{IR}6.2)_4$. The pore is formed by the $K_{IR}6.2$ unit and surrounded by SUR1 units, regulating the activity

of the K_{IR}6.2 potassium channel (Babenko *et al.*, 1998). This ABC transporter is closely related to diabetes (Matsuo et *al.*, 2003).

1.1.3.2 MRP transporters in yeast

Saccharomyces cervisiae contains six open reading frames for MRP-type ABC transporters (Rea et *al.*, 1998a). While YorI is localized in the plasma membrane, the others are most likely to be targeted to the vacuolar membrane (Klein, Kuchler and Valachovic Essay, 2011). The best-characterized MRP is the yeast cadmium factor-1 protein (*Sc*YCF1) located at the tonoplast. *Sc*YCF1 is responsible for vacuolar sequestration of heavy metals by transporting complexes between a metal ion and two glutathiones or organic glutathione S-conjugates (GS conjugates). Functional complementation in yeast and transport studies revealed their ability to act as GS-X pumps (Szczypka *et al.*, 1994; Li *et al.*, 1996 and 1997). Expression of YCF1 in Arabidopsis confers an improved heavy metal resistance to this plant (Song *et al.*, 2003).

1.1.3.3 MRP/ABCC transporters in plants

The first ABC transporter isolated from plants was an MDR-like gene from *Arabidopsis thaliana* (*At*PGP1; Dudler and Hertig, 1992). Further experiments showed that *At*PGP1 is localized in the plasma membrane and involved in hypocotyl elongation in light-grown seedlings (Sidler *et al.*, 1998). Accumulating evidence suggests that plant PGP-type ABC transporters are involved in polar and non-polar auxin transport and represent parts of the auxin efflux machinery (Geisler *et al.*, 2005).

The second observation presenting evidence that ABC transporters occur in plants, was that GS-X transport into vacuoles depended directly on MgATP hydrolysis and was independent of the electrochemical potential created by the vacuolar proton pumps (Martinoia *et al.*, 1993).

The observation that *Hs*MRP1 and the MRP homologue *Sc*YCF1 (Szczypka *et al.*, 1994) exhibit GS-X transport activity (Li *et al.*, 1996; Tommasini *et al.*, 1996) as well as high sequence similarities to plant MRPs, resulted in the isolation and functional characterization of MRP-like genes as GS-X transporters from *Arabidopsis* (Lu *et al.*

1997 and 1998; Tommasini *et al.*, 1998). First reports on plant ABC transporters showed that they are involved in detoxification processes. Sequence analysis of the Arabidopsis databases revealed that in this organism 15 genes are coding for MRPs/ABCCs (Martinoia *et al.*, 2001; Burla *et al.*, 2006). The fact that such a large number of MRP-like proteins are present in plants raises the question whether they exhibit a specific role and if yes, what could be their function.
Strong sequence homology is found in many cases and a large number of genes in the MRP sub-cluster suggest functional redundancy. One reason for the high number of genes could be the duplication of large segments of *Arabidopsis* chromosomes (Martionia *et al.*, 2002). Nonetheless, the question remains whether the duplicated ABC transporters are only redundant or whether they gained new functions.

Some of the MRPs characterized so far are specifically localized in the vacuolar membrane (*At*MRP1 and *At*MRP2) where they function in herbicide detoxification, protection against oxidative damage, pigment accumulation and the storage of antimicrobial compounds. A recent proteomic work identified 10 MRPs in the vacuolar membrane (*At*MRP1-8, *At*MRP10 and *At*MRP14) of *Arabidopsis thaliana* (Jaquinod *et al.*, 2007). *At*MRP2 and *At*MRP3, unlike *At*MRP1, catalyse the transport of chlorophyll catabolites. It was also shown that at least *At*MRP2 accepts glucuronides as an additional substrate class (Liu *et al.*, 2001). For *At*MRP1 and *At*MRP4, methotrexate transport was observed (Klein *et al.*, 2004; Rea *et al.*, 1998b). Therefore, as in animals, MRPs can function as glutathione conjugate pumps as well as transporters of certain non-glutathionated compounds such as chlorophyll catabolites and glucoronides. Very recently it was shown, that *At*ABCC1 and *At*ABCC2 are also responsible for apo-phytochelatine and phytochelatine-As (Song *et al.,* 2010). Double mutants in these ABC transporters are extremely sensitive to As and quite sensitive to Cd (Song *et al.*, 2010, Park *et al.*, 2011). In contrast to *At*MRP1, 2 and 5, *At*MRP3, 4 and 7 were able, at least partially, to restore cadmium resistance in the cadmium hypersensitive *Δycf1* yeast strain (Burla *et al.*, 2006), while in the case of *At*ABCC1 and *At*ABCC2 increased As resistance was only observed in phytochelatine synthesizing yeasts (Song *et al.,* 2010). After cadmium treatment of *A. thaliana* a significant up-regulation of *At*MRP6 could be detected in roots, even though the *Δycf1* yeast strain could not be complemented with

*At*MRP6 (Gaillard *et al.*, 2008). Interestingly, data from fission yeast has shown that Hmt1p, a vacuolar half-size ABC transporter, which is unrelated to ABCCs, is able to transport phytochelatins, as well as cadmium-phytochelatin complexes (Ortiz *et al.*, 1995). Like *At*MRP5 (discussed in the next chapter), *At*MRP4 is involved in guard cell regulation, but in contrast to *At*MRP5, *A. thaliana* T-DNA insertion mutants of *At*MRP4 lead to a decreased water-use-efficiency and increased drought susceptibility (Klein *et al.*, 2004). Furthermore, it was reported that *Zm*MRP3 is required for anthocyanin transport in maize (Goodman *et al.*, 2004).
In contrast to animals and fungi (especially *Saccharomyces cervisiae*), only few plant-borne substrates for MRPs have been identified (Hinder *et al.*, 1996; Klein *et al.*, 2000).

Further studies indicate that, as in animals, ion fluxes may be mediated or controlled by ABC transporters. Leonhardt *et al.* (1997 and 1999) showed that stomata opening in *Commelina communis* guard cells can be induced by treatment with the sulfonylurea compound glibenclamide and other drugs that are known to affect ion conductance controlled by SUR and CFTR.

1.1.4 AtMRP5 (AtABCC5), a MRP transporter protein in Arabidopsis thaliana

*At*MRP5 encodes a 167 kDa protein with a low glutathione conjugate and glucuronide conjugate transport activity. Promotor–ß-glucuronidase fusion constructs showed that it is mainly expressed in the vascular bundle and in the epidermis, especially in guard cells (Gaedeke *et al.,* 2001) and, according to the Genevestigator database, also in seeds (Zimmermann *et al.*, 2004).

Investigations on *At*MRP5 indicated that this protein exhibits functions beyond the direct energized organic anion transport. *At*MRP5 is in some way involved in signal transduction or a process that is closely linked to a signal transduction pathway. Experiments showed that wild type *A. thaliana* guard cells (on epidermal leaf strips) open in the dark in the presence of glibenclamide (Leonhardt *et al.*, 1997 and 1999). In contrast, a T-DNA mutant, identified by reverse genetics (*atmrp5-1*), was insensitive to glibenclamide. The glibenclamide-elicited opening in the dark was postulated to be due

to affected outward K^+ or S-type anion channel properties in the mutant lacking *At*MRP5 (Gaedeke *et al.*, 2001). According to the pharmacological similarities to SUR1 and CFTR it was suggested that *At*MRP5 may function as an ion channel regulator (Gaedeke *et al.*, 2001). Later studies revealed that guard cells of *atmrp5-1* plants were insensitive to external calcium and abscisic acid (ABA), a phytohormone responsible for stomatal closure during drought stress, but also did not open in the presence of external auxin (Klein *et al.*, 2003). Whole cell patch clamp experiments on wild type and T-DNA mutant guard cell protoplasts showed reduced ion fluxes, but no total inhibition of the ion fluxes (Suh *et al.*, 2007). Furthermore, impaired function in cytosolic Ca^{2+}-activated slow (S-type) anion channels in the plasma membrane of *atmrp5-1* guard cells was shown, as well as impaired Ca^{2+}-permeable channel currents after abscisic acid (ABA) treatment in mutant protoplasts. These data supported the hypothesis that *At*MRP5 is a central regulator of ion channels during ABA and Ca^{2+} signal transduction in guard cells.
In the light, the aperture of *atmrp5-1* knockout plant stomata was reduced, resulting in a decreased transpiration rate and water uptake. Finally, if plants were not watered, *atmrp5-1* plants resisted longer to drought conditions compared to wild-type plants due to reduced water loss. Analysis of CO_2 uptake and transpiration rates showed that *mrp5-1* plants have an increased water-use-efficiency (Klein *et al.*, 2003).

The mutant *atmrp5-1* exhibited decreased primary root growth and increased lateral root formation on half-strength Murashige & Skoog (MS)-medium. *atmrp5-1* and wild-type seedlings grown for 10 days after germination (dag) on a medium corresponding to full-strength MS-medium showed a reversion of this phenotype. Auxin levels in the roots of *atmrp5-1* plants were increased (Gaedeke *et al.*, 2001). This observation indicated on one hand that *At*MRP5 is involved in stomata regulation, possibly by exhibiting a channel or channel activity. On the other hand it could be postulated that *At*MRP5 is also involved in auxin signalling, possibly by transporting auxin conjugates.

1.2 Regulation of plant transpiration through stomata[1]

As mentioned above, the *At*MRP5 mutant phenotype involves deregulation of guard cell movements. At the beginning of my thesis, however, the function of *At*MRP5 in regulating stomata was not understood.
To get an idea on the role of *At*MRP5 in stomata regulation, it was important to integrate the data obtained from our *At*MRP5 work with the existing knowledge and models of guard cell function. Therefore, the most important mechanisms, pathways and observations made on stomatal movement are summarized below.

1.2.1 Role of the stomata complex

In contrast to water plants, land plants face the challenge to take up CO_2 from the atmosphere while limiting water loss. Plants developed different mechanisms to limit water loss. Most importantly and ubiquitously spread among land plants is the cuticle, a hydrophobic layer that covers the leaf surface as an efficient barrier to limit water loss. Additionally, trichomes, which increase the size of the boundary layer (see below) close to the leaf surface, or reduction of leaf size or number (great diversity of morphological forms of leaves and leaf structures) reduces water loss. However, if water loss is reduced, also CO_2 uptake is minimized. Furthermore, the concentration gradient for CO_2 uptake is much smaller than the concentration gradient driving water loss.
Stomata are regulated pores formed by two guard cells mostly present at the lower leaf surface that are responsible to maximize CO_2 uptake and minimize water loss. They can react to environmental and internal signals, such as light, water availability and high or low CO_2 partial pressure. These various signals trigger signalling processes in guard cells, which regulate the stomata complex.

[1]All information in this chapter are, if no other source is mentioned, from Taiz, l., Zeiger, E., Plant Physiology 2nd Edition, Spectrum Verlag

1.2.2 Physical features of transpiration

Transpiration of leaves is defined as water vapour moving from the leaf to the atmosphere by diffusion, mostly through stomata.

It depends on two major factors:

- Difference in water vapour concentration between the leaf air spaces and the external air and
- Diffusional resistance (r) of this pathway

$$E = \frac{c_{wv(leaf)} - c_{wv(air)}}{r_s + r_b}$$

E: transpiration rate
[E]: $mol \cdot m^{-2} \cdot s^{-1}$
c_{wv}: water vapour conc.
$[c_{wv}]$:$mol \cdot m^{-3}$
r_s: resistance stomatal pore
r_b: resistance boundary layer
[r]: $s \cdot m^{-1}$

A high resistance is equivalent to a low conductance (mathematically speaking: conductance is the inverse of resistance). In the leaf, the total resistance is mostly due to the diffusion limitation encountered by the stomatal pore, but other parts of the pathway for water loss, such as the boundary layer, may contribute significantly to r.
The boundary layer is a thin film of still air that embraces the surface of the leaf, and its resistance to water vapour diffusion is proportional to its thickness. The thickness of the boundary layer is primarily determined by the wind speed. Absence of wind, leads to a “stacking” of molecules and results in a thick layer of air around the leaf, comparable to an air cushion. This layer of air builds a barrier and reduces water vapour loss almost to zero. The increase of stomata aperture under such conditions has little effect on the transpiration rate. Contrarily, if there is a high wind speed, the layer becomes thin and its resistance reduced. Under these conditions, the stomatal resistance has the largest impact on the control over water loss by leaves. This situation is more likely appearing in nature.
Stomatal pores provide a low-resistance pathway for diffusion movement of gases across the epidermis. Changes in stomatal resistance are important in regulating water loss by the plant and controlling the rate of CO_2 uptake necessary for sustained CO_2 fixation during photosynthesis.

The water-use-efficiency is a measure of the relation between transpiration and carbon assimilation:

$$\text{Water-use-efficiency (WUE)} = \frac{\text{Moles of } CO_2 \text{ fixed}}{\text{Moles of } H_2O \text{ transpired}}$$

C3 plants (the first stable product is a C3 molecule; 3-phosphoglycerate) loose around 600 water molecules (referring to Dietrich *et al.*, 2001) per CO_2 molecule fixed (WUE=0.002).
C4 plants have a reduced water loss per CO_2 fixed, since they fix CO_2 using the phosphoenolpyruvate carboxylase that exhibits a much higher affinity towards CO_2 compared to Rubisco (WUE =0.004). CAM plants, which fix CO_2 during the night, may exhibit water-use-efficiencies around 0.02.

The large H_2O efflux to CO_2 influx ratio has two reasons:

1. In most cases the concentration gradient driving water loss is much larger than that driving CO_2 influx. The CO_2 concentration in the air is very low (~0.039%) and the water vapour concentration in the leaf air spaces is high.

2. CO_2 diffuses about 1.6 times slower through air than water vapour. Furthermore CO_2 has to diffuse through the plasmalemma, the cytoplasm and the chloroplast envelope before its fixation occurs.

1.2.3 Guard cells

Guard cells are specialized epidermal cells, which surround the stomatal pore. Two main types are described:

1. Gramineae-type stomata (barbell-shaped): typical for grasses and a few other monocots (palms)
2. Helleborus-type stomata (kidney-shaped): all dicots, many monocots, mosses, ferns and gymnosperms

Subsidiary cells are pairs of differentiated epidermal cells, flanking the guard cells.

- Gramineae-type: Subsidiary cells, which help to control the guard cells.
- Helleborus-type: Subsidiary cells not untypical but often absent.

In contrast to the usual thickness of a cell wall (1-2 μm), guard cell walls are extremely thick (up to 5 μm).
The kidney shaped pattern results in very thick inner and outer (lateral) walls, a thin dorsal wall (in contact with the epidermal cells) and a thickened ventral (pore) wall. The walls contain cellulose microfibrils, which reinforce and shape the cell. They form a kind of a steal-belted radial tire.
To withstand the great changes in size between the open and the closed state, the cell walls of guard cells are especially flexible. It was shown that the polysaccharide arabinan (a polymer of arabinose) seems to be an important component for the flexibility of cell walls (Jones *et al.*, 2003). It was postulated that arabinan prevents the formation of homogalacutronan polymers and, thus, to avoid stiffening of the cell walls. Another parameter could be acidification, which gives more elasticity to the cell walls during opening (Bittisnich *et al.*, 1987).

Guard cells sense different environmental changes like light intensity and quality, temperature, relative humidity and intracellular CO_2 concentrations, which are integrated into well-defined stomatal responses.

In C3 and C4 plants no photosynthesis takes place during the night. Consequently, there is no demand for CO_2inside the leaf tissue. Stomata close and water loss is avoided. During the day, the radiation on the leaf surface favours high photosynthetic activity. There is a high demand for CO_2 and the stomatal pores open, as long as water supply is sufficient. No or limited water availability keeps stomata closed to avoid lethal dehydration.

1.2.4 Stomata opening

To balance CO_2 entry and water loss, the stomata complex is very precisely regulated. It is able to react to diverse stimuli to reach the highest possible efficiency between carbon dioxide uptake and water loss. Therefore, not just the closure is tightly controlled; also the opening is accurately regulated.

The process, leading to the swelling of the guard cells and resulting in opening of the stomatal pore is caused by osmotic pressure. During the opening of the stomatal pore, the plasma membrane ATPase is activated and hyperpolarizes the plasma membrane. The central role of the H^+ATPase in initiating the first step of stomata opening is well documented (Zhao *et al.* 2000; Kinoshita *et al.*, 2001; Roelfsema and Hedrich, 2005). More recently Merlot *et al.* (2007) showed that constitutive activation of one of these pumps, AHA1 preventedabscisic acid-mediated stomata closure. Interestingly the effect on high CO^2- or darkness-mediated closure was much less pronounced, highlighting the complexity of the guard cell signalling pathways. Hyperpolarization of the plasma membrane leads to an activation of voltage-gated K^+ influx channels (Schroeder *et al.*, 1987) that are the driving force for K^+ uptake (Kwak *et al.*, 2001, Roelfsema and Hedrich, 2005). This uptake is followed by chloride (nitrate, malate) uptake into guard cells and malate synthesis within these cells. The consequence is a higher osmolite concentration leading to water influx and swelling of the guard cells. Ca^{2+} oscillations play an important role as an internal signal, for example for the activation and inactivation of the ATPase during stomatal movements. During the opening process, the Ca^{2+} levels in the cytosol are lower as during closure (Kwak *et al.,* 2003; Roelfsema and Hedrich, 2005, Iba and Schroeder, 2006)).

The main stimulus for stomatal movements is the day/night cycle, connected to the ability of driving photosynthesis.

Photobiological and metabolic studies have shown two distinct systems for opening:

1. Guard cell photosynthesis consumes CO_2 and, thus, changes its intercellular concentration
2. Specific reaction to blue light (activation of a proton pumping ATPase) and to red light (namely photosynthesis) (Serrano *et al.*, 1988, Sharkey and Raschke, 1981)

Stomata respond to CO_2 levels: They close in response to high CO_2 levels. If the CO_2 concentration in the substomatal cavity decreases, for instance when photosynthetic activity is high, the stomata open and permit the influx of CO_2. It was shown that different levels of CO_2 are sensed by Ca^{2+} concentration oscillations, leading to membrane potential changes. Studies revealed that a decrease in CO_2 concentration leads to hyperpolarization; in contrast, an increase in CO_2 leads to a depolarization of the guard cell plasma membrane (Brearley *et al.*, 1997, Ishikawa *et al.*, 1983, Rob *et al.*, 2002, Hedrich *et al.*, 2001).

The opening responses to blue light are rapid, reversible and sensed in this single cell type. Red light-mediated stomatal opening is dependent on photosynthetic electron transport in guard cell chloroplasts. It is not always easy to distinguish between blue light reaction and CO_2 concentration effects. But, working with epidermal strips and constant CO_2 concentrations it was shown that there are specific stomatal responses to light. The mechanism how light stimulates stomatal opening is still not fully understood (Assmann *et al.*, 1999; Assmann and Shimazaki, 1999; MacRobbie *et al.*, 1998).

Four blue light receptors have been identified in *Arabidopsis* by analysis of mutants deficient in specific blue-light-mediated responses: phototropin1 (PHOT1) and phototropin 2 (PHOT2) as well as cryptochrome 1 (CRY1) and cryptochrome 2 (CRY2). The stomata of double mutants of the flavoproteins PHOT1 and PHOT2 failed to

respond to blue light even though the mutant plants looked phenotypically normal (Kinoshita *et al.*, 2001).

Different opening signals lead to an increase of potassium, malate, and chloride and, at least in some plants, nitrate concentrations in guard cells. In *A. thaliana,* the potassium concentration rises from around 100 mM K^+ in closed to 400-800 mM K^+ in the open state. Anions such as chloride, nitrate and malate balance the increase in electric charges caused by K^+-influx. While Cl^- and NO_3^- are taken up from the apoplast, malate is mainly synthesized within the cell through carbon skeletons generated by starch hydrolysis. The question whether chloride, nitrate or malate balance potassium ions appears to be a matter of the environment and possibly also of the plant: In *Vicia faba* plants grown in the field, mainly Cl^- balanced K^+ in guard cells, while in *Vicia faba* grown in a phytotron, large portions of potassium ions were balanced by malate. Thereby, chloride ions are thought to enter the cytoplasm through a Cl^-/H^+- symporter.

Depending on the growth conditions and time of the day, stomatal movements may also rely on sugar accumulation (Talbott and Zeiger, 1998; Tallman and Zeiger, 1998). From the start of the photosynthetic period in the morning, the sucrose content of guard cells increases steadily. Throughout the day sucrose becomes the dominant osmotically active solute. At the end of the day, stomatal closure parallels a decrease in the sucrose content of guard cells. For the consistent daily opening that occurs at sunrise, K^+ is the primary active solute, while sucrose could functionally couple the stomatal conductance in the epidermis to photosynthetic activity in the mesophyll (Talbott and Zeiger, 1998). According to Tallman and Zeiger (1988) and Talbott and Zeiger (1998), the sucrose in the guard cells emerges from three sources: starch degradation, guard cell photosynthesis and uptake of apoplastic sucrose.

The role of sucrose in guard cell regulation as described by Tallman and Zeiger (1988) and Talbott and Zeiger (1998), was intensively discussed during the past years. More recent papers show that the breakdown of starch, produced from the guard cell photosynthetic activity, generates just a limited amount of sucrose (Outlaw *et al.*, 2003; Vavasseur and Raghavendra, 2005). Furthermore, it was shown that the sucrose concentration increases mainly in the apoplast (~150 mM, Lu *et al.*, 1995). It was stated that this is the main source for sucrose accumulation in guard cells. Several studies

support this statement: sucrose movement to guard cells *in planta* (Lu *et al.*, 1997), sucrose uptake by guard cells in vitro (Reddy and Das, 1986; Lu *et al.*, 1995; Ritte *et al.*, 1999), sugar transporters in guard cells (Stadler *et al.*, 2003), guard cell enzyme patterns that are typical for a sucrose sink (Hite *et al.*, 1993) and pulse labelling methods, showing that the apoplastic sucrose derives from recent photosynthesis in mesophyll cells (Lu *et al.*, 1997). In addition, the apoplastic sucrose itself plays a role in regulating stomatal aperture size. Thus, the sucrose concentration in the apoplast is sufficient to osmotically decrease stomatal aperture size by 3 µm (Lu *et al.*, 1995).

One of the various features of the phytohormone auxin (indole-3-acetic acid; IAA) is that IAA is able to trigger stomata opening even in the dark. Likewise, in auxin-induced stomatal opening, cytoplasmic Ca^{2+} has been proposed as a transmitter of the signal (Irving *et al.*, 1992). There is also evidence that IAA controls different fluxes; most importantly it modulates potassium fluxes in *Vicia faba*, like inward rectifying K^+ channels (Blatt and Thiel, 1994). As mentioned before, K^+ currents play an important role in the "central" regulation mechanisms of the stomatal pore. Furthermore, it was shown in *Vicia faba* guard cell protoplasts that IAA activates the plasma membrane H^+-ATPase, which hyperpolarizes the membrane (Lohse and Hedrich, 1992). However, the underlying mechanisms as well as the physiological role of auxin in guard cell regulation are still not fully understood.

1.2.5 Stomatal closure

Stomata of C3 and C4 plants close during night. When light fades the blue-light signals decrease and blue light-stimulated proton pumping in guard cells disappears. In addition, the CO_2 concentration in the substomatal cavity rises. As a result, the membrane is no longer hyperpolarized and the inward K^+ channels close. The subsequent depolarization of the membrane activates R- and S-type anion channels causing the release of Cl^-. In contrast to potassium channels, which are known since many years, these two types of channels have been identified only recently at the molecular level. The slow, voltage-independent anion channel is encoded by the *SLAC1* gene (Negi *et al.,* 2008, Vahisalu *et al.,* 2008) and requires the OST1 and CPK protein

kinase (Geiger *et al.,* 2009, Geiger *et al.,* 2010, Brandt *et al.* 2012). Several members of the Aluminium Metal Transporter (ALMT) family - most probably - encode rapid channels. *At*ALMT12 exhibits the characteristics of the R-type anion channel and ALMT12 T-DNA insertion mutants are strongly impaired in stomatal movement. However, in the mutant residual R-type channel activity is still present (Meyer *et al.*, 2010). Release of Cl^- ions results in further depolarization, inducing the release of K^+ through outward rectifying K^+ channels (Roelfsema and Hedrich, 2005). This leads to an osmotically triggered water loss, shrinking of the guard cell and finally to stomata closure.

ABA is the classical water stress hormone causing rapid stomatal closure when water is limiting. Under drought conditions, the ABA concentration in leaves can increase up to 50 times. Apoplastic ABA can be taken up by two types of transporters, ABC-proteins (Kang *et al.*, 2010) and by some members of the low affinity nitrate transporters (NRT1s) (Kanno *et al.,* 2012). For long time it was believed that the ABA signal was exclusively due to ABA transport from the root to the shoot. However, during the last years it was revealed that the response to drought was faster than the transport of ABA from the root. Therefore it must be suggested that the fast response to drought-induced stomata closure is triggered by ABA redistribution and biosynthesis within the leaf (Lemitri-Chlieh and MacRobbie, 1993, Christmann *et al.,* 2005). However, the exact cooperation between root and leave produced ABA remains elusive. To complicate the ABA synthesis story even more, it has very recently been shown that guard cells can produce ABA and that this ABA plays an important role for stomatal closure under reduced atmospheric humidity (Bauer *et al.,* 2013).

Due to ABA signalling, Ca^{2+} is released from internal compartments and the calcium concentration in the cytosol increases. This induces the above-mentioned S-type anion channel activation while the R-type channel is probably induced by the depolarization due to the inactivation of the plasma membrane H^+-pump. Efflux of anions induces a further membrane depolarisation and activates the K+-out channel GORK (Roelfsema and Hedrich, 2005). It was suggested that ABA-induced depolarisation events result from activation of calcium channels (Schroeder and Hagiwara, 1990).

ABA transported into the cytosol of guard cells or produced in guard cells binds to soluble ABA receptors, so-called called RCARs (regulatory component of ABA receptor). RCARs belong to a family of 14 members and bind to protein phosphatase 2Cs (PP2Cs), namely ABI1 and ABI2 (Ma *et al.*, 2009). ABI1 and ABI2 are known as key players in ABA signal transduction and repress ABA responses (Merlot *et al.*, 2001). ABA is, in the presence of e.g. RCAR1, able to fully block the protein phosphatase activity of ABI2 (Ma *et al.*, 2009).

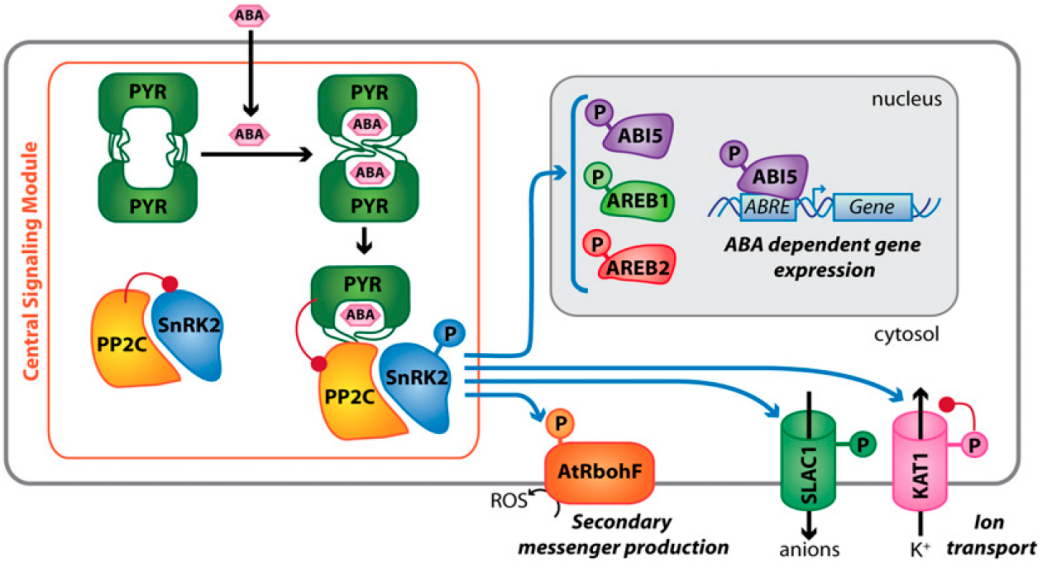

Figure 3 The core ABA signalling pathway

The PYR/RCAR-PP2C-SnRK2 signal transduction Model according to Hubbard *et al.* (2010): Without ABA present in guard cells, PP2C inhibits snRK2 activity (protein kinase) by removing the activating phosphatases. In presence of ABA, PYR/PYL dimers dissociate and form ABA receptor-PP2C complexes. These complexes inhibit, in an ABA dependent manner, the activity of the PP2C and therefore allowing the activation of SnRK2s. SnRK2 targets where localized in the plasma membrane, as well as in the nucleus. Activation of SnRK2s was shown to result in control of ion channels, secondary messenger production and gene expression. Inhibitory interactions are displayed as red connections.

Phytic acid, also known as inositolhexa*kis*phosphate ($InsP_6$) is thought to act as a signalling molecule triggered by ABA. $InsP_6$ is responsible for the release of calcium ions from internal compartments such as the central vacuole, leading to an increase in cytosolic calcium from 50-350 nM up to 1.1 μM. On the other hand, $InsP_6$ signalling leads to a reduced inward K^+ current (Lemitri-Chlieh *et al.* 2000 and 2003). In patch-clamp experiments of *Vicia faba* and *S. tuberosum* guard cells it has been shown that

nanomolar concentrations of $InsP_6$ mimicked the inhibitory effects of ABA and internal calcium on the inward rectifying K^+ currents (Lemitri-Chlieh *et al.*, 2000). It was therefore concluded that $InsP_6$ is the compound, which triggers the release of Ca2+ from internal stores, and the inhibition of inward K^+ channels was ultimately due to $InsP_6$. However, it must be a close link between ABA and $InsP_6$, which has to be elucidated.

Ethylene is a gaseous plant hormone involved in diverse seasonal, developmental and physiological processes. No general role in guard cells can be distinguished as its function varies among different plant families. In *Arabidopsis*, ethylene is able to inhibit the ABA-induced stomatal closure. A possible explanation for the physiological function of the antagonistic relationship between ABA and ethylene can be the maintenance of a minimal supply of carbon dioxide to ensure a minimum level of photosynthesis during long periods of drought stress (Tanaka *et al.*, 2005). Both hormones are affected by drought stress and their levels increase during desiccation (Xu and Zou, 1993). Ethylene production was found to be regulated by a circadian clock and by light (Thain *et al.*, 2004).

Ethylene inhibitors, such as AVG (1-aminoethoxyvinylglycine), inhibit the auxin-induced stomatal opening in *Vicia faba*. The inhibition of ethylene synthesis in guard cells with AVG did not inhibit the light- or the fusicoccin-induced opening of stomata. These findings support the hypothesis that auxin-induced stomatal opening is mediated through auxin-induced ethylene production by guard cells (Merritt *et al.*, 2001).

2 Aim of the work

The aim of this work was to further elucidate the role of *At*MRP5 in guard cell regulation by investigating transport specificity as well as the regulatory entities of *At*MRP5. Seed nutrient measurements, transport experiments with microsomes from *Saccharomyces cervisiae*, expressing *At*MRP5 and the yeast two-hybrid approach were chosen to elucidate specific transport substrates and possible interaction partners of *At*MRP5. As mentioned in the Introduction, *At*MRP5 affects stomatal movement and root growth. However, at the beginning of my thesis the mechanisms responsible for the observed phenotype were largely unknown. During this work Suh *et al.* (2007) showed that *At*MRP5 affected ion channel activity but very probably does not represent an anion channel itself. However, the mode of action, how the anion channel activity is affected, remains mainly unknown.

THE JOURNAL OF BIOLOGICAL CHEMISTRY VOL. 284, NO. 48, pp. 33614–33622, November 27, 2009

The *Arabidopsis* ATP-binding Cassette Protein AtMRP5/AtABCC5 Is a High Affinity Inositol Hexa*kis*phosphate Transporter Involved in Guard Cell Signaling and Phytate Storage*[S]

Received for publication, June 5, 2009, and in revised form, September 17, 2009 Published, JBC Papers in Press, September 21, 2009, DOI 10.1074/jbc.M109.030247

Réka Nagy[‡1], Hanne Grob[‡], Barbara Weder[‡], Porntip Green[§], Markus Klein[¶], Annie Frelet-Barrand[‡], Jan K. Schjoerring[‖], Charles Brearley[§2], and Enrico Martinoia[‡]**

*From the [‡]University of Zurich, Institute of Plant Biology, Zollikerstrasse 107, CH-8008 Zürich, Switzerland, **POSTECH-UZH Global Research Laboratory, Division of Molecular Life Sciences, Pohang University of Science and Technology, Pohang 790-784, Korea, [¶]Tobacco Technologies, Tobacco Applied Biology, Philip Morris International, R & D Innnovation Cube, Quai Jeanrenaud 5, CH-2000 Neuchatel, Switzerland, the [‖]University of Copenhagen, Faculty of Life Sciences, Thorvaldsensvej 40, DK-1871 Frederiksberg C, Denmark, and the [§]University of East Anglia, School of Biological Sciences, Norfolk NR4 7TJ, Norwich, United Kingdom*

Arabidopsis **possesses a superfamily of ATP-binding cassette (ABC) transporters. Among these, the multidrug resistance-associated protein AtMRP5/AtABCC5 regulates stomatal aperture and controls plasma membrane anion channels of guard cells. Remarkably, despite the prominent role of AtMRP5 in conferring partial drought insensitivity upon *Arabidopsis*, we know little of the biochemical function of AtMRP5. Our phylogenetic analysis showed that AtMRP5 is closely related to maize MRP4, mutation of which confers a low inositol hexa*kis*phosphate kernel phenotype. We now show that insertion mutants of *AtMRP5* display a low inositol hexa*kis*phosphate phenotype in seed tissue and that this phenotype is associated with alterations of mineral cation and phosphate status. By heterologous expression in yeast, we demonstrate that AtMRP5 encodes a specific and high affinity ATP-dependent inositol hexa*kis*phosphate transporter that is sensitive to inhibitors of ABC transporters. Moreover, complementation of the *mrp5-1* insertion mutants of *Arabidopsis* with the AtMRP5 cDNA driven from a guard cell-specific promoter restores the sensitivity of the mutant to abscisic acid-mediated inhibition of stomatal opening. Additionally, we show that mutation of residues of the Walker B motif prevents restoring the multiple phenotypes associated with *mrp5-1*. Our findings highlight a novel function of plant ABC transporters that may be relevant to other kingdoms. They also extend the signaling repertoire of this ubiquitous inositol polyphosphate signaling molecule.**

Guard cells form pairs of cells, which are conjoined at their ends, in the epidermis of the aerial tissues of plants. The cells surround a central pore, the stoma, through which gas exchange occurs. The principal gases exchanged are CO_2 and water vapor, and the function of the stomatal complex may be considered as the maximization of CO_2 assimilation by photosynthesis for the minimization of water loss.

Guard cells and hence the aperture of the central pore are sensitive to environmental factors including light, temperature, CO_2, and ozone (1). Stomatal closure is initiated by the drought stress hormone abscisic acid (ABA).[3] The closure of stomata is a result of a loss of turgor of the delimiting guard cells as a consequence of ion efflux, predominantly Cl^- and K^+, and metabolic conversion of organic acids into starch (2).

Although the molecular identity of genes encoding the outward and inward K^+ conductances are known for *Arabidopsis thaliana* (3), it remains to be demonstrated whether the recently identified SLAC protein (4, 5) encodes the S-type anion channel or is a subunit thereof.

The ATP-binding cassette family of membrane proteins is among the most ubiquitous and variable group of membrane proteins and is most commonly associated with membrane transport phenomena. The substrates transported are especially diverse, and consequently a major obstacle to the interpretation of ABC transporter function, particularly pertinent in the context of guard cell function, is the identification of the substrate transported.

A recent study identified the ABC transporter AtABCB14 as an apoplast to symplast malate importer capable of modulating stomatal response to CO_2 (6), whereas plants bearing mutations in the MRP type ABC transporter *AtMRP5* show partial inhibition of ABA-induced stomatal closure (7); impairment of activation of S-type anion channels by both ABA and cytosolic Ca^{2+} (8); and, additionally, impairment of the activation of plasma membrane Ca^{2+}-permeable channel activity by ABA (8). A number of hypotheses have been proposed to explain the phenotype of *atmrp5* mutants; these hypotheses include that *AtMRP5* encodes an anion channel or that AtMRP5 directly regulates a guard cell anion channel (8). Both of these possibil-

* This work was funded by Swiss National Foundation Grant 3100AO-117790 (to E. M.), by funds from the Forschungskredit der Universität Zürich (to R. N.), by European Union Project Public Health Impact on Long Term, Low Level Mixed Element Exposure (PHIME) Contract FOOD-CT-2006-0016253 (to J. K. S.), and by Biotechnology and Biological Sciences Research Council Grant BB/C514090/1 (to C. B.).

[S] The on-line version of this article (available at http://www.jbc.org) contains supplemental text and Figs. S1–S6.

[1] To whom correspondence may be addressed. Tel.: 41-44-6348283; Fax: 41-44-6348204; E-mail: rnagy@botinst.uzh.ch.

[2] To whom correspondence may be addressed. Tel.: 44-1603592197; Fax: 44-1603592250; E-mail: C.Brearley@uea.ac.uk.

[3] The abbreviations used are: ABA, abscisic acid; ABC, ATP-binding cassette; HPLC, high pressure liquid chromatography; AMPPNP, adenyl-5′-yl imidodiphosphate; MES, 4-morpholineethanesulfonic acid; insP_6 inositol hexa*kis*phosphate.

ities have precedent in the cystic fibrosis transmembrane conductance regulator, a mammalian ABC protein that has ion (Cl^-) channel activity and that also modulates the activity of associated ion channels (9).

The activity of other Cl^- conductances, but not cystic fibrosis transmembrane conductance regulator, have been shown to be influenced by inositol polyphosphate signaling molecules (10, 11). Most recently, inositol 3,4,5,6-tetra*kis*phosphate was identified as a physiological regulator of a specific chloride conductance, that of the CIC-3 channel of mammalian secretory epithelia (12).

Inositol 3,4,5,6-tetra*kis*phosphate and inositol 1,4,5-trisphosphate are not the only inositol phosphates that directly regulate ion channels. In guard cells, inositol hexa*kis*phosphate mobilizes calcium from endomembrane stores (13) and inhibits the inward rectifying K^+ conductance (14).

We were fascinated by a recent report that disruption of a gene encoding the ATP-binding cassette protein *ZmMRP4* reduced inositol hexa*kis*phosphate accumulation in maize kernels (15). One interpretation of this report is that ZmMRP4 is responsible for transport of inositol hexa*kis*phosphate or a precursor across the vacuole membrane of inositol hexa*kis*phosphate storage tissues of maize kernels.

Our experiments have addressed the function of AtMRP5, an orthologue of ZmMRP4, *in planta*. By a combination of biochemical, physiological, and genetic analysis, we identify a hitherto undescribed inositol polyphosphate transport function in *Arabidopsis* for this example of the most ubiquitous class of membrane transport proteins. Our work links inositol hexa*kis*phosphate transport to the regulation of stomatal response to ABA.

EXPERIMENTAL PROCEDURES

Chemical Analysis of AtMRP5 Loss-of-function Mutants—Fifty milligrams of dried seed material was incinerated for 8 h at 550 °C, and subsequently the ash was solubilized in 2 ml of 6 N HCl, briefly heated up to 100 °C, purified through Whatman No. 40 ashless filter paper, and transferred to double-distilled water to a total volume of 50 ml. Element contents were measured by inductively coupled plasma emission-spectroscopy analysis with a Varian Liberty 220 (Varian Inc., Palo Alto, CA) equipped with an ultrasonic nebulizer (CETAC U-5000 AT^+) according to standard procedures. Inositol hexa*kis*phosphate and inorganic phosphate were determined by suppressed ion conductivity HPLC of acid extracts of *Arabidopsis* seeds (16). Seeds, 2–4 mg, were boiled in 0.8 ml of 0.6 M-HCl for 30 min, and the supernatant was diluted 10 times in water. The samples (50 μl) were analyzed on a Dionex ICS2000 chromatography system fitted with a 25-cm × 2-mm internal diameter Dionex AS11 anion exchange column, with an associated AG11 guard column. The column was eluted with a gradient of KOH (0 min, 0 mM KOH; 20 min, 100 mM KOH) at a flow rate of 0.25 ml/min. The inositol hexa*kis*phosphate and P_i content of samples was determined from a calibration curve of peak area *versus* the amount injected in the range 0.2–4 and 0.2–2 nmol, respectively. In our hands, leaf inositol hexa*kis*phosphate levels were below the limit of detection of this method.

Functional Analysis in Yeast—The *ycf1* yeast mutant was transformed with the expression vector pNEV harboring no insert (pNEV) or *AtMRP5* cDNA (pNEV-MRP5). Microsomal vesicles were isolated as described previously (17). For the transport of inositol hexa*kis*phosphate, Ins(1,[^{33}P]2,3,4,5,6)P_6 prepared according to (18) was added to the reaction mix consisting of transport buffer, 1 mM dithiothreitol, 5 mM ATP, 10 mM $MgCl_2$, 10 mM creatine phosphate, and 100 μg/ml creatine kinase. Yeast microsomes were added to start the transport assay. The assays were performed at room temperature. At intervals, inositol hexa*kis*phosphate uptake was terminated by the transfer of three aliquots, equivalent to 18.9 nCi (700 Bq) of starting material, onto 0.45-μm-diameter pore size nitrocellulose filters. Under these conditions, the rate of net transport was linear with time during the first 5.5 min. The values are corrected for corresponding controls with vesicles isolated from *ycf1* yeasts transformed with the empty pNEV vector. ATP-independent inositol hexa*kis*phosphate uptake was assessed in the absence of ATP. Transport assays for all treatments were performed with the same vesicle preparation. The experiments were repeated three times, with independent vesicle preparations. Labeled material recovered on the filter was analyzed by Partisphere SAX HPLC. For the experiments with the nonhydrolyzable ATP analogue AMPPNP, the 4 mM ATP from the reaction mix was replaced with the equivalent concentration of AMPPNP. For the experiments on ice, the tubes containing the reaction mix and the labeled $InsP_6$ were placed on ice immediately after the addition of the yeast microsomes.

Inhibition Studies—Yeast microsomes were incubated at room temperature in the reaction mix that contained the indicated potential inhibitors (see Table 1). After 8 min, Ins(1,[^{33}P]2,3,4,5,6)P_6 was added to the reaction mix, and inositol hexa*kis*phosphate uptake was determined as above. The different inhibitors were always tested with the same vesicle preparation as the Ins(1,[^{33}P]2,3,4,5,6)P_6 uptake control. The number of repetitions is indicated in Table 1. For experiments with different inositol polyphosphates (see Table 2), the putative inhibitors/competitors were added to the reaction mix at the concentration indicated in Table 2. The transport assay was started by the addition of microsomes. The assays were performed at room temperature. After 5.5 min, uptake was terminated by the transfer of three replicates onto 0.45-μm-diameter pore size nitrocellulose filters. The number of repetitions of the experiment is indicated in Table 2. ATP-dependent AtMRP5-mediated transport was considered as 100%. The reaction mix contained labeled $InsP_6$ at 1.85 kBq/nitrocellulose filter.

Partisphere SAX HPLC—Extracts of radiolabeled *Arabidopsis* seedlings, products of transport assays, and preparations of Ins(1,[^{33}P]2,3,4,5,6)P_6 were all analyzed by anion exchange HPLC on a 23.5-cm × 4.6-mm internal diameter Partisphere SAX WVS cartridge with guard cartridge (18). The column was eluted at a flow rate of 1 ml/min with a gradient derived by mixing of A, water; B, 1.25 M-$(NH_4)_2HPO_4$ adjusted to pH 3.8 with H_3PO_4 according to the following program: 0 min, 0% B; 5 min, 0% B; 65 min, 100% B; 75 min, 100% B. Radioactivity (^{3}H or ^{33}P) in column eluates was estimated by admixture of Optima Flo^{TM} AP (Canberra Packard, Pangbourne, UK) scintillation fluid at 2 ml/min in a

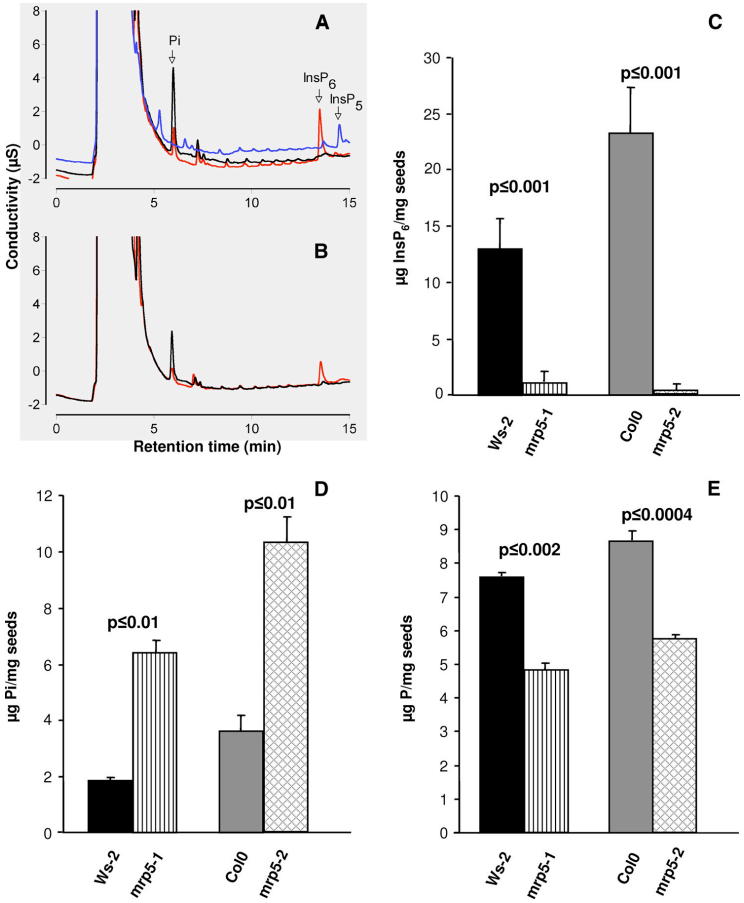

FIGURE 1. **Ablation of AtMRP5 disturbs inositol hexa*kis*phosphate, phosphate, and phosphorus levels in seeds.** The conductivity profiles of seed extracts is shown. *A*, traces for Col0 (*red line*), *mrp5-2* (*black line*), and *ipk1-1* (*blue line*). *B*, traces for Ws-2 (*red line*) and *mrp5-1* (*black line*). Individual traces are offset on the *y* axis to aid visualization. *C*, seed $InsP_6$. *D*, inorganic phosphate (*Pi*). *E*, total phosphorus (*P*) content of two independent AtMRP5 mutants and their corresponding wild types. The data represent the means and standard deviations of four to eight independent measurements.

Canberra Packard A515 flow detector fitted with a 0.5-ml flow cell. The integration interval was 0.2 min.

Analysis of Stomatal Apertures—*Arabidopsis* (Ws-2) leaves were transformed with the *GUS* reporter gene under control of the *MYB60* promoter (19) by particle bombardment. For detection of GUS activity, the leaves were incubated for 8 h at 37 °C in 1 mM X-glucuronic acid, 0.5% Triton X-100, 50 mM $NaHPO_4$, pH 7.2, and subsequently cleared in 70% ethanol. The *AtMRP5* cDNA under the control of the *MYB60* promoter was cloned into Gateway™ compatible plant transformation vectors (20). The resulting constructs were used to transform *mrp5-1* mutants by the floral dipping method using *Agrobacterium* (21). *Arabidopsis* plants (Ws-2, *mrp5-1*, and *MYB60*::*MRP5*, independent homozygous transformed lines from the T3 generation) were grown in soil in a phytotron (8-h light/16-h dark cycle; 21 °C, 70% relative humidity). For stomatal aperture measurements, the leaves of 6-week-old plants were harvested and incubated for 3 h in the light in a solution, 30 mM KCl, 1 mM $CaCl_2$, 5 mM MES-KOH, pH 5.8, with or without 5 µM ABA. Epidermal strips, prepared from the abaxial surface, were analyzed by light microscopy.

Radiolabeling of A. thaliana—Seeds of Ws-2 and *mrp5-1* were germinated and grown on a lab prepared half-strength Murashige and Skoog medium containing 2% agar. The medium was prepared to match the Duchefa (Haarlem, The Netherlands) M0221 product. The inorganic phosphate (KH_2PO_4) content of the medium was 0.625 mM. The seedlings were grown for 12 days at 22 °C under long day conditions (16-h light/8-h dark cycle) in a Sanyo (Biomedical Europe BV) MLR-351 light cabinet at a fluence rate of 120 µmol/m^2/s. The seedlings were subsequently transplanted to agar medium containing either 0.625 mM or 5 µM phosphate and grown for a further 3 days, before transfer to liquid medium with the same phosphate concentration. The seedlings were labeled in 0.5 ml of liquid medium containing 1.125 MBq *myo*-[2-^{3}H]inositol (PerkinElmer Life Sciences; specific activity, 752 GBq/mmol) in the wells of a multiwell plate for the 5-day duration of growth on liquid medium. The medium was supplemented with 0.2 ml of medium lacking radiolabel after 2 days.

RESULTS

Ablation of AtMRP5 Reduces Inositol Hexakisphosphate Level—In a recent paper it was shown for maize that the absence of an ATP-binding cassette protein, *ZmMRP4*, reduced inositol hexa*kis*phosphate accumulation in kernels (15). Phylogenetic studies of ZmMRP4 revealed that AtMRP5 is a very close homologue. Because *AtMRP5* is strongly expressed in seeds, we were interested whether knock-out mutants of this ABC transporter exhibit the same low inositol hexa*kis*phosphate phenotype. To this end, we used two independent T-DNA insertion mutants of *AtMRP5* in their different genetic backgrounds to determine their corresponding inositol hexa*kis*phosphate contents. Inositol hexa*kis*phosphate accumulates as mixed salts of mineral cations in the globoids of specialized vacuoles in *Arabidopsis* (22) as in other seeds (23).

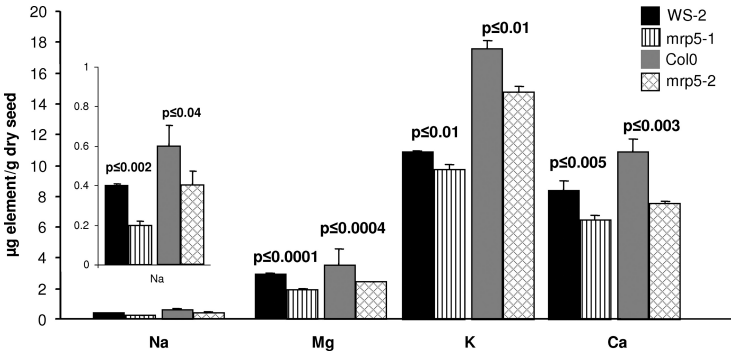

FIGURE 2. **Analysis of cation reserves in seeds of *Arabidopsis*.** Seed content of cations that differ significantly in the two independent AtMRP5 mutants (*mrp5-1* and *mrp5-2*) as compared with their corresponding wild types. The data represent the means and standard deviations of four independent measurements. *Na*, sodium; *Mg*, magnesium; *K*, potassium; *Ca*, calcium.

Seed inositol hexa*kis*phosphate was measured by suppressed ion conductivity (16, 24). Example profiles are shown in Fig. 1*A*, (note that the identity of the inositol hexa*kis*phosphate peak was confirmed for all genotypes by spiking extracts from these genotypes with an inositol hexa*kis*phosphate standard). Fig. 1*A* includes a profile of the biosynthetic mutant *ipk1-1*. On the Dionex AS11 column used, inositol 1,3,4,5,6-penta*kis* phosphate and inositol 3,4,5,6-tetra*kis*phosphate, both of which accumulate in *ipk1-1* elute after inositol hexa*kis*phosphate (24). Our analysis showed that *mrp5-1* and *mrp5-2* mutants do not accumulate inositol hexa*kis*phosphate in the seed; nor do they accumulate lower inositol phosphates, in contrast to *ipk1-1*, which accumulates inositol 1,3,4,5,6-penta*kis*phosphate and inositol 3,4,5,6-tetra*kis*phosphate predominantly among tetra*kis*phosphate species (25). Our measurements of seed inositol hexa*kis*phosphate in the Col0 genetic background of *mrp5-2*, 24.8 ± 4.1 nmol/mg of dry weight, agrees favorably with the data in Ref. 25 (22.3 ± 0.4 nmol/mg). Seed inositol hexa*kis*phosphate was reduced to 0.3 ± 0.6 nmol/mg in the *mrp5-2* mutant (Fig. 1*C*). This value and that of the *mrp5-1* mutant (1.1 ± 1.1 nmol/mg) as compared with its Ws-2 parent (14 ± 3.1 nmol/mg) are significantly greater depletions than that reported for the biosynthesis mutant *ipk1-1*, 3.9 ± 0.4 nmol/mg (25), for which we obtained a value of 4.1 ± 2.9 nmol/mg (data not shown). These data provide genetic evidence that AtMRP5 is required to accumulate inositol hexa*kis*phosphate in seeds. Measurement of inorganic phosphate levels in *mrp5* mutants and their parents (Fig. 1, *A*, *B*, and *D*) revealed that depletions of inositol phosphates in the mutants are accompanied by accumulation of inorganic phosphate. The values obtained for seeds of Col0 (35.9 ± 5.4 nmol/mg of dry weight), *mrp5-2* (103.9 ± 9.4 nmol/mg), Ws-2 (18.5 ± 1.0 nmol/mg), and *mrp5-1* (65.0 ± 4.3 nmol/mg), when compared with *atipk1-1* (30.2 ± 1.2 nmol/mg), indicate that inositol hexa*kis*phosphate transporter mutants show a seed inorganic phosphate accumulation phenotype that is more severe than that of the biosynthetic mutant *atipk1*. The measurements of total phosphorus (Fig. 1*E*) revealed a reduction, relative to wild type, respectively, of 37% in the *mrp5-1* mutant and of 34% in *mrp5-2*. We also attempted to measure inositol hexa*kis*phosphate levels in leaf tissue of *Arabidopsis*. In our hands, the levels were below the level of detection by suppressed ion conductivity, a consequence in part of a number of unidentified anions eluting in the region of inositol hexa*kis*phosphate.

It has already been extensively reported that *mrp5* mutants have pronounced phenotypes, some of which manifest in guard cells (7, 8, 26). Determinations of cations (Fig. 2) that form chelates with inositol hexa*kis*phosphate (phytin) revealed concurrent reductions in mineral composition of seeds of *mrp5-1* and *mrp5-2*. Those minerals that differed significantly between wild type parent and mutant included sodium, which was present only in very low amounts and which was reduced by 41 and 32%. Magnesium was reduced by 34 and 31%, whereas calcium was reduced by 23 and 31%. A small reduction was observed for potassium (17%), whereas no significant reduction was determined for iron, manganese, zinc, nickel, and copper. It is known that several divalent cations strongly bind to phytate, but the species can differ from plant to plant. Our data suggest that iron is not associated with phytate in *Arabidopsis*. Additional data for other minerals that were not found to differ significantly between mutant and wild type genotypes is provided in supplemental Fig. S1.

AtMRP5 Encodes a High Affinity Inositol Hexakisphosphate Transporter—The absence of lower inositol phosphates in the conductivity profiles (Fig. 1, *A* and *B*) contrasts with the biosynthetic mutant *ipk1-1* and with biosynthetic mutants, for example, of barley (27, 28) and maize (29, 30). To test whether AtMRP5 is an inositol hexa*kis*phosphate transporter or a membrane protein participating, but not directly catalyzing inositol hexa*kis*phosphate transport, we expressed AtMRP5 in yeast deficient in the YCF1 ABC transporter. Preliminary transport experiments with different mutants of MRP-type ABC transporters revealed that *ycf1* exhibited only 10–20% of the MgATP-dependent transport activity compared with the corresponding wild type strain (W303). This residual activity might be due to one of the MRP-like genes still present in *ycf1*. We were unsuccessful in our attempts to transform AtMRP5 into double and triple MRP knock-out mutants, so we used AtMRP5-transformed *ycf1* for further analysis. Microsomes were prepared and used to perform studies of [^{33}P]inositol hexa*kis*phosphate uptake. Inositol hexa*kis*phosphate transport was dependent on *AtMRP5* and ATP and was linear with respect to time up to 5.5 min (Fig. 3*A*). In the absence of AtMRP5, a low level of ATP-dependent inositol hexa*kis*phosphate uptake was observed. Expression of AtMRP5 induced a slight increase in inositol hexa*kis*phosphate transport in the absence of ATP, whereas the addition of ATP, to microsomes isolated from AtMRP5-transformed *ycf1* cells, resulted in a 6-fold increase of the ATP-dependent transport activity.

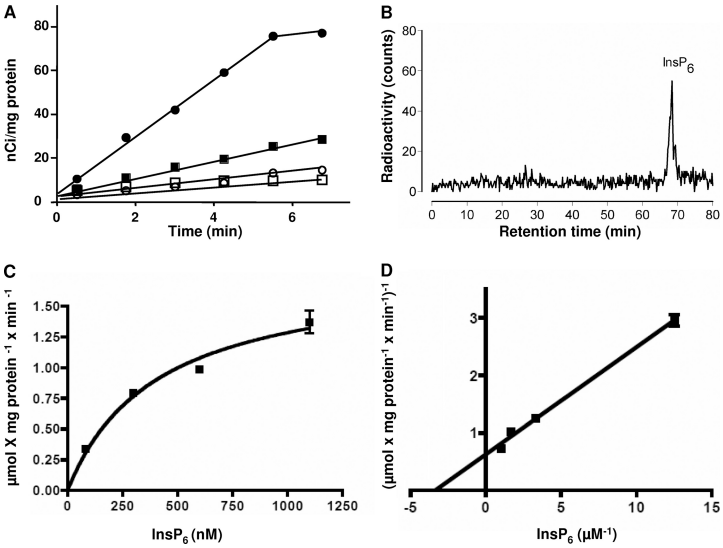

FIGURE 3. **AtMRP5 is a high affinity inositol hexa*kis*phosphate transporter.** *A*, inositol hexa*kis*phosphate uptake into microsomes isolated from yeast *ycf1* mutant cells transformed with an empty vector (pNEV) or with vector harboring *AtMRP5* cDNA (pNEV-MRP5). For non-ATP-dependent uptake, the reaction mix lacked ATP. Transport under all conditions was performed with the same vesicle preparation. *Open square*, pNEV-ATP; *filled square*, pNEV+ATP; *open circle*, pNEV-AtMRP5-ATP; *filled circles*, pNEV-AtMRP5+ATP. The $InsP_6$ concentration used for the time-dependent uptake was 80 nM. *B*, partisphere SAX HPLC analysis of the ^{33}P recovered from filtered and washed microsomes showing the integrity of inositol hexa*kis*phosphate after transport. *C*, inositol hexa*kis*phosphate uptake by microsomes isolated from yeast cells harboring AtMRP5. Uptake velocities were measured at different inositol hexa*kis*phosphate concentrations, as indicated. *D*, a double reciprocal plot was used to determine the K_m value of AtMRP5.

TABLE 1

The effect of ABC transport inhibitors on AtMRP5-mediated inositol hexa*kis*phosphate transport

Yeast microsomes were incubated in the reaction mix with the potential inhibitors at room temperature. After 8 min inositol hexa*kis*phosphate was added to the reaction mix. For the experiments with the nonhydrolyzable ATP analogue (AMPPNP), the 4 mM ATP from the reaction mix was replaced with the equivalent concentration of AMPPNP. For the experiments on ice, tubes containing the reaction mix and the labeled $InsP_6$ were placed on ice immediately after the addition of the yeast microsomes. The $InsP_6$ uptake was terminated by transfer of three aliquots onto 0.45-µm diameter pore size nitrocellulose filters after 5.5 min. The values are corrected for corresponding controls with vesicles isolated from ycf1 yeasts transformed with the empty pNEV vector. The different inhibitors and competitors were always tested using the same vesicle preparation. The reaction mix contained labeled $InsP_6$ at 1.85 kBq/nitrocellulose filter.

Condition	Percentage	Repetitions
+ ATP	100	6
+ AMPPNP	0	2
+ 5 mM NH_4Cl	77.6 ± 15.5	3
+ 150 µM glibenclamide	28.8 ± 17.8	3
+ 1 mM vanadate	62 ± 11.2	3
+ 1 mM probenicide	−12.5 ± 22.9	3
Ice	7.3 ± 7.9	2

Replacement of ATP by the nonhydrolyzable ATP analogue AMPPNP abolished transport (Table 1). This result further confirms that transport of inositol hexa*kis*phosphate is strictly ATP-dependent.

HPLC analysis of the ^{33}P recovered from filtered and washed microsomes revealed that, within the timeframe of our uptake experiments, there was no discernible metabolism of Ins(1,[^{33}P]2,3,4,5,6)P_6 to lower inositol phosphate species, nor to inorganic phosphate (Fig. 3*B*). Thus, the phosphate in the 2-position of inositol hexa*kis*phosphate, and the whole molecule, was metabolically stable. We did not observe phosphorylation of inositol hexa*kis*phosphate, as catalyzed by the KCS1 (31) or VIP1 (32) proteins of *Saccharomyces cerevisiae*. Inclusion of a range of ABC transport inhibitors revealed that the sufonylureas glibenclamide and probenicid had a very strong inhibitory effect on AtMRP5-mediated inositol hexa*kis*phosphate uptake (Table 1). Vanadate, which is an efficient inhibitor for most ABC-type protein-mediated transport processes, had only a partial inhibitory effect. NH_4Cl, which abolishes pH gradients had a very minor inhibitory effect, confirming that the ΔpH plays no or only a minor role in ABC transporter-mediated processes.

Transport experiments performed on ice showed that transport was abolished under these conditions, discounting the possibility that the transport activity reflected binding of inositol hexa*kis*phosphate only, or that transport was a facet of nonspecific permeability of yeast microsomes. A kinetic analysis of inositol hexa*kis*phosphate uptake was undertaken at room temperature. Uptake followed saturation kinetics. A double reciprocal plot of uptake against inositol hexa*kis*phosphate concentration yielded a linear relationship and estimations of K_m of 310 nM in one experiment and 263 nM in another (Fig. 3*C* and supplemental Fig. S2). V_{max} values reflecting the expression level of AtMRP5 were estimated at 1.6–2.5 µmol min^{-1} mg^{-1} microsome protein (Fig. 3*C*). The ATP-dependent inositol hexa*kis*phosphate transport activity from nontransformed yeast microsomes corresponded only to 10–20% of that observed with AtMRP5 expressing yeast. Therefore, the obtained K_m values should reflect closely the characteristics of AtMRP5-mediated transport.

To characterize the substrate specificity of AtMRP5, we performed competition experiments with a range of inositol polyphosphates identified in plants (Table 2). At a concentration corresponding to a 2-fold K_m of inositol hexa*kis*phosphate (600 nM), no significant inhibition was observed for Ins(1,4,5)P_3, Ins(1,3,4,6)P_4, and Ins(1,4,5,6)P_4. With Ins(1,3,4,5,6)P_5, transport was reduced by 20%. *Scyllo*-inositol hexa*kis*phosphate did not inhibit transport at 600 nM, suggesting that substrate binding exhibits stereospecificity and is not exclusively a consequence of high density of negative charge on the substrate. Estradiol glucuronide, a com-

TABLE 2

The effect of inositol polyphosphates on AtMRP5-mediated inositol hexa*kis*phosphate transport

The putative inhibitors and/or competitors were added to the reaction mix consisting of transport buffer, 1 mM dithiothreitol, 5 mM ATP, 10 mM $MgCl_2$, 10 mM creatine-phosphate, and 100 μg/ml creatine kinase at the concentration indicated above. Yeast microsomes were added to start the transport assay. The assays were performed at room temperature. After 5.5 min, inositol hexa*kis*phosphate uptake was terminated by the transfer of three aliquots/repetition onto 0.45-μm-diameter pore size nitrocellulose filters. The putative inhibitors and/or competitors were always tested using the same vesicle preparation. ATP-dependent AtMRP5-mediated transport was considered as 100%. The reaction mix contained labeled inositol hexa*kis*phosphate at 1.85 kBq/nitrocellulose filter.

Condition	Percentage	Repetitions
+ ATP	100	6
+ 600 nM		
$Ins(1,4,5)P_3$	111.7 ± 17.6	3
$Ins(1,3,4,6)P_4$	104.1 ± 18.4	3
$Ins(1,4,5,6)P_4$	100.6 ± 16.8	3
$Ins(1,3,4,5,6)P_5$	80.5 ± 6.6	2
Scyllo $InsP_6$	119.8 ± 12.5	3
$Ins(1,2,3,4,5,6)P_6$	52.7 ± 1.8	2
Estradiol glucuronide	122.6 ± 16.2	3
+1200 nM		
$Ins(3,4,6)P_3$	157.3 ± 3.8	3
$Ins(1,3,4,6)P_4$	100.8 ± 30.3	2
$Ins(1,4,5,6)P_4$	80.2 ± 20.2	3
$Ins(1,3,4,5,6)P_5$	61.0 ± 7.1	2
Scyllo $InsP_6$	57.7 ± 13.6	2
$Ins(1,2,3,4,5,6)P_6$	0 ± 0	2
Estradiol glucuronide	92.4 ± 4.9	3

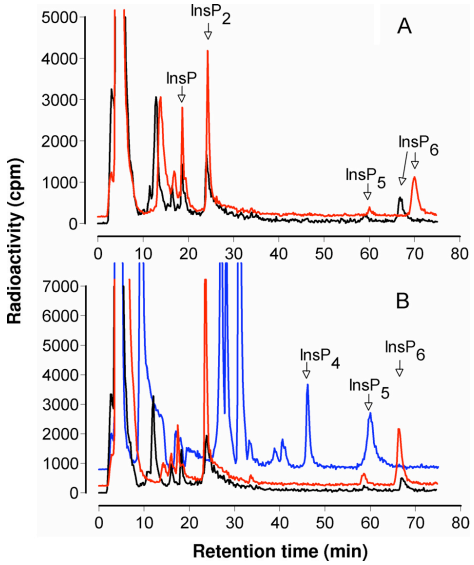

FIGURE 4. **Profiles of inositol phosphates from [^{3}H]inositol-labeled seedlings.** *A*, traces for Ws-2 labeled with low phosphate (*black line*) and high phosphate (*red line*). *B*, traces for *mrp5-1* labeled with low phosphate (*black line*) and high phosphate (*red line*) and for *ipk1-1* labeled with high phosphate (*blue line*). Note that the retention time of inositol phosphates can vary; $InsP_6$ was confirmed for all genotypes by spiking parallel samples with an $InsP_6$ standard. The *traces* for *mrp5-1* and Ws-2 labeled with high phosphate and the *ipk1-1* trace have been offset on the *y* axis to aid visualization.

pound shown to be transported by AtMRP5 (26), had a slight stimulatory effect. Increasing the concentration of the inhibitors to 1200 nM resulted in an ~40% inhibition of *myo*-inositol hexa*kis*phosphate uptake by both $Ins(1,3,4,5,6)P_5$ and *scyllo*-inositol hexa*kis*phosphate. Interestingly, at this concentration $Ins(1,4,5)P_3$ exhibited a stimulatory effect of about 50%. From this result it is tempting to speculate that $Ins(1,4,5)P_3$ at a higher concentration can accelerate the depletion of the cytosolic $InsP_6$ and thus the termination of the $InsP_6$ signaling pathway. In summary, these data ascribe novel function to AtMRP5, that of a specific high affinity *myo*-inositol hexa*kis*phosphate transporter.

The Inositol Phosphate Metabolism of atmrp5 Mutants Is Sensitive to External Phosphate—In the context of reduced vacuolar deposition of inositol hexa*kis*phosphate and accumulation of inorganic phosphate, the *atmrp5* transporter mutants potentially afford the opportunity to assess the interplay, previously untested, of intracellular inositol phosphate transport and inositol phosphate metabolism. Inositol hexa*kis*phosphate synthesis is responsive to phosphate supply in suspension culture of *Arabidopsis* (33). We labeled Ws-2 and *mrp5-1* seedlings with inositol and analyzed the responsiveness of inositol hexa*kis*phosphate synthesis to phosphate concentration in the growth and labeling media. Our analysis (Fig. 4) revealed that the profile of ^{3}H-labeled peaks of increasing phosphorylation, from inositol up to inositol hexa*kis*phosphate, were similar for Ws-2 and *mrp5-1* mutants treated and labeled in low phosphate. The absence of major peaks of label in the inositol 1,4,5-trisphosphate to 1,3,4,5,6-penta*kis*phosphate region is typical of plant tissues. Material eluting before the InsP peak includes inositol and, likely, cell wall sugars derived from inositol. In a typical experiment, at 5 μM phosphate, the label recovered in inositol penta*kis*phosphate and inositol hexa*kis*phosphate peaks were, respectively, 0.25 and 0.96% for Ws-2 and 0.07 and 0.60% for *mrp5-1*. These results and the seed inositol phosphate data (Fig. 1) suggest that the control exerted by AtMRP5 on inositol hexa*kis*phosphate accumulation in seeds or whole seedlings is not manifest as an accumulation of metabolic precursors. Moreover, seedlings of Ws-2 and *mrp5-1* grown and labeled on high phosphate accumulated ~2-fold more label in inositol hexa*kis*phosphate than those transferred to and labeled in low phosphate media. Similar conclusions have been drawn from measurements of inositol hexa*kis*phosphate in suspension cultures of *Catharantheus roseus* and *Arabidopsis* grown in low and high phosphate, with *Arabidopsis* showing weaker responses to phosphate than *C. roseus* (33). In our experiments, the proportions of label recovered in inositol penta*kis*phosphate and inositol hexa*kis*phosphate were 0.15 and 1.89% for Ws-2 and 0.25% and 1.46% for *mrp5-1* grown and labeled on high phosphate. These data show that, in respect to metabolic flux from inositol to inositol hexa*kis*phosphate, the *mrp5-1* mutant is responsive to environmental phosphate status like its wild type Ws-2 parent. We conclude that, unlike the *ipk1-1* mutant, which is deficient in recognition of external phosphate (25), *mrp5* mutants are not defective in sensing environmental phosphate. The data presented above indicate that AtMRP5 makes a dominant contribution to accumulation of inositol hexa*kis*phosphate in seeds of *Arabidopsis*. Although we are not aware of gene expression studies of inositol hexa*kis*phosphate accumulation in *Arabidopsis*, of the biosynthetic gene prod-

ucts, IPK1 has a dominant contribution to inositol hexa*kis*phosphate accumulation (25). We undertook expression analysis of the effect of mutation of AtMRP5 on transcript levels of AtIPK1 and of four members of the inositol tris/tetra*kis*phosphate kinase family whose contribution to inositol hexa*kis*phosphate synthesis, while undefined in *Arabidopsis* (34), is anticipated from studies of maize (30). The data presented in the supplementary information (supplemental Fig. S3) indicate that mutation of *AtMRP5* was without effect on *IPK1* or *ITPK1* (At5G16760) in either background, whereas a doubling of the other transcripts was evident in *mrp5-1* only.

Atmrp5 Mutants Show Defective Stomatal Responses That Are Partially Relieved by Guard Cell-targeted Expression of AtMRP5—The foregoing data point not only to a novel inositol hexa*kis*phosphate transport function for AtMRP5 but also to a dominant contribution to inositol hexa*kis*phosphate accumulation. ABC transport proteins have not been extensively characterized in plants, but among them AtMRP5 and AtABCB14 have been shown to exert control over a number of cellular targets, particularly ion channels whose regulation underlies the control of stomatal function. Because we have shown that inositol hexa*kis*phosphate is a physiological regulator of vacuolar (Ca^{2+}-permeable) and plasma membrane (inward rectifying K^+) conductances (13, 14), we sought to determine a role for AtMRP5 in guard cell function. We tested the effectiveness of ABA as an inhibitor of stomatal opening in response to light, because this response is a well documented physiological indicator of MRP5 function, one to which anion channel activity contributes markedly. The data of Fig. 5*C* were obtained from epidermal peels of wild type (Ws-2), the *mrp5-1* mutant, and a series of lines of *mrp5-1* that had been independently transformed with an *AtMRP5* construct driven from a promoter, MYB60, that is strongly expressed in guard cells but not in epidermal cells (Fig. 5, *A* and *B*). Stomatal opening was strongly inhibited by ABA in Ws-2 but not in the *mrp5-1* mutant (Fig. 5*C*). Significantly, transgenic expression of AtMRP5 restored ABA responsiveness to the *mrp5-1* mutant, a result that was confirmed for several independent transgenic lines. Detailed physiological analyses of the above mentioned transgenic lines revealed that guard cell-targeted expression of AtMRP5 did not restore wild type seed $InsP_6$ content (Fig. 5*D*) and did not restore the root phenotype (supplemental Fig. S4).

It remains a matter of debate whether the observed stomatal phenotype of *mrp5-1* is the result of an interaction between AtMRP5 and unknown proteins and/or the AtMRP5-mediated transport of a specific molecule. Therefore, to get further insights as to whether a functional transporter is required, site-directed mutagenesis of AtMRP5 was undertaken, and the mutated cDNAs driven by the CaMV35S promoter were transformed into *mrp5-1* (supplemental Fig. S5*A*). The *mrp5-1* related phenotypes (seed $InsP_6$ content, root length, drought resistance, and stomatal aperture) were analyzed for all constructs in the T3 generation. Most of mutants showed an intermediate phenotype as compared with Ws-2 and *mrp5-1* for all traits. Only those plants with either a D771A or a D1429A exchange in the Walker B domain of NBD1 or NBD2 behaved like *mrp5-1* (supplemental Fig. S5, *b–e*). Because the Walker B

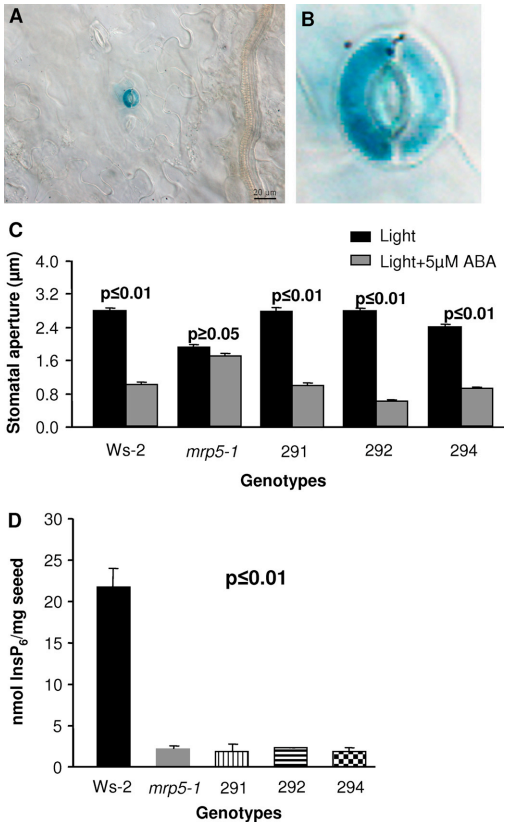

FIGURE 5. **Guard cell-targeted expression of AtMRP5 restores stomatal phenotype in AtMRP5 mutant.** *A* and *B*, the MYB60 promoter targets *GUS* exclusively to guard cells. *C*, the *mrp5-1* mutant is insensitive to ABA (ABA inhibits opening of stomata in response to light). The *MYB60::AtMRP5* transgene restores ABA sensitivity to *mrp5-1*. The results for Ws-2, *mrp5-1*, and three independent transgenic T3 lines are shown. At least 200 stomates of abaxial epidermal strips were measured for each genotype. Two independent experiments were performed, and three additional T3 lines of the transgenic gave the same results (data not shown). The *error bars* represent the S.E. *D*, the *MYB60::AtMRP5* transgene does not complement the seed inositol hexa*kis*phosphate content of *mrp5-1*. The data represent the means and standard deviations of three independent measurements. For *C*, the *p* value indicates the confidence of significance between light treatment and light+ABA treatment within the same genotype. For *D*, the *p* value indicates the confidence of significance between wild type and the four other genotypes.

domain is known to be essential for the transport activity of most ABC transporters (35), this result suggests that AtMRP5-mediated $InsP_6$ uptake and the stomatal phenotype are both dependent on a functional AtMRP5.

DISCUSSION

Inositol polyphosphates and inositol pyrophosphates contribute to diverse cell biological and developmental phenomena including activated exocytosis (36), mRNA export (37, 38), cell cycle activities (39), and establishment of left-right asymmetry

of organ development in zebra fish (40). In plants, inositol hexa*kis*phosphate mobilizes calcium and inhibits the inward rectifying K^+ conductance of guard cells (13, 14).

Despite all of these elaborations of higher inositol polyphosphate function, remarkably little is known of the compartmentation of inositol polyphosphate synthesis or of the contribution of compartmentation to the roles identified above. Interestingly, inositol hexa*kis*phosphate is a component of basal resistance to fungal, bacterial, and viral pathogens in *Arabidopsis*, with an indication that a discrete subcellular pool of inositol hexa*kis*phosphate contributes to these phenomena (41). In higher plants, inositol hexa*kis*phosphate accumulates as mixed salts of alkali and other metal cations in the globoids of specialized vacuoles of storage tissues (23). By corollary, inositol hexa*kis*phosphate is a major component of the laminal layer of hydatid cysts, the reproductive stage of the animal parasite *Echinococcus granulosus* (24). Both of these examples imply vectorial transport of inositol hexa*kis*phosphate or a precursor across cellular membranes, noncytosolic synthesis of inositol hexa*kis*phosphate, and/or trafficking of membrane-bound inositol hexa*kis*phosphate. These possibilities are all highlighted by the apparent enigma that human multiple inositol polyphosphate phosphatase localizes within the lumen of the endoplasmic reticulum, whereas its inositol phosphate substrates are considered to be exclusively cytosolic (42).

Our elaboration of AtMRP5 as an inositol hexa*kis*phosphate transporter, taken with the analysis of *ZmMRP4* mutants (15), provides a mechanistic explanation of the accumulation of inositol hexa*kis*phosphate in storage tissues of plants that differs from established conventions. Previous explanations of inositol hexa*kis*phosphate accumulation in membrane-bound protein bodies, including the aleurone bodies of cereals, are tightly linked to morphological examination of vesicle trafficking phenomena as ontogenetic explanations of the origins of protein bodies themselves (43, 44). We are reminded of analysis of natural variation of inositol hexa*kis*phosphate accumulation in *Arabidopsis*, which mapped a trait in inositol hexa*kis*phosphate accumulation to a 99-kb region that harbored a tonoplast membrane ATPase G-subunit (16). Although the exact locus of the trait was not identified, one possible explanation of the variation in inositol hexa*kis*phosphate is that accumulation of inositol hexa*kis*phosphate is dependent on vacuolar transport processes.

We now show that two distinct insertion mutants of *AtMRP5* (Col0 and Ws-2) in different, genetic backgrounds both display a low phytic acid phenotype in seed tissue. We show that the low inositol hexa*kis*phosphate seed phenotype is associated with alterations of mineral cation and phosphate status in both genetic backgrounds. The low seed phytate phenotype is a direct consequence of the missing transport activity. Our data demonstrate that AtMRP5 is a specific, high affinity inositol hexa*kis*phosphate transporter.

Beyond our identification of the molecular identity of an inositol phosphate transporter, our analysis reveals, in the context of existing literature, that disruption of a gene encoding an inositol hexa*kis*phosphate transporter contributes to stomatal biology. Because we show that MRP5 expression, exclusively, in guard cells of the *mrp5-1* mutant restores sensitivity of these cells to ABA, we hypothesize that AtMRP5 is involved in stomatal regulation because of its capacity to transport inositol hexa*kis*phosphate. The physiology of guard cells is dominated by the multitude of ion channels and transporters whose

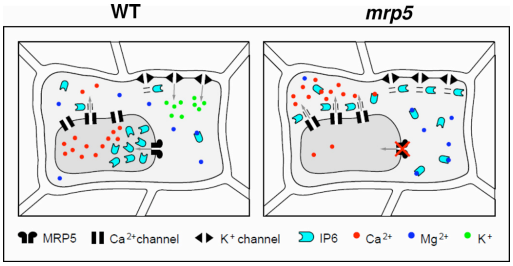

FIGURE 6. **Hypothetical model that links AtMRP5, $InsP_6$ signaling and guard cell movements.** In wild type plants, inositol hexa*kis*phosphate stimulates the release of Ca^{2+} by specific channels and inhibits the K^+ inward channel. To avoid continuous $InsP_6$ signaling, inositol hexa*kis*phosphate has to be transported into the vacuole by AtMRP5. AtMRP5 mutant plants are impaired in the export of $InsP_6$ into the vacuole. Increased concentrations of cytosolic $InsP_6$ might complex divalent cations or induce continuous Ca^{2+} release, thus disturbing Ca^{2+}-dependent signaling pathways. Furthermore, during the light period, increased $InsP_6$ levels may reduce K^+ uptake into guard cells by inhibiting K^+ inward rectifying channels.

regulation is integrated in this specialized epithelial cell, with tonoplast transport playing a central role (2). It may be significant that the fast and slow Ca^{2+}-permeable conductances of the tonoplast are both targets of inositol hexa*kis*phosphate (13). For the meantime, in the absence of direct studies of electrophysiological targets of inositol hexa*kis*phosphate in our transgenics of *mrp5-1*, it remains plausible that perturbation of cytosolic and/or vacuolar inositol hexa*kis*phosphate concentration because of the absence of its transporter will necessarily deregulate the transport processes that underlie guard cell physiology (Fig. 6).

In consideration of tonoplast function, we suggested in a first report (8) that Ca MV35S promoter-driven AtMRP5-GFP was localized to the plasma membrane of root cells. It is possible that plasma membrane localization is an ectopic consequence of MRP5 overexpression. Indeed, proteomic analysis predicts AtMRP5 to reside in the vacuolar membrane (45). The latter interpretation is consistent with the low seed inositol hexa*kis*phosphate phenotype of *mrp5-1* and *mrp5-2* mutants; $InsP_6$ is recognized to accumulate in membrane-bound protein bodies of vacuolar nature. To further address the physiological location of AtMRP5, we have examined the location of AtMRP5 expressed under the control of its native promoter. No GFP signal was detected when plants were cultivated under control conditions. Because transcriptomic studies indicated that *AtMRP5* transcript levels are increased upon drought stress (46), we subjected *mrp5-1* plants expressing AtMRP5 under the control of its native promoter to 14 days of drought stress. Under such conditions, a weak fluorescence signal associated with the vacuolar membrane was detected (supplemental Fig. S6).

These localization studies raise the intriguing question of how a vacuolar inositol hexa*kis*phosphate transporter could affect guard cell signaling and the plasma membrane anion channel activity. A hypothetical model linking the phenomena mentioned above is presented in Fig. 6. The impaired AtMRP5-dependent transport of inositol hexa*kis*phosphate into the vacuole could lead to an increase in cytosolic $InsP_6$, which could act either by complexing divalent cations such as Mg^{2+} and Ca^{2+} or triggering a continuous efflux of Ca^{2+} into the cytosol by an $InsP_6$-regulated channel. This could lead in both cases to a dis-

turbance of Ca^{2+}-dependent signaling pathways. This hypothesis could explain the impaired ABA and Ca^{2+} signaling observed in *mrp5* mutants. However, it cannot be excluded that the impaired stomatal aperture observed in the *mrp5* mutants during the light phase is not additionally the result of increased $InsP_6$ binding to unidentified targets or Ca^{2+}-dependent inhibition of the K^+ inward channel (14).

In conclusion, our identification of a high affinity inositol hexa*kis*phosphate transport associated with the tonoplast membrane adds to the diversity of functions assigned to the ABC transporter class of membrane proteins and also answers a long standing question of how inositol phosphates traverse membranes. Given the ubiquity of this class of proteins, we can anticipate that inositol phosphate transport will contribute not only to the regulation of diverse cellular signaling phenomena, perhaps to human disease, but also potentially to the acquisition of environmental inositol hexa*kis*phosphate, which comprises one of the most abundant sources of organic phosphate in the environment (47).

Acknowledgments—We are grateful to Thomas Flura (Eidgenössische Technische Hochschule, Zürich, Switzerland) for the inductively coupled plasma measurements and to Maik Hadorn for drawing the model.

REFERENCES

1. Hetherington, A. M. (2001) *Cell* **107,** 711–714
2. MacRobbie, E. A. (1998) *Philos. Trans. R. Soc. Lond. B Biol. Sci.* **353,** 1475–1488
3. Lebaudy, A., Vavasseur, A., Hosy, E., Dreyer, I., Leonhardt, N., Thibaud, J. B., Véry, A. A., Simonneau, T., and Sentenac, H. (2008) *Proc. Natl. Acad. Sci. U.S.A.* **105,** 5271–5276
4. Vahisalu, T., Kollist, H., Wang, Y. F., Nishimura, N., Chan, W. Y., Valerio, G., Lamminmäki, A., Brosché, M., Moldau, H., Desikan, R., Schroeder, J. I., and Kangasjärvi, J. (2008) *Nature* **452,** 487–491
5. Negi, J., Matsuda, O., Nagasawa, T., Oba, Y., Takahashi, H., Kawai-Yamada, M., Uchimiya, H., Hashimoto, M., and Iba, K. (2008) *Nature* **452,** 483–486
6. Lee, M., Choi, Y., Burla, B., Kim, Y. Y., Jeon, B., Maeshima, M., Yoo, J. Y., Martinoia, E., and Lee, Y. (2008) *Nat. Cell Biol.* **10,** 1217–1223
7. Klein, M., Perfus-Barbeoch, L., Frelet, A., Gaedeke, N., Reinhardt D., Mueller-Roeber, B., Martinoia, E., and Forestier, C. (2003) *Plant J.* **33,** 119–129
8. Suh, S. J., Wang, Y. F., Frelet, A., Leonhardt, N., Klein, M., Forestier, C., Mueller-Roeber, B., Cho, M. H., Martinoia, E., and Schroeder, J. I. (2007) *J. Biol. Chem.* **282,** 1916–1924
9. Schwiebert, E. M., Egan, M. E., Hwang, T. H., Fulmer, S. B., Allen, S. S., and Cutting, G. R. (1995) *Cell* **81,** 1063–1073
10. Yang, L., Reece, J., Gabriel, S. E., and Shears, S. B. (2006) *J. Cell Sci.* **119,** 1320–1328
11. Vajanaphanich, M., Schultz, C., Rudolf, M. T., Wasserman, M., Enyedi, P., Craxton, A., Shears, S. B., Tsien, R. Y., Barrett, K. E., and Traynor-Kaplan, A. (1994) *Nature* **371,** 711–714
12. Mitchell, J., Wang, X., Zhang, G., Gentzsch, M., Nelson, D. J., and Shears, S. B. (2008) *Curr. Biol.* **18,** 1600–1605
13. Lemtiri-Chlieh, F., MacRobbie, E. A., Webb, A. A., Manison, N. F., Brownlee, C., Skepper, J. N., Chen, J., Prestwich, G. D., and Brearley, C. A. (2003) *Proc. Natl. Acad. Sci. U.S.A.* **100,** 10091–10095
14. Lemtiri-Chlieh, F., MacRobbie, E. A., and Brearley, C. A. (2000) *Proc. Natl. Acad. Sci. U.S.A.* **97,** 8687–8692
15. Shi, J., Wang, H., Schellin, K., Li, B., Faller, M., Stoop, J. M., Meeley, R. B., Ertl, D. S., Ranch, J. P., and Glassman, K. (2007) *Nat. Biotechnol.* **25,** 930–937
16. Bentsink, L., Yuan, K., Koornneef, M., and Vreugdenhil, D. (2003) *Theor. Appl. Genet.* **106,** 1234–1243
17. Tommasini, R., Evers, R., Vogt, E., Mornet, C., Zaman, G. J., Schinkel, A. H., Borst, P., and Martinoia, E. (1996) *Proc. Natl. Acad. Sci. U.S.A.* **93,** 6743–6748
18. Sweetman, D., Johnson, S., Caddick, S. E., Hanke, D. E., and Brearley, C. A. (2006) *Biochem. J.* **394,** 95–103
19. Cominelli, E., Galbiati, M., Vavasseur, A., Conti, L., Sala, T., Vuylsteke, M., Leonhardt, N., Dellaporta, S. L., and Tonelli, C. (2005) *Curr. Biol.* **15,** 1196–1200
20. Curtis, M. D., and Grossniklaus, U. (2003) *Plant Physiol.* **133,** 462–469
21. Clough, S. J., and Bent, A. F. (1998) *Plant J.* **16,** 735–743
22. Otegui, M. S., Capp, R., and Staehelin, L. A. (2002) *Plant Cell* **14,** 1311–1327
23. Lott, J. N. (1984) in *Seed Physiology* (Murray, D. R., ed) Vol. 1, pp. 139–166, Academic Press, New York
24. Casaravilla, C., Brearley, C., Soulé, S., Fontana, C., Veiga, N., Bessio, M. I., Ferreira, F., Kremer, C., and Díaz, A. (2006) *FEBS J.* **273,** 3192–3203
25. Stevenson-Paulik, J., Bastidas, R. J., Chiou, S. T., Frye, R. A., and York, J. D. (2005) *Proc. Natl. Acad. Sci. U.S.A.* **102,** 12612–12617
26. Gaedeke, N., Klein, M., Kolukisaoglu, U., Forestier, C., Müller, A., Ansorge, M., Becker, D., Mamnun, Y., Kuchler, K., Schulz, B., Mueller-Roeber, B., and Martinoia, E. (2001) *EMBO J.* **20,** 1875–1887
27. Hatzack, F., Hübel, F, Zhang, W., Hansen, P. E., and Rasmussen, S. K. (2001) *Biochem. J.* **354,** 473–480
28. Dorsch, J. A., Cook, A., Young, K. A., Anderson, J. M., Bauman, A. T., Volkmann, C. J., Murthy, P. P., and Raboy, V. (2003) *Phytochemistry* **62,** 691–706
29. Raboy, V., Gerbasi, P. F., Young, K. A., Stoneberg, S. D., Pickett, S. G., Bauman, A. T., Murthy, P. P., Sheridan, W. F., and Ertl, D. S. (2000) *Plant Physiol.* **124,** 355–368
30. Shi, J., Wang, H., Wu, Y., Hazebroek, J., Meeley, R. B., and Ertl, D. S. (2003) *Plant Physiol.* **131,** 507–515
31. Saiardi, A., Erdjument-Bromage, H., Snowman, A. M., Tempst, P., and Snyder, S. H. (1999) *Curr. Biol.* **9,** 1323–1326
32. Mulugu, S., Bai, W., Fridy, P. C., Bastidas, R. J., Otto, J. C., Dollins, D. E., Haystead, T. A., Ribeiro, A. A., and York, J. D. (2007) *Science* **316,** 106–109
33. Mitsuhashi, N., Ohnishi, M., Sekiguchi, Y., Kwon, Y. U., Chang, Y. T., Chung, S. K., Inoue, Y., Reid, R. J., Yagisawa, H., and Mimura, T. (2005) *Plant Physiol.* **138,** 1607–1614
34. Sweetman, D., Stavridou, I., Johnson, S., Green, P., Caddick, S. E., and Brearley, C. A. (2007) *FEBS Lett.* **581,** 4165–4171
35. Frelet, A., and Klein, M. (2006) *FEBS Lett.* **580,** 1064–1084
36. Illies, C., Gromada, J., Fiume, R., Leibiger, B., Yu, J., Juhl, K., Yang, S. N., Barma, D. K., Falck, J. R., Saiardi, A., Barker, C. J., and Berggren, P. O. (2007) *Science* **318,** 1299–1302
37. York, J. D., Odom, A. R., Murphy, R., Ives, E. B., and Wente, S. R. (1999) *Science* **285,** 96–100
38. Odom, A. R., Stahlberg, A., Wente, S. R., and York, J. D. (2000) *Science* **287,** 2026–2029
39. Lee, Y. S., Mulugu, S., York, J. D., and O'Shea, E. K. (2007) *Science* **316,** 109–112
40. Sarmah, B., Latimer, A. J., Appel, B., and Wente, S. R. (2005) *Dev. Cell* **9,** 133–145
41. Murphy, A. M., Otto, B., Brearley, C. A., Carr, J. P., and Hanke, D. E. (2008) *Plant J* **56,** 638–652
42. Craxton, A., Caffrey, J. J., Burkhart, W., Safrany, S. T., and Shears, S. B. (1997) *Biochem. J.* **328,** 75–81
43. Adams, C., Norby, S. W., and Rinne, R. W. (1985) *Crop Sci.* **25,** 255–262
44. Marty, F. (1997) in *Advances in Botanical Research: The Plant Vacuole* (Leigh, R. A., and Sanders, D., eds) Vol. 25, pp. 1–42, Academic Press, London
45. Jaquinod, M., Villiers, F., Kieffer-Jaquinod, S., Hugouvieux, V., Bruley, C., Garin, J., and Bourguignon, J. (2007) *Mol. Cell. Proteomics* **6,** 394–412
46. Zimmermann, P., Hirsch-Hoffmann, M., Hennig, L., and Gruissem, W. (2004) *Plant Physiol.* **136,** 2621–2632
47. Turner, B. L., Papházy, M. J., Haygarth, P. M., and McKelvie, I. D. (2002) *Philos. Trans. R. Soc. London B Biol. Sci.* **357,** 449–469

3.2. Supplementary Material

THE ARABIDOPSIS ATP-BINDING CASETTE PROTEIN ATMRP5/ATABCC5 IS A HIGH-AFFINITY INOSITOL HEXA*KIS*PHOSPHATE TRANSPORTER INVOLVED IN GUARD CELL SIGNALING AND PHYTATE STORAGE

The following supplementary material is available online:

Experimental Procedures

Real time PCR- Total RNA was extracted from frozen plant material using an RNeasy plant mini kit, incorporating an RNAse-free DNAse step (Qiagen). 1µg of RNA, quantified with a NanoDrop 1000 (Thermo Scientific), was used for cDNA synthesis using random hexamer primers and Superscript II reverse transcriptase (Invitrogen, UK). Real-time PCR was performed with non-inventoried small scale TaqMan Gene Expression Assays, each containing a FAM dye-labelled TaqMan MGB probe and a PCR primer pair (Applied Biosystems). Each reaction of 25 µl volume contained the equivalent of 5 ng of reverse transcribed RNA, 33% TaqMan PCR Master Mix (Applied Biosystems), 200 nM each of the forward and reverse primer, and 100 nM of probe. Reactions were performed in microtiter plates in an ABI Prism 7900 Fast Real-Time PCR System (Applied Biosystems), according to the manufacturer's protocol. Standard curves were prepared for all samples in the range equivalent to 20–0.625 ng RNA. Expression levels were quantified relative to the gene *ACTIN2*. The details of the TaqMan Gene Expression Assays are shown below.
Small scale TaqMan Gene Expression Assays used for real-time PCR

Gene	AGI Number	Assay ID
ACTIN2	At3G18780	At02329915_s1
ITPK1	At5G16760	At02200756_g1
ITPK2	At4G08170	At02210121_g1
ITPK3	At4G33770	At02249483_g1
ITPK4	At2G43980	At02173051_g1
IPK1	At5G42810	At02314554_g1

Note, the gene names for ITPKs are those designated at the tair website http://www.arabidopsis.org/news/news.jsp. We have previously (1) *FEBS lett* 581: 4165-4171. designated ITPK2, At4G33770; and ITPK3, At4G08170.

Site-directed mutagenesis-Single amino acid exchanges in conserved domains of AtMRP5 (Fig S5A) were generated using the QuikChange®Multi Site-Directed Mutagenesis Kit (Stratagene) using the following primers bearing mismatching bases (in bold characters):
For NBD1:
Walker A_MRP5KA1: GGC ACA GTT GGC TCT GGA **GCA** TCA AGT TTT ATC TCT TGC
Walker B_MRP5DA1: GCT GAC ATT TAT TTA CTA **GCC** GAC CCT TTT AGT GCT C
ABC signature_MRP5RA1: CAG CGT GTA CAA CTT GCA **GCG** GCA TTA TAT CAA GAT GC
For NBD2:
Walker A_MRP5KA2: GGG CGA ACG GGA AGC GGA **GCG** TCG ACT TTG ATT CAA GCT
Walker B_MRP5DA2: GCC AAA ATA CTT GTT CTT **GCT** GAA GCA ACA GCA TCGG
ABC signature_MRP5RA2: CAG CTT GTG TCA CTT GGA **GCA** GCA TTA CTG AAA CAA GCC
Plasmid DNA of individual clones was isolated and sequenced to confirm the presence of the desired mutations. Mutated AtMRP5 cDNAs were cloned into the pMDC83 vector (2). Thus, the various mutated AtMRP5 cDNAs had a C-terminal GFP tag, and the AtMRP5-GFP was driven by the CaMV35S promoter. The obtained construct pCaMV35S::AtMRP5(mutated)-GFP was used to transform *mrp5-1* mutants by the floral dipping method using *Agrobacterium* GV3101 (3). Seeds were harvested and selected on $^1/_2$MS agar plates containing 1% sucrose and 25 µg/ml Hygromycin until reaching the T3 generation. Major difficulties were encountered while performing Western blots. Probably due to a very low expression we failed detecting the GFP signal, both via localization and Western blotting. Thus, all transformants (T1, T2, T3) were analyzed at DNA and RNA level. Transcripts levels were comparable to that of the wild type. cDNAs corresponding to the mutated regions were cloned and sequenced. We can state, that at least at DNA and RNA level the

mutagenized AtMRP5 cDNAs are integrated in the plant genome. Homozygous T3 plants having single amino acid exchanges in the conserved domains were subjected to a series of physiological experiments in order to monitor how their phenotype changes as compared to *mrp5-1* and Ws-2, *i.e*. stomata aperture upon treatment with ABA, drought resistance, water loss, root length, seed InsP6 content.

Subcellular localization of AtMRP5- A 1.9 kb long AtMRP5 promoter sequence was amplified from Arabidopsis genomic DNA using the following primers: promMRP5-s 5'-CCCAAGCTTGTGGAAGAACGTAGAATTCCC-3', and promMRP5-as 5'-TCCACTAGTCATGATCGGGAAAGATTTGTG-3'. By excising the CaMV35S promoter from the pMDC83 vector (2), the amplified AtMRP5 promoter was fused to the already cloned *AtMRP5–GFP* fusion. The resulting *pAtMRP5*::AtMRP5-GFPconstruct was used to transform *mrp5-1* mutants by the floral dipping method using *Agrobacterium* GV3101 (3). Seeds were harvested and selected on $^1/_2$MS 1% sucrose containing 25 µg/ml Hygromycin until T3 was reached. Homozygous T3 plants were grown for 4 weeks in the phytotron under normal growth conditions (8h dark /16 h light cycle; 21ºC, 70% relative humidity). No GFP signal was detected in vacuoles released from protoplasts isolated from those plants. As next, the plants were subjected to 14 days drought stress (8h dark /16 h light cycle; 21ºC, 70% relative humidity, no watering). Vacuoles were released by osmotic lysis from leaf protoplasts isolated from drought stressed plants. Images were captured by laser scanning confocal microscopy (DM IRE2; Leica Microsystems) using the 63X magnification objective, and an appropriate zoom.

Legends for the supplementary figures:

Figure S1 Seed content of elements that do not significantly differ in the two independent AtMRP5 mutants as compared to their corresponding wild types. The data represent the mean of four independent measurements. Error bars correspond to the standard deviation.

Figure S2 AtMRP5 encodes for a high affinity inositol hexa*kis*phosphate transporter. A second experiment of inositol hexa*kis*phosphate uptake by microsomes isolated from yeast cells harbouring AtMRP5 was performed. Uptake velocities were measured at different inositol hexa*kis*phosphate concentrations, as indicated.

Figure S3 Expression analysis of genes of inositol polyphosphate synthesis. Real-Time PCR based expression levels of IPK1 and of four members of the inositol tris/tetra*kis*phosphate kinase family in the two AtMRP5 mutants and their corresponding wild types. Error bars indicate the SD of three independent experiments. The gene names for ITPKs are those designated at the tair website http://www.arabidopsis.org/news/news.jsp

Figure S4 Guard-cell targeted expression of AtMRP5 does not restore *mrp5-1*-type root phenotype to wild type status. Seedlings of wild type, *mrp5-1* and independent transgenic T3 lines harbouring AtMRP5 driven by the MYB60 promoter were grown on vertically oriented 1/2 MS agar plates for 10 days prior to root analysis.

Figure S5 Site-directed mutagenesis of MRP5 was undertaken to elucidate the domains which play a key role for the functionality of the transporter. (*A*) Position and type of the single amino acid exchanges undertaken in key domains of AtMRP5. T3 homozygous plants carrying *pCaMV35S*::*AtMRP5* constructs with either a D771A or a D1429A exchange in the Walker B domain of NBD1 or NBD2 exhibit *mrp5-1* type seed $InsP_6$ content (*B*), root length (*C*) drought resistance (*D*) and ABA-insensitive stomatal aperture phenotype (*E*). The experiments were repeated at least three times. Error bars represent SEM. For *B*) The "p-value" indicates the confidence of significance between wild type and the three other genotypes. For *E*) The "p-value" indicates the confidence of significance between Light- and Light+ABA treatments within the same genotype. Note, while in wild type plants the stomatal aperture is significantly reduced upon ABA treatment, in *mrp5-1*, DA1 and

DA2 the stomatal apertures are significantly increased. The aperture of *mrp5-1* mutants in the light is always smaller than that of the wild type plants (4,5), but it is still significantly larger than that of ABA treated wild type plants ($p \leq 0.01$).

Figure S6 Subcellular localization of AtMRP5. An *AtMRP5–GFP* construct under the control of the native *AtMRP5* promoter was used to transform *mrp5-1* plants. Since the GFP signal was very weak, vacuoles were released by osmotic lysis from leaf protoplasts isolated from homozygous T3 plants subjected to drought stress. To verify vacuolar localization, images were captured by laser scanning confocal microscopy with the 63X magnification objective, and an appropriate zoom. (*A*) differential interference contrast (DIC) image (*B*) fluorescence signal in green, corresponding to GFP (emission λ_{em}= 500-530nm) (*C*) chlorophyll autofluorescence signal in red (emission λ_{em}= 620-750nm) (*D*) merged images of *A*, *B* and *C*.

References

1. Sweetman, D., Stavridou, I., Johnson, S., Green, P., Caddick, S.E., and Brearley, C.A. (2007) *FEBS lett* **581**, 4165-4171
2. Curtis, M., and Grossniklaus, U. (2003) *Plant Physiol* **133**, 462-469
3. Clough, S.J., and Bent, A.F. (1998) *Plant J* **16**, 735-743
4. Klein, M., Perfus-Barbeoch, L., Frelet, A., Gaedeke, N., Reinhardt D., Mueller-Roeber, B., Martinoia, E., and Forestier, C. (2003) *Plant J* **33**, 119-129
5. Gaedeke, N., Klein, M., Kolukisaoglu,U., Forestier, C., Mueller, A., Ansorge, M., Becker, D., Mamnun, Y., Kuchler, K., Schulz, B., Mueller-Roeber, B., and Martinoia,E. (2001) *The EMBO J* **20,** 1875-1887

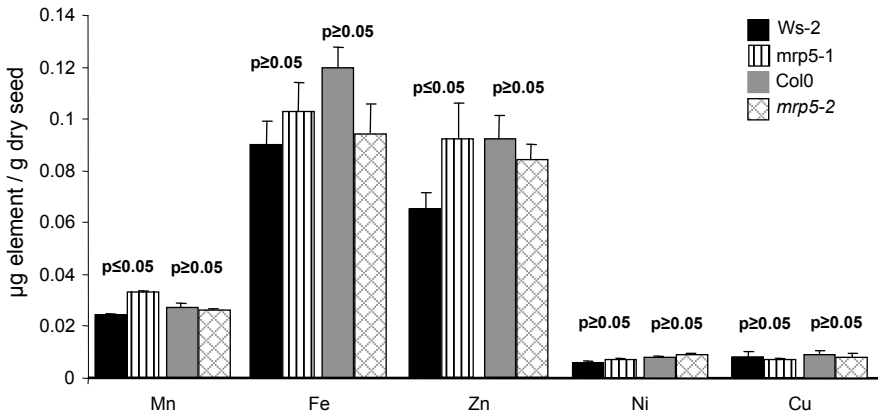
µg element / g dry seed
0.14
0.12
0.1
0.08
0.06
0.04
0.02
0
Ws-2
mrp5-1
Col0
mrp5-2
p≤0.05
p≥0.05
p≥0.05
p≥0.05
p≤0.05
p≥0.05
p≥0.05
p≥0.05
p≥0.05
p≥0.05
Mn
Fe
Zn
Ni
Cu

Figure S1

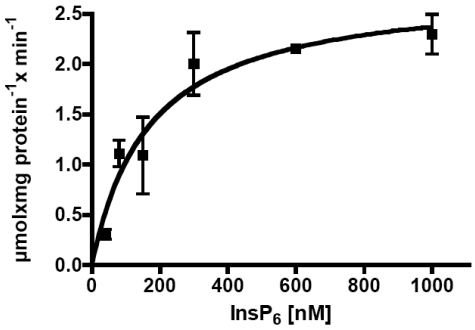
2.5
2.0
1.5
1.0
0.5
0.0
µmolxmg protein-1 x min-1
0
200
400
600
800
1000
InsP6 [nM]

Figure S2

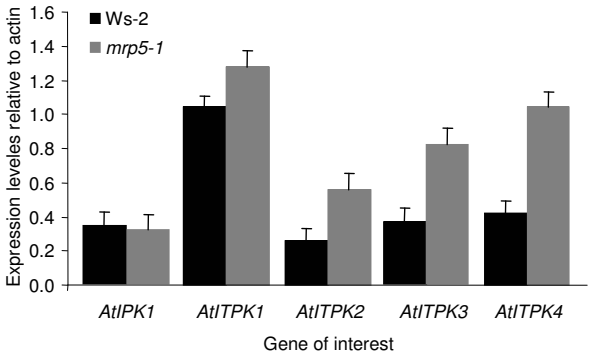
Ws-2
mrp5-1
Expression leveles relative to actin
1.6
1.4
1.2
1.0
0.8
0.6
0.4
0.2
0.0
AtIPK1
AtITPK1
AtITPK2
AtITPK3
AtITPK4
Gene of interest

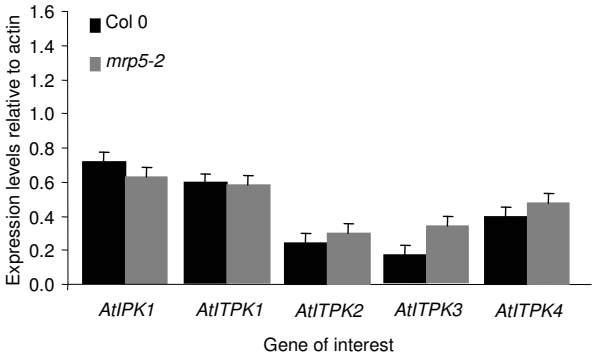
Col 0
mrp5-2
Expression levels relative to actin
1.6
1.4
1.2
1.0
0.8
0.6
0.4
0.2
0.0
AtIPK1
AtITPK1
AtITPK2
AtITPK3
AtITPK4
Gene of interest

Figure S3

A

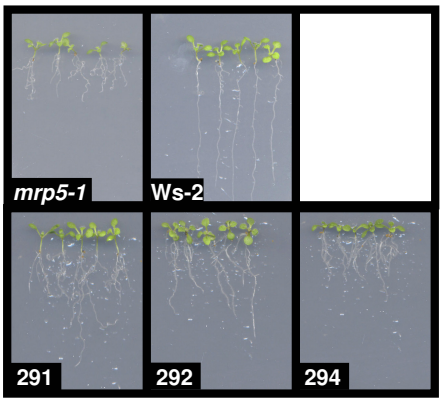

Figure S4

A

NBD1

Walker A	K663A
Walker B	D771A (DA1)
ABC signature	R759A

NBD2

Walker A	K1308A
Walker B	D1429A (DA2)
ABC signature	R1417A

B

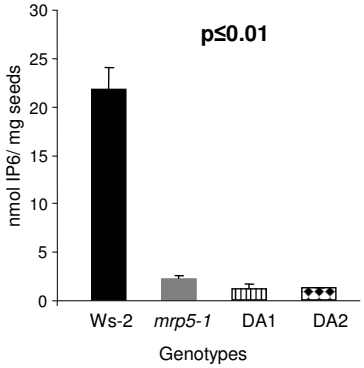

C

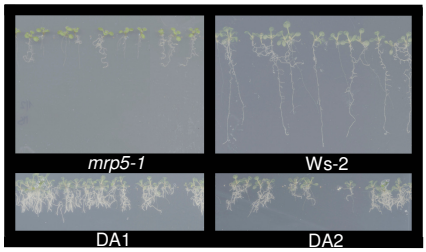

D

E

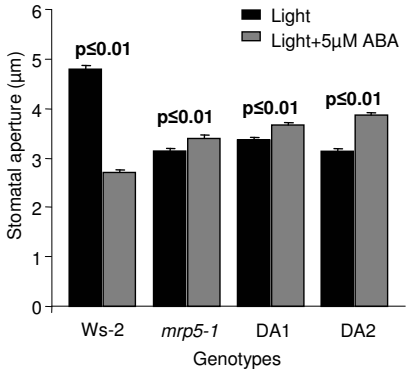

Figure S5

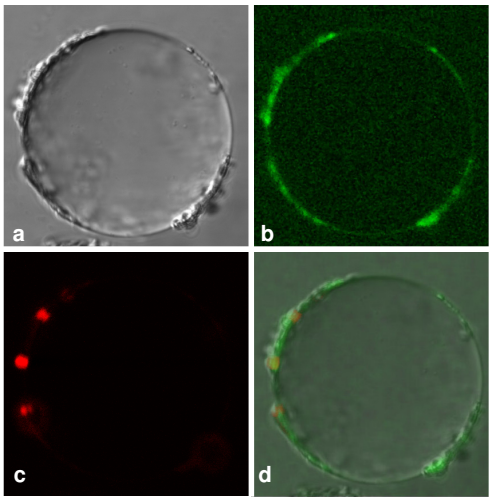

Figure S6

4 *At*MRP5/*At*ABCC5 - An Inositolhexa*kis*phosphate transporter interacts with Hookless 1, a protein involved in ethylene signaling

4.1 Introduction

Land plants often encounter the risk of irregular water supply and hence to wither. To overcome this danger, they evolved mechanisms to face this problem. In temperate zones they possess a water-impermeable cuticule. In arid zoned they produce xeromorphe leaves, which serve as water stores. The cuticula efficiently reduces the transpiration rate, but does not allow regulating the exchange of H_2O_2, CO_2 and O_2. Stomata, formed by a pair of guard cells, are pores in the leaf surface, able to open and close in response to environmental signals, like light or drought stress. The main function of stomata is to minimize water loss and optimize CO_2 uptake required for photosynthesis. To this end, guard cells have evolved complex regulatory mechanisms, involving phytohormones like abscicicabscisic acid (ABA), signaling compounds such as Ca^{2+} or H_2O_2, as well as a large number of channels and transporters. In this study we focus on one specific transporter *At*MRP5/*At*ABCC5, belonging to the super family of the ATP-binding cassette (ABC) proteins, more precisely to the Multidrug resistance associated protein transporters (MRP).

Over the past years several studies were carried out on *At*MRP5, but still its function in stomata regulation is poorly understood. *At*MRP5 loss-of-function *Arabidopsis* plants display a decreased stomatal aperture compared to wild type plants, which results in an increased water-use-efficiency. Furthermore *Arabidopsis mrp5-1* T-DNA insertion mutants are insensitive towards ABA, a phytohormone responsible for stomata closure during drought stress and Ca^{2+}, a major secondary messenger during ABA signaling. Stomata also show an impaired response against auxin and glibenclamide (Klein *et al.,* 2003). In patch-clamp experiments it has been shown that guard cell protoplasts from *mrp5-1* plants, exhibit a reduced S-type anion channel activity, indicating that AtMRP5 directly or indirectly influences S-type anion channels (Suh *et al.,* 2007). In a recent study Nagy *et al.* (2009) showed that AtMRP5 is a highly specific and high affinity phytic acid ($InsP_6$) transporter. Phytic acid consists of a *myo*-inositol moiety bearing 6 phosphates and represents the principal phosphorus storage in many plants seeds and was documented as a new signaling molecule. Still, all these findings do not fully explain the impaired stomatal function of *mrp5-1* plants.

Upon drought, the drought stress hormone abscicabscisic acid (ABA) is produced in the

roots and cells of the vascular tissue of leaves. ABA is subsequently transported in the water stream to the guard cells. When ABA enters the cytosol of a leave cell, it binds to the soluble ABA receptors of the RCAR (Regulatory component of ABA receptor) family. It was shown, that RCAR1 binds to ABA to mediate the inactivation of ABI1 and ABI2 in an ABA-depending manner (Ma *et al.*, 2009, Park et *al.*, 2009) Inactivation of the phosphatases allow to phosphorylate and activate the S-type anion channels (Hubbard *et al.,* 2011; Geiger *et al.,* 2011) resulting depolarization in opening of potassium outward currents. It has been postulated that $InsP_6$ acts by activating vacuolar Ca^{2+} channels and inhibiting K^+ inward channels (Pei *et al.,* 1997, Lemtiri-Chlieh *et al.,* 2003)). $InsP_6$ is synthesized in response to ABA and contributes to stomata closure by Ca^{2+} release from internal compartements (Lemtiri-Chlieh *et al.,* 2003).

Ethylene is a gaseous phytohormone involved in fruit ripening, seedling germination, seedling growth, stem and flower development, organ senescence and abscission. Ethylene synthesis is regulated by developmental cues and hormones, such as auxin, gibbereline (GA), cytokinin and brassinorides (Yoo *et al.,* 2009). Stresses like wounding, salts, drought, cold, ozone, flooding, pathogen and insect attacks enhance ethylene synthesis (Yoo *et al.,* 2009). However, the molecular mechanisms behind these diverse actions of ethylene remain largely elusive.

One of the most interesting features of ethylene, for this work, is that ethylene inhibits the ABA-induced stomatal closure. Two possible explanations for these reactions have been, proposed i) ethylene ensures a minimum amount of carbon dioxide for photosynthesis by keeping the stomata partially open during drought stress ii) ethylene allows some photosynthesis during leaf senescence for instance in autumn (Tanaka *et al.,* 2005). These results provide evidence that ethylene interacts with the ABA signaling pathway at least in the case of guard cells. The situation is even more complicated, since it was observed that auxin-induced stomatal opening is mediated through auxin-induced ethylene production by guard cells (Merritt *et al.,* 2001). All these findings implicate that ethylene plays a complex role in guard cell signaling by interfering with the ABA and the auxin signaling pathways.

In this work, we show that Hookless 1, a soluble protein involved in ethylene sensing, interacts with the nucleotide binding domain 1 of *At*MRP5 and that both loss-of-function

Arabidopsis mutants exhibit an altered stomata phenotype. This raises the question how Hookless 1 and *At*MRP5 are involved in guard cell signaling.

4.2 Material and Methods

4.2.1 AtMRP5 interaction partner search using the conventional yeast two hybrid system

The protocols concerning buffers, solutions, plasmid maps, instruments and devices, which are not listed in the text, will be found in the supplementary data.

4.2.2 Creating the bait constructs pLexA_kan-NBD1 and pLexA_kan-NBD2 and transformation of the Saccharomyces cervisiae strain LH40

The **N**ucleoid **B**inding **D**omain 1 (NBD1) and NBD2 from *At*MRP5 were amplified from a cDNA derived from *Arabidopsis thaliana* (Columbia-0) RNA, utilizing the primers NBD1-s (5' -G**GAATTC**CGGAACTTTCCTGATCTGG-3'), NBD1-as (5' - GCG**GGATCC**ATATGCAGCACCCATGTATG-3'), NBD2-s (5' - G**GAATTC**CCACATGGAACCATTGATCCA-3') and NBD2-as (5' - GCG**GGATCC**TCATAATTCAGGGATTCCAGT-3'). The sense primers contained an EcoRI and the anti-sense primers a BamHI restriction site (in bold). The polymerase chain reaction (PCR) was carried out with the Advantage Hot Start Taq polymerase (Clonetech). The PCR, as well as the program, were designed as written in the accompanying protocol.

The NBD1 fragment began started at base pair 1729 and ends at 2832bp (approximately 1.1 kb, ~57 kDa) and the NBD2 fragment started at 3586bp and ended at 4545bp (approximately 1 kb, ~52 kDa). After restriction of the NBD1/2 fragments and the plasmid pLexA-kan (map see appendix) with the enzymes BamHI and XhoI, a ligation reaction was performed and the reaction was transformed into *E.coli*. Plasmids of the colonies were confirmed by restriction analysis and sequencing (Data not shown). Yeast cells of the strain LH40 (MATa, trp1, leu2, his3; LYS2::lexA-His; URA3::lexA-lacZ) were grown overnight in 5 ml YPAD liquid media at 28°C and transformed with the bait contruct (see.suppl. data)

4.2.3 Crude yeast cytosolic protein extraction and Western blot analysis

5 ml of selective SD liquid media, lacking tryptophan were inoculated with LH40 yeast cells containing either pLexA-kan_NBD1 or pLexA-kan_NBD2. The cells were grown over night and subsequently centrifuged at 3'000 rpm for 5 minutes. The resulting pellets were washed with MilliQ water and centrifuged again. The pellet was resuspended in 1 ml MilliQ water and placed on ice (the following steps were also preceded on ice). 150 µl of yeast extraction buffer (YEC: 1.85 M NaOH, 7.5% ß-mercaptoethanol, 1 tablet of protein inhibition mix (Roche)) per 25 ml of YEC liquid media were added and vortexed. Subsequently, 150 µl of 50% TCA (Trichloroacetic acid) were added. The solution was shaken vigorously and incubated for 10 minutes. The suspensions were centrifuged at 3'000 rpm for 5 minutes and the pellets were resuspended in protein sample buffer. The samples were incubated for 10 minutes at 65°C and a Western Blot was performed (see suppl. Data)

4.2.4 High efficiency transformation of cDNA library (prey) into yeast containing the bait constructs

The screens on the different bait constructs were performed twice and the data of the two screens were assembled. The Arabidopsis cDNA library was cloned in the pACT2 plasmid and kindly provided by Dr. Csaba Koncz. The cDNA library was transformed into yeasts, which have already been transformed with the bait construct. Both transformations were performed according to the High efficiency transformation protocol (see suppl. Data) and plated on SD media lacking tryptophan, leucine and histidine.

4.2.5 Yeast two hybrid Screen

To exclude false-positive colonies and to control the tightness of the system, yeast cells containing the bait constructs (autotroph for tryptophan) and the empty prey vector pACT2 (autotroph for leucin) were grown on SD plates containing different 3-Amino-1,2,4-triazole concentrations (3-AT). The results indicated that the system was tight without supplementing 3-AT.

A high-efficiency transformation of the cDNA library was performed (Gietz and Woods, 2002). Yeast cells were streaked out on selective plates and incubated at 30°C. In the yeast two hybrid screen, using NBD1 as bait construct, approximately 15'380 colonies grew on plates and 387 colonies gave a positive signal in the X-Gal screen. The yeast two hybrid screen using NBD2 resulted in approximately 1720 colonies on screening plates; in the X-Gal screen 38 colonies gave a positive blue sign*al.*

4.2.6 X-Gal assay and yeast plasmid extraction/verification of positive prey clones

The X-Gal assay was used as an additional confirmatory assay that could exclude false positive results.

A sterile, circular, marked nitrocellulose membrane disc was placed on the plate, containing the yeast colonies and the position of the disc was, as well marked (three times with a sterile needle). After the nitrocellulose had full contact, the membrane was removed carefully and frozen in liquid nitrogen. The membrane was shortly thawed and placed on a round Petri dish (Ø145 mm; Greiner), containing a Whatman paper disc, soaked with Z-buffer (see appendix) and incubated at 30°C for at least 30 minutes. The incubation was stopped after the first colonies turned deep blue. The plasmids of the positive clones were recovered, transformed into *E.coli* and incubated on selective LB plates. The plasmids harvested from liquid cultures were rescued and sent for sequencing with a prey specific primer. From the 387 positive colonies of the NBD1 screen, 247 plasmids transformed into *E.coli* grew on plates and 39 revealed no sequencing results. 208 plasmids could be further characterized (Table 1A in the supplementary Data), corresponding to 53.75% of the colonies, which had turned blue. In the NBD2 screen 25 plasmids transformed into *E.coli* grew and 1 sequence could not be retrieved. 24 plasmids were sequenced, corresponding to 63.16% of the colonies giving a positive sign*al.*

Possible interaction candidates were chosen, depending on the number of appearance in the screen and/or the probability that they are involved in stomata regulation, the root phenotype of *mrp5-1* plants or general ABC transporter mechanisms (see table 1A and B in the supplementary Data in bold)

To see if there were strong interactions, a Co-immunoprecipitation was performed using a non-denaturing protein extraction method and the Dynabead system from Sigma Aldrich. Co-immunoprecipitates were loaded on a polyacrylamid gel and a Western blot was performed (see suppl. Data).

4.2.7 Phenotypical analysis of potential interaction partners of AtMRP5

4.2.7.1 Plant growth conditions

For each candidate gene (full list see supplementary data) a, knockout or at least a knock-down plant was selected from the SALK database (http://sign*al.*salk.edu/cgi-bin/tdnaexpress) and retrieved from the Nottingham Arabidopsis Stock Center (http://arabidopsis.info/BasicForm). All mutant plants were grown under short day conditions in the phytotron (light/dark cycle: 8h/16h; light intensity: 250-300µmol^{-2}sec^{-1} PAR; humidity: ~60% d/n; Temperature d/n: 18.5°C) on soil (Einheitserde) for 4-6 weeks.

4.2.7.2 Screen for altered stomatal aperture

To screen for altered guard cell movements in the mutants of the potential interaction partner genes, a basic stomata experiment was performed, verifying the aperture states in the light or in the dark. Single plants were removed from the phytotron before the light cycle started and kept in the dark until the start of the experiment.

From two individual mutant plants, belonging to the same population, the tenth and eleventh leaves were harvested (in the dark) and placed in two Petri dishes on stomata buffer (30mM KCl, 5mM MES pH5.8), one Petri dish was kept in the dark, the other exposed to light (illumination apparatus). To equilibrate the biological variance in between single plants, the leaves were distributed according to the following pattern: Petri dish one contained the tenth leaf from plant A and the eleventh leaf from plant B, whereas the second Petri dish contained the eleventh leaf from plant A and the tenth leaf from plant B. The Petri dishes were kept either in the dark or the light for 2.5h.

After 2.5h incubation time, ten pictures of the epidermal strips were taken with the 40x magnification objective. The stomatal aperture was measured with the Leica Software. A third sample (epidermal strips) of another single mutant plant was taken, directly after

removing the plants from the phytotron to verify the aperture at the starting point of the experiments. Too small stomata (fully round pair of guard cells), too old stomata (no visible round chloroplasts inside the guard cells) and destroyed guard cells were not taken into account.

4.2.8 Stomata aperture experiments with mutant plants displaying altered stomata movements in the screen

To investigate the role of probable interaction partners of *At*MRP5, more detailed experiments were performed with the following mutant plants and their corresponding wild type (written in brackets): *mrp5-1* (WS-2); *mrp5-2* (Col-0); *hookless1* (Col-0 SALK wild type: N60'000); *At4g01590* (knock out mutant of a T-DNA insertion into a gene of unknown function, containing a putative calcium binding EF hand motive similar to a gene in *Medicago truncatula*).

Leaves were incubated by floating on stomata buffer with or without 10µM AVG (L-α-(2-Aminoethoxyvinyl)glycine hydrochloride; inhibitor of the ACC oxidase), using the same distribution pattern as described before for 2.5h in the light (illumination apparatus). After 2.5h, 5µM abscisic acid (ABA) was added and the leaves were kept for 3h in the light.

4.2.9 Drought stress experiments with Col-0 and hls-1 plants in the dark

The plants used for the experiments were grown on soil for 4 - 5 weeks. The drought stress experiment was performed in the dark. 10 *hls1-1* and Col-0 plants were excised directly from above the soil and the wound was closed with silicone. Plants were hanged upside down and the weight was measured at different time points (0, 15, 30, 45, 60, 75, 90, 120, 150, 180, 240, 300 min). The dry weight of the plants was determined by drying the plants for several hours in the drying cupboard.

4.3 Results

4.3.1 Identification of possible interacting partner of AtMRP5/AtABCC5 using a yeast two hybrid screen and the nucleotide binding domain 1 of AtMRP5 as a bait

As a first step, to identify potential interaction partners of AtMRP5, a yeast two Hybrid screen with the nucleotid binding domain 1 (1729bp - 2832bp of cDNA of AtMRP5) cloned into the bait vector pLexA and a plant cDNA library in the prey vector pACT2 was performed. Approximatively 15'380 colonies grew on selective SD media (lacking tryptophane, histidine and leucine). In a following X-Gal assay 387 colonies showed a positive blue sign*al.* From these 387 colonies, 247 plasmids could be rescued. 208 sequences were assigned to the *Arabidopsis thaliana* genome, 39 sequences could not be identified.

The 208 sequences encoding for proteins were classified into the following groups: auxin-related proteins, protein degradation-related proteins, cell wall and pathogen attack related proteins, Ca^{2+}-binding proteins, ubiquitin-related proteins and proteins of unknown function (list of all sequences obtained, see supplementary data)

4.3.2 Basic light/dark stomatal aperture screen

Candidates of interest were chosen (see supplementary data, written in bold letters) and the corresponding loss-of-function *Arabidopsis* plants were tested in a light/dark stomata experiment. Leaves from 4-5 weeks old plants were incubated on stomata buffer either in the dark or in the light for 2.5 h and stomatal apertures were measured (leaves were harvested in the dark) or examined for an altered response, compared to wild type plants. The most obvious altered stomatal aperture phenotype, compared to the corresponding wild type plants was the one of the *hookless 1* loss-of-function mutant in the dark (Fig. 1). The stomatal aperture was measured in the light and the dark and as shown in Figure 2, *hls1* mutant stomata are partially open in the dark. In the light, the stomatal aperture exceeds that of the wild type constituently. This result prompted us to investigate more in detail the interaction between *At*MRP5 and HLS1.

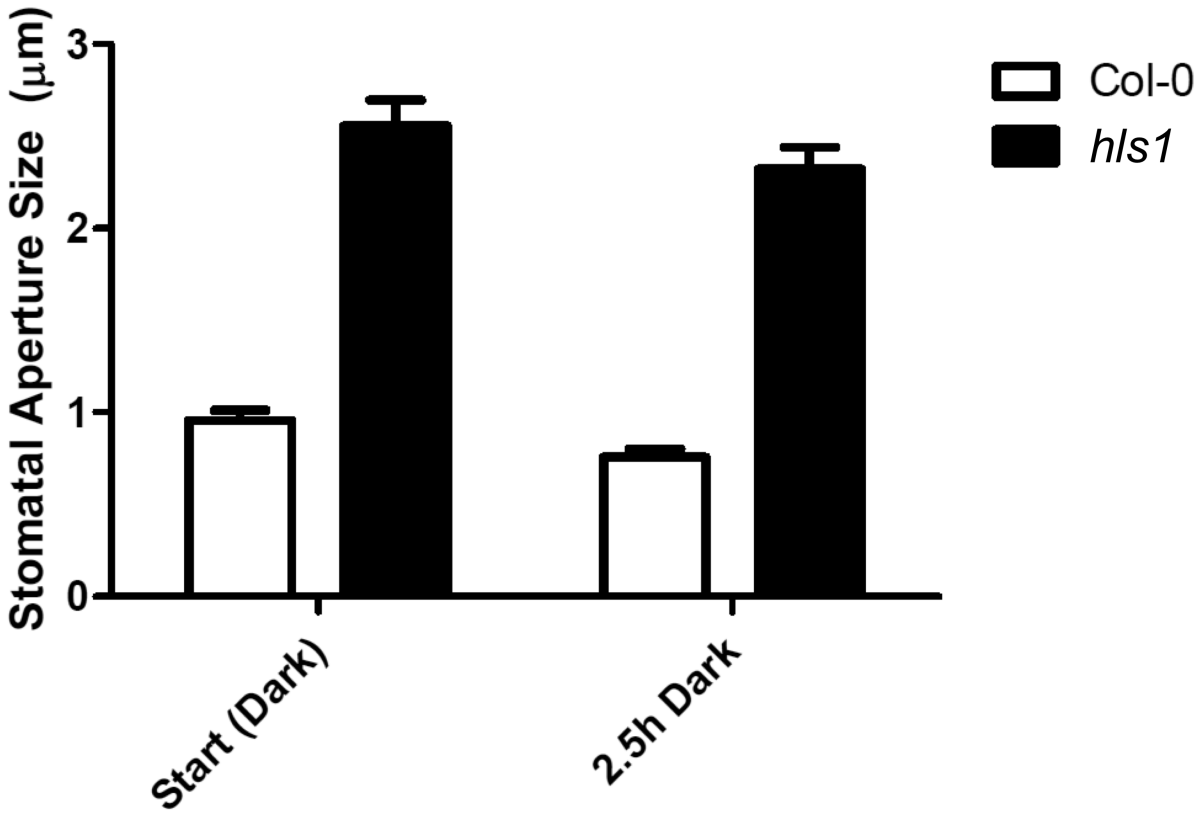

Figure 1 Stomatal aperture measurements of *hls1* mutant plants

Measurements of the average stomatal aperture (µm) of the *hls1* mutant and the corresponding wild type plants kept under dark conditions. Epidermal strips were either prepared from excised leaves from plants collected during the dark phase or after incubation of the excised leaves on stomata buffer for 2.5h in the dark (2.5h dark). Error bar stands for the standard error.

4.3.3 Verification of the full length HLS1 as interacting partner

To double check the Yeast Two Hybrid screen result, the full size Hookless 1 gene (1212 bp) was amplified, cloned into the prey vector and transformed in the *Saccharomyces cervisiae* strain LH40 carrying the bait construct containing the NBD1 of *At*MRP5. Grown colonies were tested again in an X-Gal assay together with a negative control (containing the empty prey vector, see Fig. 1). Furthermore a rough mapping was performed by testing the first half of the Hookless 1 gene (0-622bp), the second half (601bp-1212bp) and an overlapping part (301-907bp) for the interaction with *At*MRP5.

The fragments were also cloned into the prey vector and similar assays were performed as with the full size Hookless 1. As shown in Figure 2B and C the full size construct exhibited an interaction, whereas the negative control displayed just a slight background staining (Fig.2A). Furthermore it was observed that the first half of HLS1 bound the strongest (Fig.2D), whilst the second half shows (Fig.2F) nearly no interaction. The overlapping part shows an intermediate phenotype, comparable to the binding of the full size construct (Fig.2E).

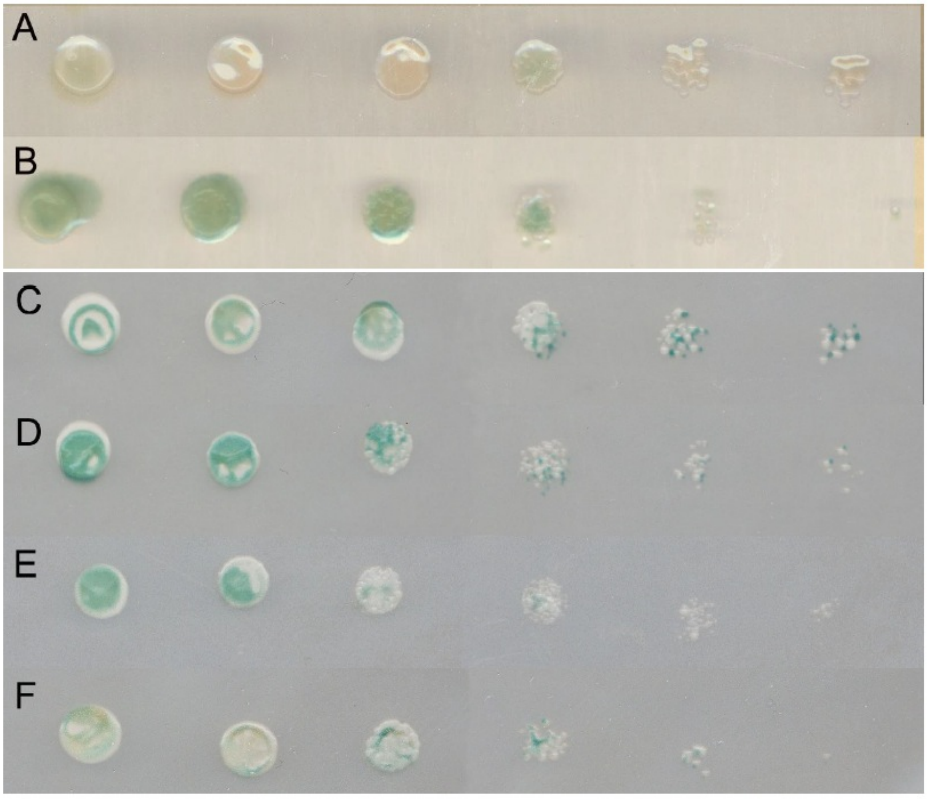

Figure 2 Verification analysis of possible yeast two hybrid candidate HLS1

Verification analysis of the interaction of *At*HLS1 with the NBD1 of *At*MRP5 (**A**, **B**), performed in *Saccharomyces cervisiae*, using the Yeast Two Hybrid System. **A** negative control, empty prey vector (pACT2) and bait vector containing the NBD1 of MRP5 (pLexA - MRP5(NBD1)); **B** full length *At*HLS1 prey construct and *At*MRP5(NBD1) (bait); **C** - **F** Mapping assay of the binding of fragments of *At*HLS1 to the MRP5(NBD1) bait construct, **C** full length *At*HLS1 and bait construct; **D** first half of *At*HLS1 (~0bp - 600bp) and bait construct; **E** fragment overlapping the middle part of *At*HLS1 (~300bp - 900bp) and bait construct; **F** second half of *At*HLS1 (~900bp - 1200bp) and bait construct. Further negative controls with the NBD2 of *At*MRP5 were performed and no colonies grew on selective media, excluding interaction of NBD2 of *At*MRP5 and *At*HLS1 (data not shown).

4.3.4 Stomatal apertures are altered in the loss-of-function mutant

To verify whether *hls1* mutants show a similar stomata phenotype as the *mrp5-2* mutants (T-DNA insertion in MRP5 in the Columbia ecotype, corresponding wild type to T-DNA insertion mutant line received from the SALK institute), *hls1* mutants and *mrp5-2* mutants were treated with 5µM absisic acid in the stomata buffer. Interestingly, *hls1* stomata were insensitive towards ABA treatment as reported for *mrp5-2* and *mrp5-1* mutant plants (Fig. 3).

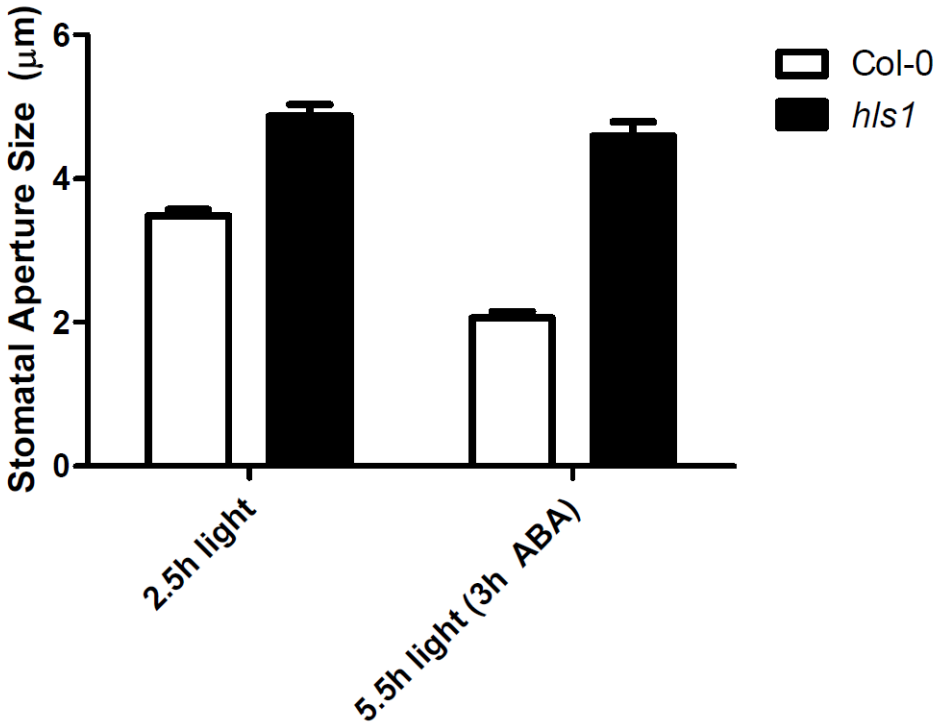

Figure 3 Stomatal aperture measurements *hls1* mutants with ABA

Measurements of the average stomatal apertures (µm) from epidermal strips of excised leaves of the *hls1* mutants and their corresponding wild type plants (Columbia). Excised leaves were kept on stomatal buffer in the light for 2.5h and measured. Subsequently ABA (5µM) was added and leaves were kept in the light for additional 3h. Error bars represent the standard errors.

Since *hls1* is involved in ethylene signaling and ethylene inhibits the ABA-induced stomatal closure (Tanaka et. al, 2005), further stomata experiments were performed by adding AVG (L-α-(2-Aminoethoxyvinyl)glycine hydrochloride, an inhibitor of ethylene synthesis) into the stomata buffer. Leaves were incubated for 2.5h in the light with or

without 10µM AVG and subsequently for 3h in the presence or absence of 5µM ABA. The results demonstrated that *hls1* loss-of-function mutants respond to ABA when pretreated with AVG (Fig. 4) and reduce their stomatal aperture size to a comparable size of the corresponding wild type. Therefore we were interested whether *mrp5-2* knockout (Columbia) exhibit a similar behavior. Indeed pretreatment of mrp5-2 plants with AVG restored ABA sensitivity also in this mutant (Fig. 5). To verify that the response of *mrp5-2* to ethylene is not depending on the Columbia ecotype, the experiment was repeated with the mrp5-1 loss-of-function mutant and its corresponding wild type WS-2 (Fig. 6). Similar results were obtained, indicating that the phenotype was not ecotype specific.

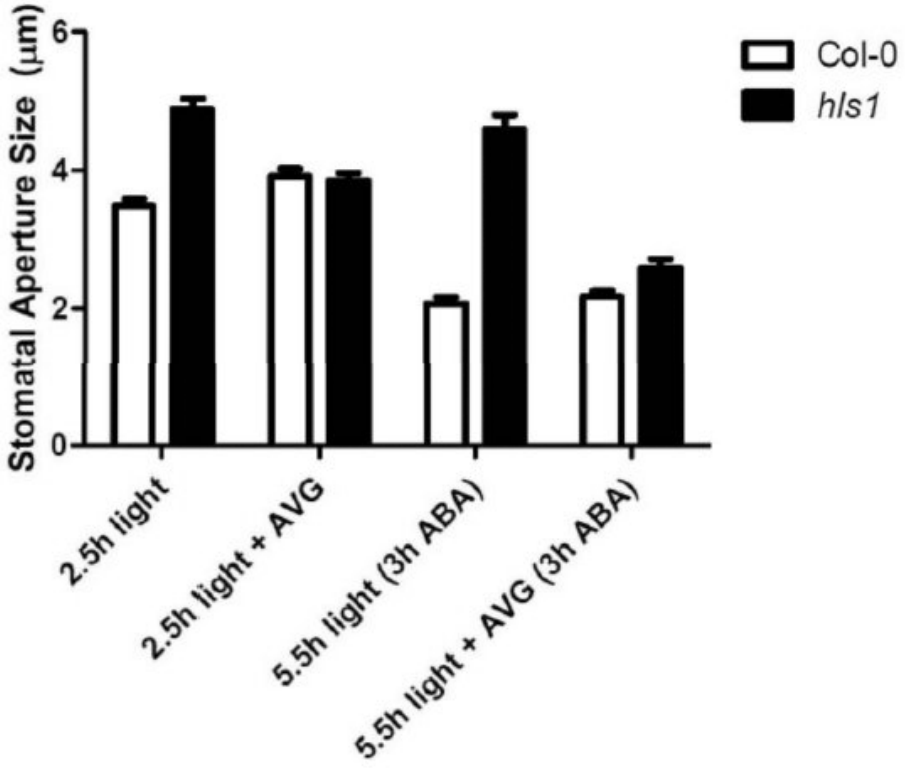

Figure 4 Stomatal aperture measurements *hls1* mutants with ABA and AVG

Measurements of the stomatal apertures (µm) from epidermal strips of excised leaves of the *hls1* mutant and their corresponding wild type plants (Columbia). Excised leaves were kept in the light for 2.5h on stomatal buffer in absence or presence of AVG (10µM). Subsequently ABA (5µM) was added and leaves were kept in the light for additional 3h. Error bars represent the standard errors.

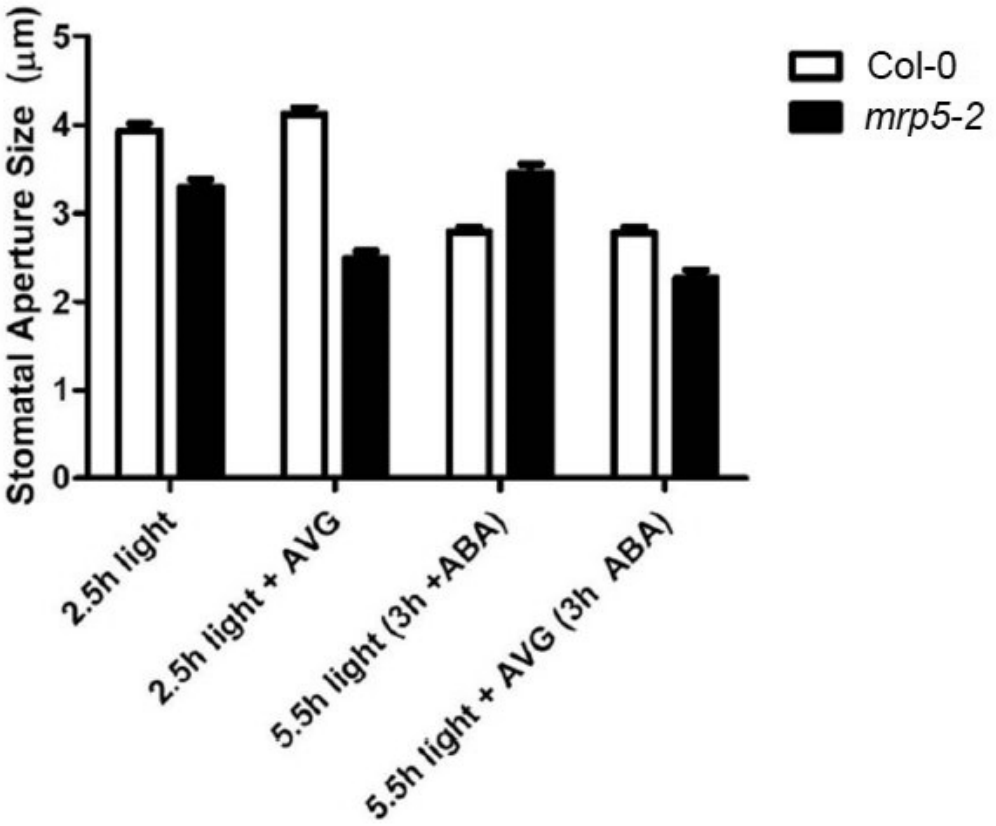

Figure 5 Stomatal aperture measurements of *mrp5-2* mutants with ABA and AVG

Measurements of the stomatal apertures (µm) from on epidermal strips of excised leaves of from the *mrp5-2* mutant and their corresponding wild-type plants (Columbia). Excised leaves were kept in the light for 2.5h on stomatal buffer with and without the addition of AVG (10µM). Subsequently ABA (5µM) was added and leaves were kept in the light for additional 3h. Error bars represent the standard errors.

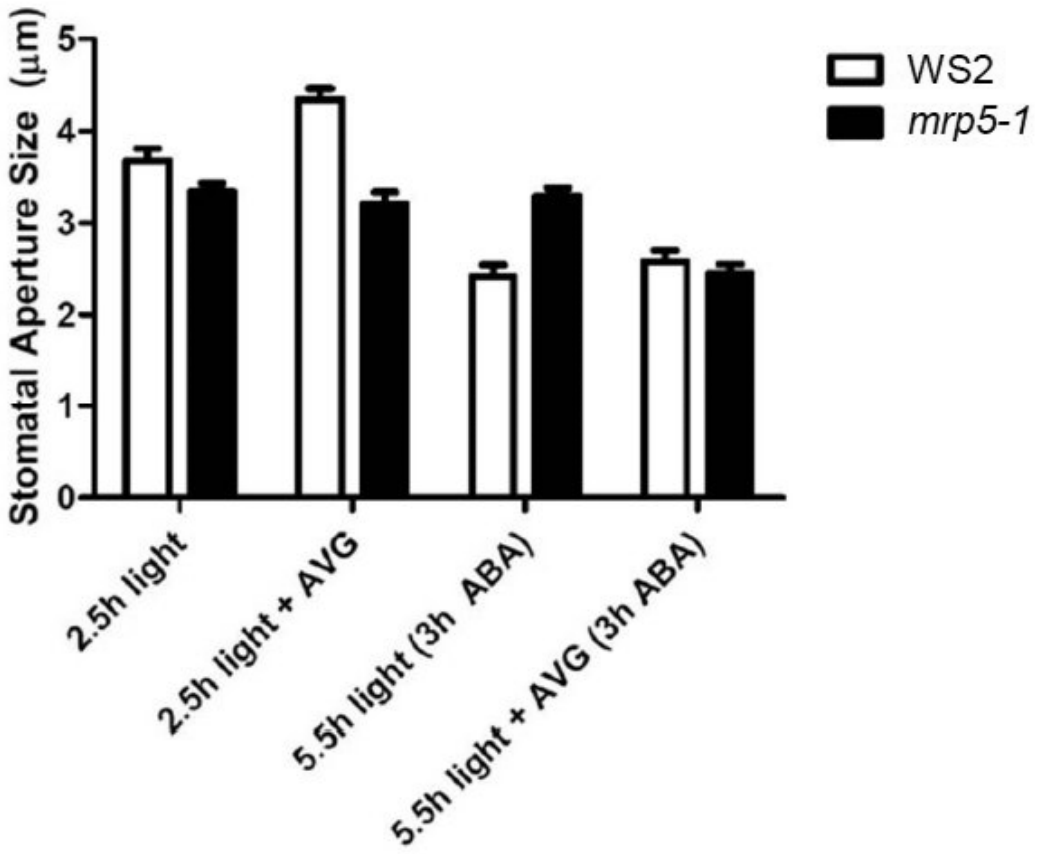

Figure 6 Stomatal aperture measurements of *mrp5-1* mutants with ABA and AVG

Measurements of the stomatal apertures apertures (µm) on epidermal strips of excised leaves of the *mrp5-1* mutant and their corresponding wild type plants (Wasslevskayia). Excised leaves were kept in the light for 2.5h on stomatal buffer with and without the addition of AVG (10µM). Subsequently ABA (5µM) was added and leaves were kept in the light for additional 3h. Error bars represent the standard errors.

Drought stress experiments indicate that hls1 loss-of-function mutants exhibit a higher transpiration rate.

Since the stomata of the *hls1* mutant seem to remain partially open in the dark, a drought stress experiment with whole plants was performed. Plants were excised directly above ground and the excision was closed with silicon to prevent water-loss via the wounded part. Plants were hanged up side down and kept continuously in the dark. The weight was initially measured in intervals of 15min and later in longer intervals. As shown in Figure 7 the hls1 mutant lost consistently more water than the corresponding wild type.

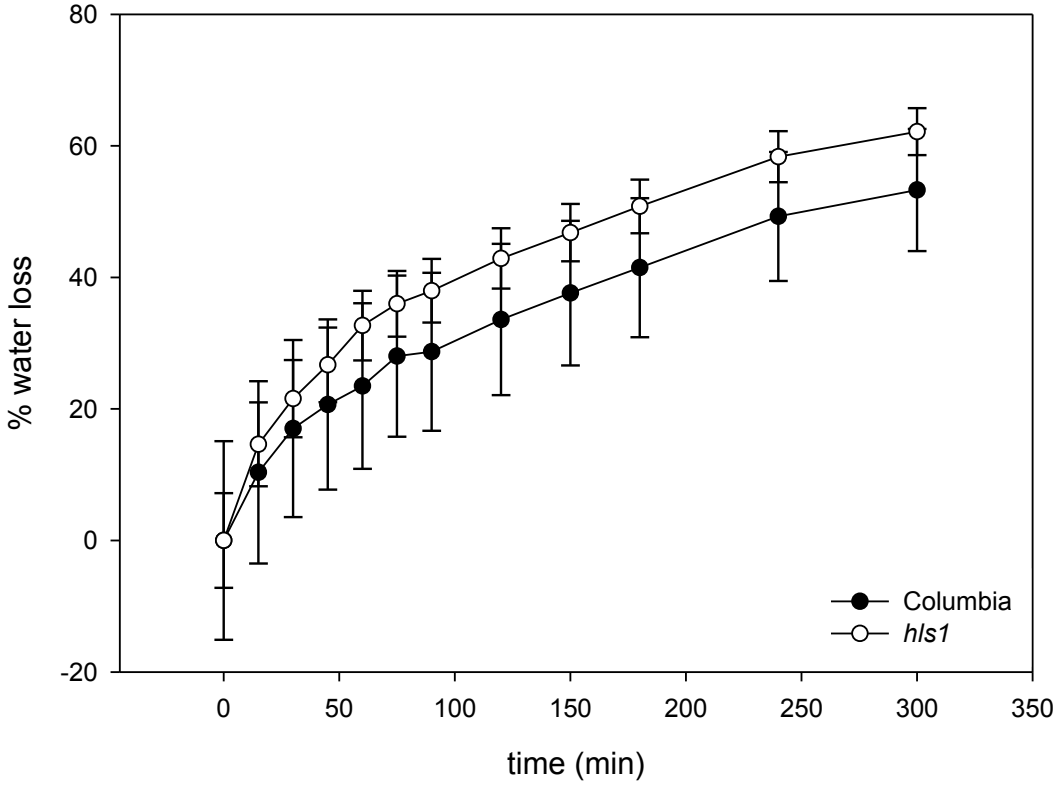

Figure 7 Water loss experiment with *hls1* and wild type plants

Water-loss (%) of excised whole *hls1* and Columbia wild type plants in the dark. Plants were excised directly above soil; the wound was closed with silicone and platns were hanged upside down. The plants, used for the experiments, were grown on soil and 4 - 5 weeks. Error bars represent the standard deviation.

4.4 Discussion

4.4.1 Yeast two hybrid screen using the nucleotide binding domain 1 of AtMRP5 as bait

As mentioned in the introduction, screening a plant cDNA library with a full length ABC-transporter as bait in the membrane based yeast two hybrid system (Split ubiquitin system) causes severe problems. This has several reasons: the large size of the proteins and additionally, as experienced in our laboratory the low levels of expression for plant ABC transporters in yeast. All these arguments led to the decision to use only the nucleotide binding domains (NBD1 and NBD2) of *At*MRP5 (purely cytosolic, small size and not functional as transporter).

The amount of positive colonies retrieved in the screen with the NBD1 compared to that found with NBD2 (results of the NBD2 screen see supplementary data), supported that the major interactions take place at the NBD1. The decision whether a candidate was interesting or not was based on the known functions of the identified proteins, as well as on the expression pattern found on the e-FP browser (Website: http://www.efp.ucr.edu). Candidates, even though having an interesting function, were not chosen if they were not expressed in guard cells. Of special interest were proteins involved in Ca^{2+} binding (important 2^{nd} messenger in stomata function), proteins believed to be involved in channel modulation as well as proteins involved in phytohormone pathways. To further elucidate the role of those proteins, loss-of-function mutants were compared with the wild type.

4.4.2 Basic light/dark stomatal aperture screen

Surprisingly, the most obvious stomatal phenotype observed was that of *hookless1*. We observed that in *hls1* stomata were not able to fully close during the dark cycle (Fig. 2). To verify if the method itself could have any impact on the stomata, the measurement was performed with leaves taken directly from the dark and leaves incubated for 2.5h on stomata buffer in the dark. *Hookless 1* (*AtHLS1*) is expressed, similarly to *At*MRP5, in the 24h imbibed seed and the stomata (source e-FP browser). Until now, the *At*HLS1 loss-of-function mutant was described as an ethylene-insensitive mutant in triple

response screens. Etiolated *hls1* mutant seedlings fail to form the apical hook and do not react with the triple response to ethylene treatment (Guzman *et al.,* 1990). *At*HLS1 is a soluble protein with a putative N-acetyltransferase moiety. This putative N-acetyltransferase was proposed to control the differential cell growth in etiolated seedlings via modulating the amount of free auxin (Lehmann *et al.,* 1996). It was suggested, that the auxin is inactivated via acetylation of the hormone. Nevertheless, these results suggest that *At*HLS1 is acting in the crosstalk between auxin signaling and the ethylene pathway and therefore is an interesting candidate. However, it is not likely that the target of acetylation is auxin, since so far no acetylated auxin has been identified and since there is no hint that such a compound could occur. Therefore it is tempting to speculate that HLS1 acetylates proteins (Lundby et *al.* 2012)

4.4.3 Stomatal aperture changes of the loss-of-function mutant hls1 towards the phytohormone ABA and the ethylene synthesis blocker AVG in the light

To verify if the drought stress hormone abscisic acid (ABA) has any impact on the *hls1* mutant, more detailed stomata aperture experiments were performed. Like the *mrp5-1* and *mrp5-2* mutants, the *hls1* loss-of-function mutant was insensitive towards ABA (Fig. 3). Figure 3 also shows that the hls1 mutant opens even further in the light, which implies that a central mechanism limiting stomatal aperture in the light is impaired.

Since it is known, that ethylene is able to inhibit the ABA response, we added AVG to the stomata buffer (an ethylene synthesis inhibitor). Surprisingly, stomata of *hls1* loss-of-function plants, which were treated with AVG in the absence of ABA, closed their stomata to a value comparable to the corresponding wild type (Fig. 4). Furthermore, as soon as AVG was added to the stomata buffer, the ABA response proceeded similarly as in the wild type (Fig. 4). This clearly indicated that a pool of ethylene in the stomata of *hls1* mutants inhibited the ABA response, as well as it was leading to a larger aperture in non-ABA treated leaves of *hls1* plants.

In contrast, the corresponding wild type does not show any alterations, when AVG was added (Fig. 4). The most important question, in this context was, whether the interaction between *At*MRP5 and *At*HLS1 circumvent the raise in ethylene concentration. If this is so, also mrp5 loss-of-function plants would have to get sensitive again towards ABA

treatment, when pretreated with AVG. As shown in Fig. 5, indeed also *mrp5-2* mutant plants exhibit ABA induced stomatal closure when pretreated with AVG. Since it is known that reactions towards ethylene are strongly varying among Arabidopsis ecotypes, the experiment was also performed with mrp5-1 and the corresponding wild type, WS-2 (Fig. 6). These results indicate that *mrp5*, as well as *hls1* loss-of-function mutants are insensitive towards ABA, because they have an internal pool of ethylene. In contrast it cannot be stated that this ethylene pool is the reason for the open state during the dark cycle (results varied strongly from experiment to experiment, data not shown). In this case it might be, that ethylene induces auxin production, which is able to open stomata in the dark. This hypothesis remains to be investigated.

4.4.4 Drought stress experiments performed with whole plants of hls1 loss-of-function mutants and corresponding wild type (Col-0) in the dark

Stomata aperture measurements are not so easy to perform, due to a large biological variability among the stomatal aperture size. Aperture sizes are considerably different between the leaves and areas of one leaf. This is the reason why a strict protocol has to be followed (see Materials and Methods). To test whether the stomata measurements reflect the situation *in planta*, drought stress experiments with whole plants were performed. It was found that also at the whole plant level the *hls1* loss-of-function mutant loses more water in the dark than the wild type (Fig. 7).

4.5 Conclusion

To understand the role of *At*MRP5 and its interaction with *At*HLS1 in a general context, it is important to know more about the role of ethylene in stomata regulation. Ethylene is a gaseous plant hormone involved in diverse seasonal, developmental and physiological processes. No general role in guard cells could be distinguished, as its function varies among different plant families. In *Arabidopsis thaliana*, ethylene is able to inhibit ABA induced stomatal closure (Tanaka *et al.,* 2005). Possible explanations for the physiological function of the antagonistic relationship of ABA and ethylene can be the insurance of a minimal supply of carbon dioxide to allow a minimum level of photosynthesis upon drought stress for a long period (Tanaka *et al.,* 2005). Both hormones are affected by drought stress and increase during desiccation (Xu and Zou, 1993). Ethylene production levels were found to be regulated by the circadian clock and light (Thain *et al.*, 2004).

As shown in Figure 8A, ABA is transported into the cytosol of guard cells (Fig.8 A-1) and there bound to soluble ABA receptors, called RCARs (regulatory component of ABA receptors) (Fig.8 A-2). RCAR1 belongs to a family of 14 members (RCARs) and binds to the protein phosphatases 2Cs (PP2Cs), namely ABI1 and ABI2 (Ma *et al.,* 2009, Park et *al.* 2009). ABI1 and ABI2 are known as key players in ABA signal transduction and repress ABA responses (Merlot *et al.*, 2001). ABA is, in the presence of RCAR1, able to fully block the protein phosphatase activity of ABI2 (Ma *et al.*, 2009). Phytic acid, also known as inositol hexa*kis*phosphate ($InsP_6$) is thought to act as a signalling molecule triggered by ABA (Fig.8 A-3) (Lemtiri-Chlieh *et al.*, 2003). $InsP_6$ is responsible for the release of calcium ions from the internal compartments such as the central vacuole, leading to an increase in cytosolic calcium from 50-350 nM up to 1.1 μM (Lemitri-Chlieh *et al.* 2000). On the other hand the presence of $InsP_6$ leads to a reduced K^+ inward current into the cytosol (Lemitri-Chlieh *et al.* 2003) (Fig.8 A-4). Elevated cytosolic Ca^{2+} concentrations cause rapid depolarization of the membrane, due to the activation of voltage dependent anion channels (Hedrich *et al.*, 1990). As shown by Nagy *et al.,* (2009), *At*MRP5 is an $InsP_6$ transporter, thought to play a role in seed phosphate storage. Since *AtMRP5* is highly expressed in guard cells (especially during drought stress), we think it could be required to remove $InsP_6$ from the cytosol and terminate the

$InsP_6$ signal (Fig.8 A-5). In this work we conclude, that the interaction between *At*MRP5 and *At*HLS1, leads to an inhibition of ethylene synthesis in guard cells (Fig.8 A-6). As a result of all these events, the stomata close in the presence of ABA.

Figure 8A-D: Hypothesis of the mechanism of the interaction between *At*HLS1 and *At*MRP5
A Model of the mechanism in the guard cells of the wild type for ABA perception **B** Model of the mechanism in guard cells of *mrp5* loss of function plants **C** Model of guard cells in the *hls1* loss-of-function plant background **D** Expected reaction model for the double knock-out plant guard cells of *mrp5/hls1*

Figure 8A Hypothesis of the mechanism of the interaction between *At*HLS1 and *At*MRP5

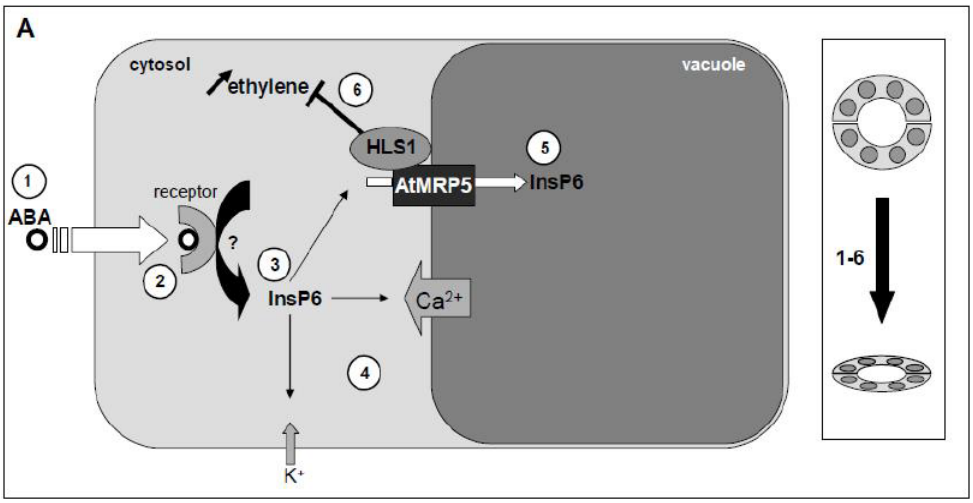

A Model of the mechanism in the guard cells of the wild type for ABA perception

To underline this conclusion, a closer look at the two mutant plants (*mrp5* and *hls1*) should be taken. In Figure 8B, we show how the regulation could work in *mrp5* mutant plants. If *At*MRP5 is missing in guard cells, $InsP_6$ cannot be removed from the cytosol anymore and $InsP_6$ levels increase and remain high (ABA present or not) (Fig.8B -1), this would mimic an ABA induced stomatal closure (Fig.8B -2). In patch-clamp experiments it has been shown that nanomolar concentrations of $InsP_6$ in *Vicia faba* and *S.tuberosum* guard cells mimicked the inhibitory effects of ABA and internal calcium by inhibiting inward rectifying K^+ currents (Lemitri-Chlieh *et al.* 2000). Since the stomata of *At*MRP5 loss-of-function plants are not closed and just display a reduced stomatal

aperture, we conclude that, if there is no interaction between *At*MRP5 and *At*HLS1, the level of ethylene increases and therefore inhibits ABA induced stomatal closure (Fig.8B -4). This is true, even in the presence of ABA (Fig. 8B -5).

Figure 8B Hypothesis of the mechanism of the interaction between *At*HLS1 and *At*MRP5

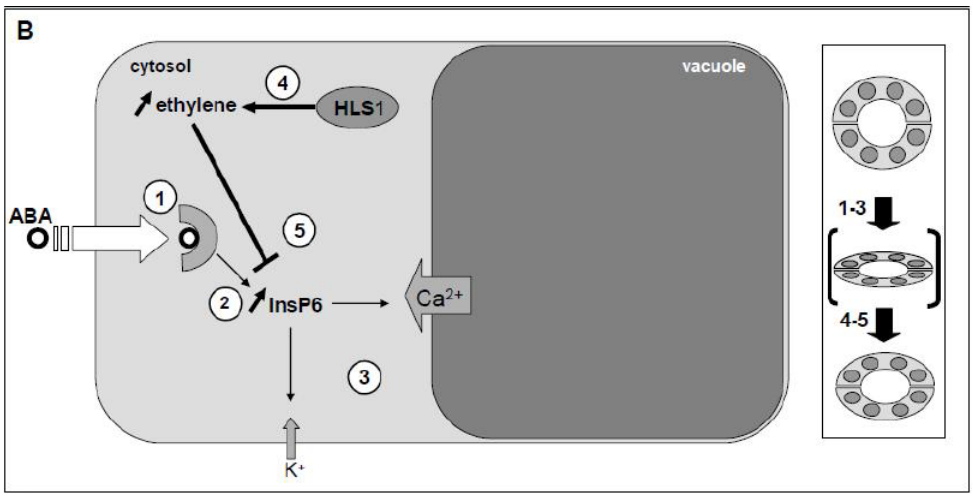

B Model of the mechanism in guard cells of *mrp5* loss of function plants

In the *hls1* mutant Arabidopsis plant the following could happen: *At*MRP5 is still functional and able to remove $InsP_6$ from the cytosol (Fig.8C -1), but since the interaction with *At*HLS1 is missing (Fig.8C -2), this function is impaired and therefore, ethylene levels increase, further opening the stomata and leading to ABA insensitivity (Fig.8C -3).

Figure 8C **Hypothesis of the mechanism of the interaction between *At*HLS1 and *At*MRP5**

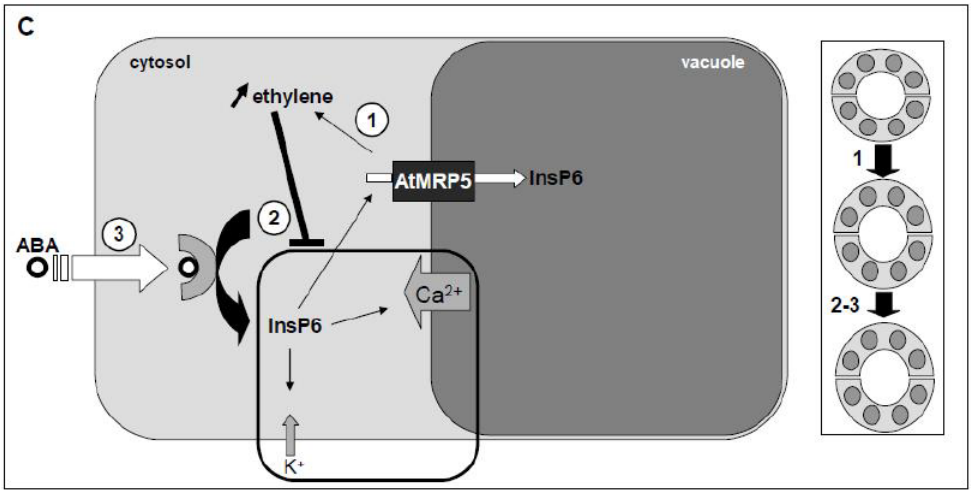

C Model of guard cells in the *hls1* loss-of-function plant background

What happens when AVG (1-aminoethoxyvinylglycine) is added to the stomata buffer? Ethylene synthesis is blocked and in both, *mrp5* and *hls1* mutant plants, ethylene levels cannot increase (Fig.8D-3 und -4) and ABA sensitivity is restored (Fig.8D-1 und -2).

Figure 8D Hypothesis of the mechanism of the interaction between *At*HLS1 and *At*MRP5

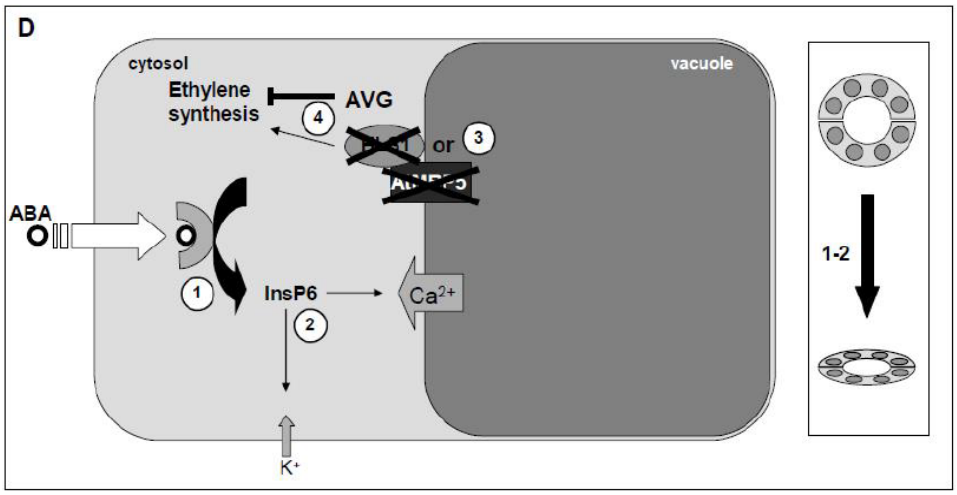

D Expected reaction model for the double knock-out plant guard cells of *mrp5/hls1*

Figure 8: Hypothesis of the mechanism of the interaction between *At*HLS1 and *At*MRP5 A Model of the mechanism in the guard cells of the wild type for ABA perception **B** Model of the mechanism in guard cells of *mrp5* loss of function plants **C** Model of guard cells in the *hls1* loss-of-function plant background **D** Expected reaction model for the double knock-out plant guard cells of *mrp5/hls1*

This still does not fully explain the open stomata of the *hls1* mutant in the dark, because ethylene alone is not known to be able to open stomata in the dark, but auxin is. It was shown that AVG inhibits the auxin-induced stomatal opening in *Vicia faba*. The inhibition of ethylene synthesis in guard cells with AVG did not inhibit the light or the fusicoccin-induced opening of stomata (Clint and MacRobbie, 1984). These findings support the hypothesis that auxin-induced stomatal opening is mediated through auxin-induced ethylene production by guard cells or ethylene induced auxin synthesis (Merritt *et al.*, 2001).

Even tough we never had a clear cut result with the *hls1* mutant kept in the dark (sometimes stomata closed, sometimes they did not, data not shown) and AVG was added to the buffer, it still could be that the stomata remain open, due to the presence of a high level of auxin in guard cells. This could as well explain the opening state of *hls1* stomata in the dark. To prove this, it would be necessary to transforme *hls1 Arabidopsis*

plants with a stomata specific construct for an IAA-lysin synthetase, which conjugates lysin to the auxin molecule and thereby inactivates the free auxin.

Furthermore by producing recombinant HLS1 protein (I made a first attempt which was not successful) and by performing transport assays with yeast vesicles isolated from *At*ABCC5 expressing yeast, iIt will be interesting to investigate, how the interaction between HLS1 and ABCC5 modulate the $InsP_6$ transport activity.

4.6 Supplementary Data

4.6.1 Results

4.6.1.1 AtMRP5 interaction partner search using the conventional yeast two hybrid system

4.6.1.1.1 Crude yeast cytosolic protein extraction and Western blot analysis

After transformation of the bait constructs into yeast, the transcription of the two nucleotide binding domains of *AtMRP5* were confirmed using the Western Blot method. The results showed that both fragments were transcribed and they were detected at the correct protein size (see Fig. 1).

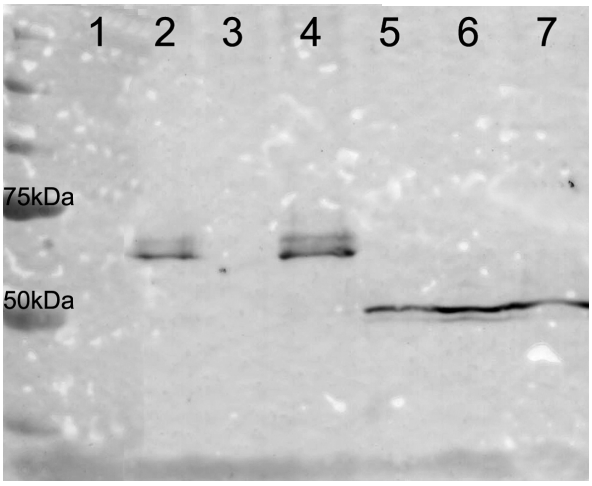

Figure 1 Western Blot analysis of the two bait fragments NBD1 and NBD2 (fFor each fragment, three colonies were examined.). **1** Negative control (LH40 protein extract), **2** NBD1-1, **3** NBD1-2, **4** NBD1-3, **5** NBD2-1, **6** NBD2-2, **7** NBD2-3

4.6.1.1.2 X-Gal assay and Yeast plasmid extraction/verification of positive prey clones

All sequences obtained in the plasmid rescue in E.coli of the positive colonies found in the Yeast Two Hybrid Screen are shown below (for NBD1 and NBD2). Written in bold, the candidates of special interest are marked and were chosen for further studies.

The criteria for follow up studies were: Number of appearance in the assay, involvement in stomatal or root-growth regulatory mechanisms, as well as possible involvement in general aspects of ABC transporter mechanisms.

Table 1A Summary of the retrieved sequences from NBD1 yeast two hybrid screen

ABI code:	**Hits**	**Description:**
At1g07210	1	30S ribosomal protein S18 family
At1g07770	1	RPS15A (RIBOSOMAL PROTEIN S15A)
At1g15385	1	Unknown protein
At1g16000	1	Similar to unknown protein
At1g20330	1	CVP1, FRL1, SMT2 (STEROL METHYLTRANSFERASE 2)
At1g22360	**1**	**UDP-glucoronosyl/UDP-glucosyl transferase Family protein**
At1g23410	1	Ubiquitin extension protein, putative /40S ribosomal protein S27A (RPS27aA)
At1g27350	1	Similar to unknown protein (TAIR:At1g27330)
At1g28190	1	Similar to unknown protein At5g12340
At1g28330	1	DRM1 (DORMANCY-ASSOCIATED PROTEIN 1)
At1g29690	1	CAD1 (CONSTITUTIVELY ACTIVATED CELL DEATH 1); oxidoreductase
At1g30510	1	AtRFNR2 (ROOT FNR 2); oxidoreductase
At1g31812	5	ACBP (ACYL-COA-BINDING PROTEIN); acyl-CoA binding
At1g31817	1	NFD3 (NUCLEAR FUSION DEFECTIVE 3) structural constituent of ribosome
At1g32580	1	Plastid developmental protein DAG, putative
At1g32920	1	Similar to unknown protein At1g32928
At1g33055	2	Unknown protein
At1g33120	1	60S ribosomal protein L9 (RPL90B)
At1g43170	1	EMB2207, RPL3A, ARP1 (ARABIDOPSIS RIBOSOMAL PROTEIN 1)

At1g43900	1	Protein phosphatase 2C, putative / PP2C (short sequence alignment)
At1g50250	1	FTSH1 (FtsH protease 1);ATP-dependent peptidase/ ATPase/ metallopeptidase
At1g50480	1	THFS (10-FORMYLTETRAHYDROFOLATE SYNTHETASE); ATP binding / formate-tetrahydrofolate ligase
At1g51060	1	Histone H2A, putative
At1g52300	2	60S ribosomal protein L37 (RPL37B)
At1g54290	1	Eukaryotic translation initiation factor
At1g55210	1	Disease resistance response
At1g55890	1	Pentatricopeptide (PPR) repeat-containing protein
At1g58684	4	40S ribosomal protein S2, putative
At1g60095	1	Jacalin lectin family protein
At1g61140	1	EDA16 embryo sac development arrest 16); ATP binding / DNA binding / helicase/ protein binding / zinc ion binding
At1g62380	**2**	**AtACO2 (ACC Oxidase 2)**
At1g63800	1	UBC5 (ubiquitin-conjugating enzyme 37)
At1g65520	1	Enoyl-CoA hydratase/isomerase family protein
At1g67430	1	60S ribosomal protein L17 (RPL17B)
At1g70600	1	60S ribosomal protein L27A (RPL27aC)
At1g70830	1	MLP28 (MLP-like protein 28)
At1g72370	1	AP40, RP40, RPSAA, P40 (40S ribosomal protein SA); structural constituent of ribosome
At1g73430	1	Sec34-like family protein
At1g76300	1	SMD3 (SNRNP CORE PROTEIN SMD3)
At1g76650	**1**	**Calcium-binding EF hand family protein**
At2g04795	1	Similar to unknown protein [Arabidopsis thaliana]
At2g05220	1	40S ribosomal protein S17 (RPS17B)
At2g17420	1	AtNTRA (NADPH-dependent thioredoxin reductase 2)

At2g21900	1	AtWRKY59, WRKY59 (WRKY DNA-binding protein 59); transcription factor
At2g28910	**1**	**CXIP4 (CAX Interacting Protein 4)**
At2g29960	**1**	**AtCYP5**
At2g30860	**1**	***A.th*. Glutathione S-transferase (class phi) 9); glutathione transferase**
At2g30870	**1**	**ERD13, AtGSTF4, AtGSTF10 (EARLY DEHYDRATION-INDUCED 13); glutathione transferase**
At2g33585	1	Similar to conserved hypothetical protein [Medicago truncatula] (GB:ABE82600)
At2g34480	1	60S ribosomal protein L18A (RPL18aB)
At2g36220	1	Similar to unknown protein (TAIR:At3g52710)
At2g36460	1	Fructose-bisphosphate aldolase, putativ
At2g37190	2	60S ribosomal protein L12 (RPL12A)
At2g39675	1	TAS1C
At2g42210	1	AtOEP16-3; protein translocase
At2g45990	1	Similar to conserved hypothetical protein (medicago truncatula)
At2g47110	2	UBQ6 (ubiquitin 6); protein binding
At3g02090	1	MPPBETA; metalloendopeptidase
At3g04120	7	GAPC-1: Glyceraldehyde-3-Phosphate dehydrogenase C subunit
At3g04730	1	IAA16 (indoleacetic acid-induced protein 16); transcription factor
At3g04840	1	40S ribosomal protein S3A (RPS3aA)
At3g09200	1	60S acidic ribosomal protein P0 (RPP0B)
At3g10860	1	Ubiquinol-cytochrome C reductase complex
At3g12050	1	Aha1 domain-containing protein
At3g12620	1	Protein phosphatase type 2C (PP2C)
At3g13080	1	AtMRP3

At3g15540	**1**	**MSG2, IAA19 | IAA19 (indoleacetic acid-induced protein 19)**
At3g16640	1	TCTP (TRANSLATIONALLY CONTROLLED TUMOR PROTEIN)
AT3g17920	1	Leucine-rich repeat family protein
AT3g21420	1	Oxidoreductase, 2OG-Fe(II) oxygenase family protein
At3g22330	1	putative DEAD box RNA helicase
At3g22850	1	Similar to unknown protein (TAIR:At5g43830)
At3g23050	**1**	**AXR2, IAA7**
At3g25290	1	auxin-responsive family protein
At3g25660	3	Glutamyl-tRNA(Gln) amidotransferase, putative
At3g25900	1	HMT-1, AtHMT-1; homocysteine S-methyltransferase
At3g25910	1	Similar to unknown protein At3g24740; similar to TRAF-like (m.t.)
At3g28180	1	CSLC04, AtCSLC4 (Cellulose synthase-like C4); transferase, transferring glycosyl groups
At3g28730	1	SSRP1, AtHMG (HIGH MOBILITY GROUP, STRUCTURE-SPECIFIC RECOGNITION PROTEIN 1) transcription factor
At3g28900	1	60S ribosomal protein L34 (RPL34C)
At3g30350	1	Unknown protein
At3g44100	1	MD-2-related lipid recognition domain-containing protein / ML domain-containing protein
At3g45980	1	Histone H2B
At3g48980	1	Similar to unknown protein similar to (TAIR:At5g23850)
At3g49010	1	BBC1, RSU2; structural constituent of ribosome

At3g52590	2	EMB2167, ERD16, UBQ1 (EARLY-RESPONSIVE TO DEHYDRATION 16, UBIQUITIN EXTENSION PROTEIN 1)
At3g53740	1	60S ribosomal protein L36 (RPL36B)
At3g59540	1	60S ribosomal protein L38 (RPL38B)
At3g61240	1	DEAD/DEAH box helicase, putative (RH12)
At3g62250	7	UBQ5 (UBIQUITIN 5); protein binding
At3g62290	**2**	**AtARFA1E (ADP-ribosylation factor A1E); GTP binding / phospholipase activator/ protein binding**
At4g00020	1	MEE43, EDA20, BRCA2(IV), (breast cancer 2 like 2A, embryo sac development arrest 20, maternal effect embryo arrest 43)
At4g00026	1	Similar to expressed protein (Oryza sativa; GB: ABF95014)
At4g01590	**1**	**Similar to unknown protein (TAIR:At4g35680); similar to Calcium-binding EF-hand [Medicago truncatula]**
At4g05050	1	UBQ11 (UBIQUITIN 11); protein binding
At4g05320	2	UBQ10 (POLYUBIQUITIN 10); protein binding
At4g08900	1	Arginase (just a few nucleotides; bad alignment)
At4g12420	**1**	**SKU5**
At4g13850	1	AtGRP2 (Glycin-rich RNA-binding Protein 2)
At4g14270	2	Protein containing PAM2 motif which mediates interaction with the PABC domain of polyadenyl binding proteins.
At4g16380	1	Metal ion binding protein
At4g20280	1	Transcription initiation factor IID (TFIID) 28 kDa subunit (TAFII-28) family protein
At4g22030	1	F-box family protein (short sequence alignment)

At4g24920	7	Protein transport protein SEC61 gamma subunit, putative
At4g26230	1	60S ribosomal protein L31 (RPL31B)
At4g27090	1	60S ribosomal protein L14 (RPL14B)
At4g27130	1	Eukaryotic translation initiation factor
At4g27450	1	Similar to unknown protein (TAIR:At3g15450)
At4g28910	1	Similar to nuclear transport factor 2 (NTF2)
At4g29040	**4**	**RPT2A | RPT2A (regulatory particle triple-A 2A); ATPase**
At4g29430	1	RPS15AE (ribosomal protein S15A E)
At4g30270	1	MERI-5, BRU1 (MERISTEM-5); hydrolase, acting on glycosyl bonds
At4g31490	1	Coatomer beta subunit, putative
At4g37580	**1**	**COP3, HLS1 | HLS1 (HOOKLESS 1)**
At4g39090	1	RD19A, EMB3005 (RESPONSIVE TO DEHYDRATION 19); cysteine-type peptidase
At5g01540	1	Lectin protein kinase, putative (short sequence)
At5g01650	3	Macrophage migration inhibitory factor family protein / MIF family protein
At5g01980	1	Zinc finger (C3HC4-type RING finger) family protein
At5g02450	1	60S ribosomal protein L36 (RPL36C)
At5g03380	1	Metal ion binding
At5g06380	1	Similar to unknown protein (TAIR:At3g11690)
At5g08130	1	BIM1 (BES1-interacting Myc-like protein1); DNA binding / transcription factor
At5g08570	3	Pyruvate kinase, putative
At5g12140	1	AtCYS1 (A. THALIANA CYSTATIN-1);cysteine protease inhibitor
At5g14090	1	Similar to unknown protein At3g27025
At5g14570	1	Promoter of AtNDRT2.7
At5g15200	3	40S ribosomal protein S9

At5g18490	1	Similar to unknown protein (TAIR:At1g04090)
At5g19860	1	Similar to unknown protein
At5g20290	1	40S ribosomal protein S8 (RPS8A)
At5g20950	1	Glycosyl hydrolase family 3 protein
At5g21105	1	L-ascorbate oxidase/ copper ion binding
At5g24300	1	SSI, AtSS1 (STARCH SYNTHASE I); transferase, transferring glycosyl groups
At5g25180	4	CYP71B14 (Cytochrom P450, family 71, subfamily B, polypeptide 14)
At5g25280	1	Serine-rich protein-related (just 48bp)
At5g37740	**4**	**C2 domain-containing protein**
At5g40530	1	Similar to protein of unknown function DUF691 (methyltransferase; Medicago truncatula)
At5g51040	3	Similar to Protein of unknown function DUF339 [Medicago truncatula]
At5g54660	1	Heat shock protein-related
At5g54940	1	Eukaryotic translation initiation factor SUI1, putative
At5g57290	1	60S acidic ribosomal protein P3 (RPP3B)
At5g59660	1	Leucine-rich repeat protein kinase, putative
At5g59850	1	40S ribosomal protein S15A (RPS15aF)
At5g60030	1	Similar to unknown protein (TAIR:At1g56660)
At5g60340	1	MaoC-like dehydratase domain-containing
At5g60670	2	60S ribosomal protein L12 (RPL12C)
At5g62300	1	40S ribosomal protein S20 (RPS20C)
At5g62770	1	Similar to unknown protein At1g23710
At5g63460	1	SAP domain-containing protein
At5g66985	4	Unknown protein
At5g67560	**1**	**AtARLA1D (ADP-ribosylation factor-like A1D); GTP binding**
Total	*208*	

Table 1B Summary of the retrieved sequences from NBD2 yeast two hybrid screen

ABI code:	**Hits**	**Description:**
At5g20520	1	WAV2 | WAV2 (WAVY GROWTH 2)
At5g67560	**2**	**AtARLA1D (ADP-ribosylation factor-like A1D); GTP binding**
At5g25180	4	CYP71B14 (cytochrome P450, family 71, subfamily B, polypeptide 14); O2 binding
At4g40040	2	Histone H3.2
At1g31812	1	ACBP (ACYL-COA-BINDING PROTEIN)
At5g21105	3	L-ascorbate oxidase/ copper ion binding
At3g28180	1	CSLC04, AtCSLC4 (Cellulose synthase-like C4); transferase, transferring glycosyl groups
At3g11910	1	Ubiquitin-specific protease, putative
At3g01470	1	AtHB1, HD-ZIP-1, HAT5 (Homeobox-leucine zipper protein HAT5); transcription factor
At5g20720	1	CPN10, CHCPN10, AtCPN21, CPN20 (CHAPERONIN 20)
At5g01650	1	Macrophage migration inhibitory factor family protein
At3g56050	1	Protein kinase family protein
At5g65165 or	1	Succinate dehydrogenase 2-3 or
At3g45090	1	2-phosphoglycerate kinase-related
At1g03560 or	1	Pentatricopeptide (PPR) repeat-containing protein or
At5g59660 or	1	Leucine-rich repeat protein kinase, putative or
At4g22030 or	1	F-box family protein or
At1g65010	1	Similar to protein transport protein-related similar to Protein kinase PKN/PRK1,effector [Medicago truncatula]
At2g03590	1	AtUPS1 (Arabidopsis thaliana ureide permease 1); allantoin transporter

At4g24920	1	Protein transport protein SEC61 gamma subunit, putative
At1g76650	1	Calcium-binding EF hand family protein
Total	*24*	

4.6.1.1.3 Co-immunoprecipitation of potential interaction partners of *At*MRP5

Western blot analysis of Co-immunporecipitation experiments showed a band for immunoprecipitate of *At*4g01590 at a size of about 20 kDa. *At*4g01590 encodes for an unknown protein in *Arabidopsis thaliana*, but is similar to a Calcium-binding EF hand protein in *Medicago truncatula* and has the size of 22,2 kDa. This result indicates that this unkown protein with similarities to a Calcium-binding EF hand protein interacts with MRP5. Nevertheless, no altered stomatal aperture size was seen, compared to wild type plants.

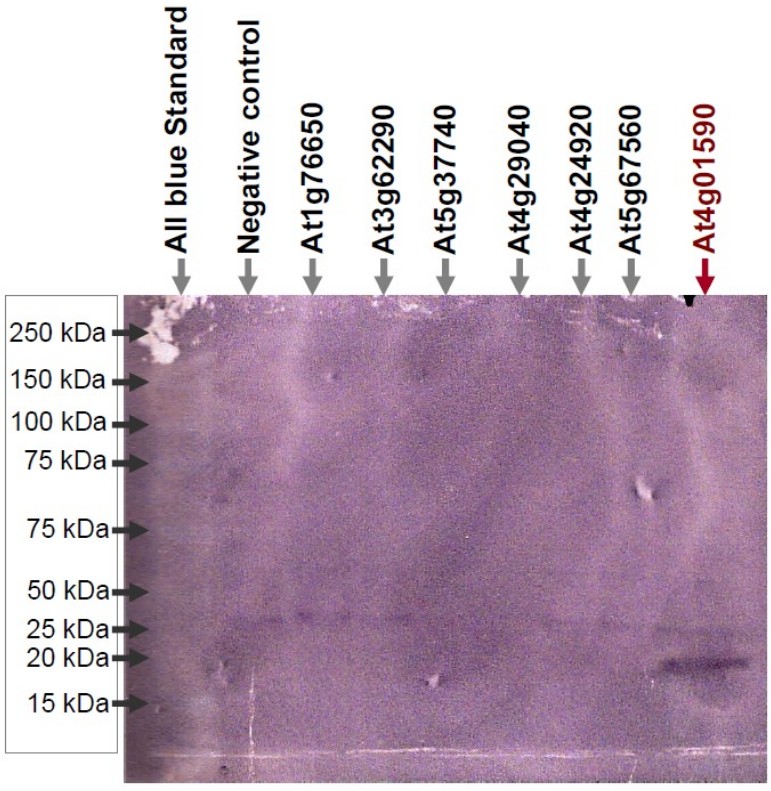

Figure 9
Western Blot results of co-immunoprecipitation analysis of selected positive colonies from yeast two hybrid assay. A band of about 20 kDa is visible in the lane of co-immunoprecipitate of *At*MRP5 with the protein from *At*4g01590.

4.6.1.1.4 Screen for altered stomatal aperture

Selected leaves of mutant plants (written in bold in Table 1A and B) and their corresponding wild types were incubated for 2.5h in the light or the dark and stomatal apertures were measured (see material and methods). For the mutant Arabidopsis plants with T-DNA insertions in the genes At1g22360, At1g62380, At2g28910, At2g29960, At2g30860, At2g30870, At3g15540, At3g23050, At3g62290, At4g01590, At4g29040, At5g37740, At5g67560, At5g67560 no significant differences in stomatal aperture compared to the wild type were observed (Data not shown). For the knock-out plants in At4g37580 (Hookless 1) and At1g76650 (a Calcium binding EF hand family protein) alterations in stomatal aperture were found. Since *hookless 1* related results were discussed before, here I report only about the differences in apertures of the Ca^{2+} binding EF hand family protein in the *Arabidopsis thaliana* mutant (At1g76650; SALK_066538c). As shown in Fig. 9 the stomata of Ca^{2+} binding EF hand family protein *Arabidopsis thaliana* mutant have a smaller aperture size in light conditions as compared to those of wild-type and mrp5-1 mutant plants.

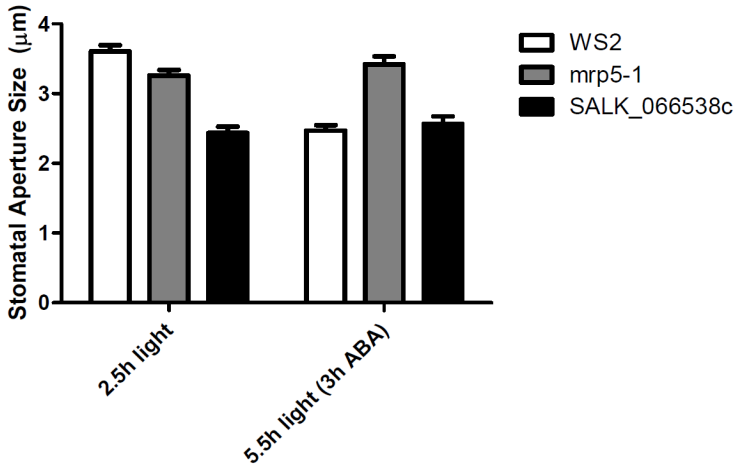

Figure 10
Measurements of the average stomatal aperture (µm) from epidermal strips of the SALK_066538c line (insertion mutant of A1t76650), the *mrp5-1* mutant and their corresponding wild type plants (Wasslevskayia). Excised leaves were kept on stomatal buffer in the light for 2.5h and measured subsequently ABA (5µM) was added and leaves were kept in the light for additional 3h. Error bars represent the standard errors.

The guard cells of the Ca^{2+} binding EF hand family protein *Arabidopsis thaliana* mutant show no reaction towards ABA, a behavior similar to the mrp5-1 mutant. However, this result could also reflect the nearly closed stomata even in the light.

4.6.1.2 Material and Methods

4.6.1.2.1 *At*MRP5 interaction partner search using the conventional yeast two hybrid system

The Yeast Two Hybrid bait plasmid pLexA_kan and the two amplified fragments NBD1 and NBD2 were digested with EcoRI and BamHI for 3 hours at 37°C and subsequently purified using the PCR Clean-up Wizard kit (Promega). The ligation was performed over night at 16°C using T4 ligase, according to the protocol of the T4 ligation kit (Promega). After incubation the entire reaction mix was transformed into the *Escherichia coli* strain Dh10b via the heat shock method (Oishi and Cosloy, 1972). Plasmids present in growing colonies were first controlled by restriction enzyme digestion (EcoRI, BamHI) and subsequently by sequencing. A sequencing reaction was set up, consisting of 6.25 µl MilliQ water, 1.5 µl BigDye buffer, 0.25 µl sequencing primer for primer pLexA-s ((5'-ccaattgtcgttgacctt-3'); approx. 5 pmol/µl), 1 µl template DNA (approx. 200 ng) and 1 µl BigDye. The Sequencing PCR was placed in a Thermocycler (sequencing PCR program: 1. 94°C for 2 min, 2. 96°C for 10 sec, 3. 50°C for 5 sec, 4. 60°C for 3 min, step 2 to 4 were repeated 60 times). The PCRs were cleaned via sepharose columns and loaded into the ABI3730 sequencing machine. Sequences were blasted on the TAIR homepage.

4.6.1.2.2 Transformation of the bait constructs into competent cells of the yeast strain LH40

Yeast cells of the strain LH40 (MATa, trp1, leu2, his3; LYS2::lexA-His; URA3::lexA-lacZ) were grown overnight in 5 ml YPAD liquid media at 28°C, by shaking at 150 rpm to an OD_{600} between 0.6 and 0.8. Cells were centrifuged at 4'000 rpm for 5 minutes and the pellet was resuspended in 4 ml ice-cold solution A (1 M sorbitol, 10 mM Bicine-NaOH (pH 8.35), 3% ethyleneglycol). The suspension was centrifuged again at 4'000 rpm for 5

minutes and resuspended in 2 ml of ice-cold solution A. The cells were then split in 200 µl aliquots and frozen at -80°C. This freezing procedure revealed to produce better competent cells than freezing in liquid nitrogen.

In order to transform competent yeast cells with the corresponding plasmid, a transformation mix of 10 µl was prepared, including 50 µg salmon sperm DNA (10 mg/ml; denatured at 96°C for 5 minutes and cooled down on ice), 1 µl of construct pLexA-kan_NBD1 or pLexA-kan_NBD2 (approx. 5 µg) and 4 µl of sterile ddH_2O. The 10 µl transformation mix was directly placed on top of the frozen competent cells and incubated for 5 minutes by shaking at 37°C. 1 ml of solution B (40% PEG and 0.2 M Bicine-NaOH (pH 8.35)) was added to the cell suspension and incubated for one hour at 28°C. After centrifugation at 3'000 rpm for 5 minutes, the pellet was resuspend in 1 ml of solution C (0.15 M NaCl and 10 mM Bicine-NaOH (pH 8.35)), centrifuged again (same conditions as mentioned before) and resuspend in 100 µl solution C. Cells (containing approximately 10^8 cells) were plated on SD plates lacking the amino acid tryptophan.

4.6.1.2.3 Crude yeast cytosolic protein extraction and Western blot analysis

The samples were incubated for 10 minutes at 65°C in protein sample buffer (5x protein sample buffer: 60 mM Tris-HCl (pH 6.8), 15% SDS, 39% glycerol, 0.1% bromophenol blue and 6.25% ß-mercaptoethanol). The denatured cytosolic protein samples and the ladder (Precision Plus Protein All Blue Standards; BioRad) were loaded on a SDS Lämmli gel consisting of a 4%* stacking and a 7%** resolving gel (6,1ml* / 5.1 ml** ddH_2O, 1,3 ml* / 2,3 ml** 30% Degassed Acrylamide/Bis, 2,5 ml 0.5 M Tris-HCl, pH6.8* or 2,5 ml 1.5 M Tris-HCl, pH8.8**, 0,1ml 10% SDS*/**, 5 µl* / 10 µl** TEMED, 50 µl 10% APS*/**) and run at 100 Volt in a Bio-Rad vertical electrophoresis chamber filled with running buffer. The gel was incubated for 5 minutes in transfer buffer (800 ml of 60 mM Tris, 50 mM glycine, 0,05 % SDS in ddH_2O plus 200 ml Methanol) and then was carefully transferred on a nitrocellulose membrane (Schleicher&Schüll) for protein transfer using a Trans-Blot SD semi-dry blotter (BioRad; 40 minutes at 16 Volts). After 40 minutes the nitrocellulose membrane was removed from the stack, incubated over night in blocking buffer (washing buffer plus 1% BSA). Afterwards, the membrane was incubated in blocking buffer containing the primary antibody (anti-LexA, mouse monoclonal antibody, Dualsystem; 1:3000 dilution; 3 hours, shaking at room

temperature). The nitrocellulose was subsequently washed three times for 5 minutes with washing buffer (10mM Tris-HCl pH7.5, 150 mM NaCl), before applying the secondary antibody (anti-mouse-antibody linked to a alkaline phosphatase) for one hour at room temperature (slowly shaking). After incubation with the secondary antibody the membrane was washed three times in washing buffer and once in alkaline phosphatase buffer (100 mM Tris, 100mM NaCl and 5mM $MgCl_2$). Detection with NBT and BCIP was performed according to the protocol provided by the supplier (Roche Applied science).

4.6.1.2.4 Defining the amount of 3-Amino-1,2,4-triazole in screening plates to reduce false-positive clones

Five µl of yeast cells of the LH40 strain in liquid culture, containing the bait construct pLexA-kan_NBD1 or pLexA-kan_NBD2 and the empty prey vector pACT2 (transformed into bait containing yeast cells like mentioned above) were dropped on either non-selective YPAD plates (positive control), selective SD plates lacking tryptophan, histidine and leucine, comprising different concentrations of 3-Amino-1,2,4-triazole (0 mM, 5 mM, 10 mM, 15 mM, 20 mM, 25 mM, 30 mM, 35 mM, 40 mM, 45 mM, 50 mM) or SD plates containing no amino acids (negative control). The plates were incubated at 30°C for 3 days.

4.6.1.2.5 High efficiency transformation of a cDNA library (prey) into yeast containing the bait constructs

Competent yeast cells carrying the bait constructs were thawed on ice (each batch; approx. 10^8 cells), centrifuged (5 minutes at 3'000 rpm; 4°C) and the supernatant was removed. A transformation mix (360 µl) was prepared, consisting of 240 µl PEG 3500 50%, 0.1 M LiAc (36µl 1 M LiAc), 50 µl boiled single-strand-carrier DNA (10 mg/ml, salmon sperm DNA) and 34 µl cDNA library (1 µg/µl). The transformation mix was pipetted on top of the cells, vigorously vortexed and incubated for 40 minutes at 42°C. Afterwards, the cells were centrifuged (5 minutes at 3'000 rpm; RT) and the supernatant removed. 10 ml of sterile MilliQ water were added to the pellet and the pellet was resuspended. 0.5 ml aliquots of cell suspension were plated on big round plates (Ø145 mm; Greiner) containing SD media lacking tryptophan, leucin and histidine, until all 10ml were distributed. The plates were incubated for 3 to 4 days at 30°C.

4.6.1.2.6 X-Gal assay of grown yeast colonies on screening SD plates

A sterile circular nitrocellulose membrane disc was placed on the plate and the position of the disc was marked three times with a sterile needle. After that, the nitrocellulose was placed in order to have full contact to yeast colonies and the plate surface. Afterwards the membrane was removed carefully and frozen with liquid nitrogen. The membrane was shortly thawed and placed on a round Petri dish (Ø145 mm; Greiner), containing a Whatman paper disc, soaked with Z-buffer (Z buffer: 60 mM $NaHPO_4 \cdot 2H_2O$, 40 mM $NaH_2PO_4 \cdot H_2O$, 10 mM KCl, 1 mM $MgSO_4 \cdot 2H_2O$, freshly added 38.5 mM ß-mercaptoethanol, 1 mg/ml X-G*al.*) and incubated at 30°C for at least 30 minutes (incubation was stopped after the first colonies turned deep blue). Positive yeast colonies were picked, the prey plasmid rescued, transformed into *E.coli* and the harvested plasmid sequenced (see Table 1). To see if there were strong interactions, a Co-immunoprecipitation was performed using a non-denaturing protein extraction method and the Dynabead system from Sigma Aldrich. Co-immunoprecipitates were loaded on a polyacrylamid gel and a Western blot was performed (see Appendix)

4.6.1.2.7 Yeast plasmid extraction and verification of positive prey clones

Yeast plasmid extraction was basically carried out with the GeneElution HD Plasmid Miniprep Kit (Fermentas) with slight modifications (resuspension, lysis and neutralization solution: 1.5 fold more was added, than stated in the protocol). A 5 ml overnight yeast culture was spun down, resuspension solution and sterile glass beads (Ø0.5 mm) were added (filled approximately to the 300 µl mark in a 1.5 ml centrifugation tube) and the suspension was vortexed to resuspend the pellet. Lysis solution was added to the suspension and the mix was vortexed for 5 minutes. Subsequently the solution was neutralized with neutralization buffer. Afterwards the usual protocol provided with the kit was followed. The plasmid extract was then transformed with the heat shock method into competent cells of the *Escherichia coli* strain DH10b. Colonies were picked, grown in 5 ml selective liquid LB media and a plasmid extraction was performed using the GeneElution HD Plasmid Miniprep Kit (Fermentas). A sequencing reaction was set up with the sequencing primer for pACT2 (5'-TACCACTACAATGGATG-3'; approx. 5 pmol/µl) and the sequencing was performed as mentioned before using an ABI sequencer.

4.6.1.2.8 Co-immunoprecipitation of potential interaction partners of *At*MRP5

Depending on the growth stage of the yeast colonies carrying the bait and prey construct, the co-immunoprecipitation was performed either directly with the colonies grown on selective plates or the candidate from the library was amplified again via PCR and cloned into pACT2 (list of primers and PCR program see appendix). These constructs were then transformed in competent yeast cells containing the bait construct (transformation procedure mentioned above).

Yeast cells containing the bait and the prey construct of interest were grown in 10 ml selective liquid SD media (lacking tryptophan, histidine, leucin) overnight by shaking at 30°C to an OD_{600} of 0.5. At this OD the cells were harvested and spun down for 10 minutes at 4'500 g. The pellet was washed with MilliQ water and centrifuged again at 4'500 g for 10 minutes and subsequently resuspended in 500 µl breaking buffer (20 mM HEPES-KOH; pH 7.6; 100 mM KCl; 1 mM Pefablock; Complete Protease Inhibitor mix tablet, Roche). Washed glass beads were added, as far as at least three-quarter of the suspension filled up the spaces in between the glass beads. The tubes were placed in a vortex with a shaking top piece at 4°C and harshly vortexed for 40 minutes. The suspension was collected and centrifuged for 10 minutes at 4'500 g. The supernatant was removed and centrifuged at 12'000g for 10 minutes. The soluble protein extract was transferred in a fresh tube mixed 1:1 with immunoprecipitation buffer (50 mM Tris-HCl; pH 7.6; 150 mM KCl; 1 mM EDTA; 0.2% Nonidet P-40; complete protease inhibitor mix, Roche). Mouse monoclonal anti-LexA antibodies were added in a 1:3000 dilution and incubated at 4°C on a rotatory shaker for 3 hours. In 1 ml immunoprecipitation reaction (consisting of the soluble protein extract, immunoprecipitation buffer and antibody), 30 µl of Dynabeads coated with protein G were added and placed overnight on a rotatory shaker at 4°C. The Dynabeads were fixed to the wall of the tube with a magnetic rack and the supernatant was removed. The beads were washed twice with TNET (700 mM NaCl; 250 mM Tris pH 7-8; 25 mM EDTA pH 7.7; 5% Triton X-100) and then twice with TNE (TNET without Triton X-100). The supernatant was removed; Lämmli buffer was added to the beads and boiled for 10 minutes. The samples were loaded on a SDS-Page and a Western blot was performed as described previously. The only difference to the described procedure was that two identical Western blots were carried out to allow

the detection with two different antibodies (mouse monoclonal anti-LexA for NBD1/NBD2 and mouse monoclonal anti-HA antibody for library fragments, Dualsystems).

4.6.1.2.9 Screen for altered stomatal aperture

The following T-DNA insertion mutants were selected for the screen:

Table 2 T-DNA insertion mutant selection for stomatal aperture screen

AGI code	**Gene**	**T-DNA insertion mutant**
*At*2g28910	CXIP4 (CAX Interacting Protein 4)	GABI_527C02
*At*1g22360	UDP-glucoronosyl/UDP-glucosyl transferase family protein	SALK_045078
*At*1g62380	*At*ACO2 (ACC Oxidase 2)	SALK_027311c
*At*1g76650	Calcium-binding EF hand family protein	SALK_066538c
*At*2g29960	*At*CYP5	SALK_065887
*At*2g30860	*A.th*. Glutathione S-transferase (class phi) 9)	SALK_148672
*At*2g30870	ERD13 (EARLY DEHYDRATION-INDUCED 13), *At*GSTF10 (glutathione S-transferase)	SALK_072918
*At*3g15540	IAA19 (indoleacetic acid-induced protein 19)	SALK_000337
*At*3g23050	AXR2, IAA7	SALK_089809
*At*3g62290	*At*ARFA1E (ADP-ribosylation factor A1E)	GK835H10
*At*4g01590	Similar to unknown protein (TAIR: *At*4g35680); similar to Calcium-binding EF-hand [Medicago truncatula]	RAFL 15-01-E05
*At*4g12420	SKU5	SALK_070056
*At*4g29040	RPT2A (regulatory particle triple-A 2A); ATPase	SALK_005596
*At*4g37580	HOOKLESS 1 (COP3, HLS1)	SALK_136528

*At*5g37740	C2 domain-containing protein	SALK_038969
*At*5g67560	*At*ARLA1D (ADP-ribosylation factor-like A1D); GTP binding	SALK_045932

4.6.1.2.10 Verification of homozygous mutant plants

Mutant plants, containing a T-DNA insertion in the genes of interest, were tested for homozygocity with gene specific primers. Primers were ordered at Microsynth laboratories (www.microsynth.ch) and are listed in Table 3.

Table 3 Primer list for homozygous test

SALK_066538c	At1g76650	Ca2+ bdg. EF hand family protein
sense	5' - GATTGATGCTGTTGGTACCAAG - 3'	
antisense	5' - GAGCAAACTCATCAAAGC - 3'	
SALK_005596	At4g29040	AtRPT2A
sense	5' - GATTGATGCTGTTGGTACCAAG - 3'	
antisense	5' - GAGAGTCATCTTCGATGTGTG -3'	
N480158	At3g62290	AtARFA1E
sense	5'- GTGTGGGATGTCGGGGGTC - 3'	
antisense	5' - CACAGCATCTCTCAACTCATC - 3'	
SALK_045932	At5g67560	AtARLA1D
sense	5' - GAGAGAAGTCAACTCTCTG - 3'	
antisense	5' - CGAGTTCATTGCATGTTTTG - 3'	
SAIL_106_D06	At4g01590	similar to Ca2+-bdg. EF hand family protein (Medicago)
sense	5' - ATTTGCGCTTACTAATCTG - 3'	
antisense	5' - CTCCATCGTAATCGAACTG - 3'	
SALK-027311c	At1g62380	AtACO2
sense	5' - CATGAAGTTTCCAGTAGTAG - 3'	
antisense	5' - CCCAATCGACATCTTCGAC - 3'	
SALK_065887	At2g29960	AtCYP5

sense	5' - CAGTGGAGAACTTCCTCTC - 3'	
antisense	5' - GTGACACGAAATCTCTGTGG - 3'	
SALK_089809	At3g23050	AtAXR2
sense	5' - CAAGGAAACTATGGAGCAC - 3'	
antisense	5' - GGTAGAGACAAAGCCAAAG - 3'	
GABI_527C02	At2g28910	AtCXIP4
sense	5' - GAGGAGGTGAGTAGTGAAGAG - 3'	
antisense	5' - GACAGACGTGTGAAGAGAAAG - 3'	
SALK_070056	At4g12420	AtSKU5
sense	5' - CTGTGGTGCTCTCAGCAAAC - 3'	
antisense	5' - CAAGTCAGAGAAATCCAAC -3'	
GABI_235G01	At1g22360	UDP-glucuronosyl/-glucosyl transferase family protein
sense	5' - CACCGTCAAACCCAAACG - 3'	
antisense	5' - GTATACAGGATCAGAGCCAGC - 3'	
SALK_136528	At4g37580	Hookless1
sense	5' - CTCGCTTACGTCTTGGGCCTTC - 3'	
antisense	5' - GTACAACGTCTCAGCATC - 3'	
SALK_148672	At2g30860	GSTF9
sense	5' - ACACACGTTTCCACCAATC - 3'	
antisense	5' - GAAGCAAAGTGAGGTCCGTAC - 3'	
SALK_082482	At2g30870	ERD13
sense	5' - GCCACCTATACCGACACG - 3'	
antisense	5' - CTCCCTTCTCCACCAATG - 3'	
SALK_016641	At3g12620	PP2C
sense	5' - CACGGTAATGCGAGTTG - 3'	
antisense	5' - TCAGCAACTCGCATTACCGTG - 3'	
SALK_000337	At3g15540	IAA19
sense	5' - GAGGTTTCGGTTACTACATATCC - 3'	
antisense	5' - CTCAACCTCTTGCATGACTC - 3'	

SALK_038969	At5g37740	C2 domain containing protein
sense	5' - CAGAGGTGGCTCGAGGCAG - 3'	
antisense	5' - CAGTTCAATAAACGCATCAG - 3'	

To verify if the primers bind to gDNA, they were tested on Col-0 wild type gDNA. The isolated gDNA from T-DNA mutants was amplified with PCR Method and gene specific primers. Samples were loaded on a 1% agarose gel and the bands visualized using ethidium bromide.

Plant gDNA was isolated with the CTAB method. 1-2 leaves of mutant or wild type plants were collected in a 1.5 ml centrifugation tube and frozen in liquid nitrogen. After grinding the frozen leaves with a pre-frozen pistil, 700 µl of 2xCTAB (100 mM Tris-HCl pH8.0, 1.4 M NaCl, 20 mM EDTA pH 8.0, 2% (w/v) CTAB) were added. The samples were placed at 68°C for 30 min, frequently shaken and centrifuged afterwards for 5min at 13'000 rpm. The supernatant was transferred in a fresh 1.5 ml centrifugation tube and 3 µl of RNAse (10mg/ml) were added and the samples were incubated for 30 min at 37°C. The mix was extracted with one volume of phenol:choloroform:isoamylalcohol (25:24:1) and centrifuged at 13'000 rpm for 5 min. To remove phenol traces, one volume of chloroform:isoamylalcohol (24:1) was added and vortexed for 1 min. The mix was centrifuged for 5 min at 13'000 rpm. The supernatant was subsequently transferred into a new tube and gDNA was precipitated with 2.5 volumes of ice-cold 100% ethanol at -20°C overnight. After 30 min centrifuation at 13'000 rpm and 4°C, the supernatant was discarded; the pellet was washed with 80% ethanol and spun down again. Subsequently, the pellet was dried and finally resuspended in ddH_2O. The retrieved gDNA was used for PCR reactions with the following set up: 2 µl template gDNA, 1.25 µl dNTPs, 2.5 µl 10xbuffer, 1 µl sense primer, 1 µl anti-sense primer, 0.25 µl Taq polymerase (all information about the single components can be found in the Appendix, as well as the PCR program).

4.6.1.2.11 Localization of *At*MRP5

A) Construction of the Localization Vector pMDC83_*pMRP5::AtMRP5*

To achieve the promoter of *AtMRP5*, ~1900bp prior to the start codon of *AtMRP5* were amplified (Gaedeke *et al.,* 2001) using the following primers:

promMRP5-s	CCCAAGCTTGTGGAAGAACGTAGAATTCCC
promMRP5-as	TCCACTAGTCATGATCGGGAAAGATTTGTG

Underlined sequencer indicates the restriction sites; sense primer: HindIII; antisense primer: SpeI

The promoter was amplified with the GoTaq Polymerase and the reaction set up as written in the protocol delivered with the GoTaq Hot Start Polymerase (Promega). The Gateway plasmid pMDC83 (already containing a gene, practicability reasons) was chosen as a vector (map see appendix). The inserts, as well as the plasmid pMDC83 restricted with HindIII and SpeI for 2 h at 37°C. A ligation reaction with a T4 ligase was performed over night at 16°C (ligation reaction: 3 µl insert, 1µl plasmid, 4 µl ddH_2O, 1 µl T4 ligase buffer, 1µl T4 ligase). *Escherichia coli* strain DH5alpha was transformed with the ligation reaction mix and bacteria were grown on selective media. Several colonies were picked, DNA was extracted (Fermentas Miniprep Kit) and sent for sequencing. The sequencing reaction was performed with a sense primer in the sequence of pMDC83, upstream of the promoter region (5'-ccaacttaatcgccttgcagc-3') and an antisense primer, situated in the start region of the present gene (5'-ccaatcttgtactgatggacg-3'). After detecting a positive clone a LR reaction was performed with the pDONRZeo containing *AtMRP5* (according to the protocol of the Gateway system) and *E.coli* were transformed with the reaction mixture. Colonies were picked and verified by growing them in liquid culture medium; DNA was extracted (as mentioned above) and digested with Asc/Pac. Since the LR reaction involves no amplification step, the promoter was not sequenced again.

B) Complementation of *mrp5-1* plants

The correct pMDC83_*pMRP5::*MRP5 plasmid was transformed into the *Agrobacterium tumefaciens* strain GV3101 via electroporation. Firstly the electroporation Gene® Pulser cuvette (BioRad; Cat.No.165-2089) was washed with 70% EtOH and sterilized for 10

min on a UV screen. After sterilization the cuvette was packed in Parafilm and placed on ice. Bacteria were thawed on ice and 40 µl of the solution was gently mixed with 1 µl DNA (~300ng/µl). 1 ml of liquid LB media for each transformation was placed on ice. The Micropulser (BioRad, more details see appendix) was set to the appropriate conditions (RAISE: 1.4kV; LOW CAP: 25; LOW RANGE: 200; HIGH RANGE: infinite) and the mixture was transferred into the ice-cold electroporation cuvette to avoid bubbles. The cuvette was placed in the chamber slide. The chamber was closed and the pulse was given. The cuvette was rapidly removed and 1ml ice-cold LB was immediately added to avoid over-heating of the bacteria. The mix was transferred to a 2 ml centrifugation tube and incubated for 2-3 h at 28°C (shaking at 200 rpm), then struck out on selective media and incubated for 48 h at 28°C. Pre-cultures (25 ml) were initiated from single bacterial colonies and served as inoculum for a 400 ml selective liquid culture and grown until an OD_{600} of 1-1.5. *At*MRP5 loss-of-function plants were grown in the greenhouse until flowering and transformed according to the floral dip method (Clough and Bent, 1998).

Seeds were harvested and selected on $^1/_2$MS containing 1% sucrose and 25µg/ml Hygromycin until T_3 was reached.

C) Subcellular localization of *At*MRP5 using the confocal microscope

An *AtMRP5–GFP* construct under the control of the native *AtMRP5* promoter was used to transform *mrp5-1* plants. Since the GFP signal was very weak, vacuoles were released by osmotic lysis from leaf protoplasts isolated from homozygous T3 plants subjected 14 d to drought stress (*AtMRP5* is drought induced and no signal could be obtained in well-watered plants). To verify vacuolar localization, images were captured with a laser scanning confocal microscope with a 63X magnification objective, and an appropriate zoom. Differential interference contrast (DIC) image, fluorescence signal in green, corresponding to GFP (emission_em= 500-530nm) and a chlorophyll autofluorescence signal in red (emission _em= 620-750nm) were taken and images were merged with Adobe Photoshop.

4.7 References

Adams, C., Norby, S. W., and Rinne, R. W. (1985). Production of multiple vacuoles as an early event in the ontogeny of protein bodies in developing soybean seeds. Crop Science 25, 255-262

Anderson, M.P., Gregory, R.J., Thompson, S., Souza, DW ., Paul, S., Mulligan, R.C., Smith, A.E ., and Welsh, M.J. (1991). Demonstration, that CFTR is a chloride channel by alteration of its anion selectivity. Science **253**: 202-205

Assmann, S.M., and Shimazaki, K. (1999). The Multisensory Guard Cell. Stomatal Responses to Blue Light and Abscisic Acid. Plant Physiology **119**: 809-816

Babenko, A.P., Aguilar-Bryan, L., and Bryan, J. (1998). A View of SUR/K_{IR}6.X, K_{ATP} channels. Ann. Rev. of Physiology **60**: 667-687

Bar-Yosef, B., Kafkafi, U., and Bresler, E. (1972). Uptake of Phosphorus by Plants Growing Under Field Conditions: I. Theoretical Model and Experimental Determination of its Parameters. Soil Sci Soc Am Journal **36**: 783-788

Bauer, H., Ache, P., Lautner, S., Fromm, J., Hartung, W., Al-Rasheid, K.A.S., Sonnewald, S., Sonnewald, U., Kneitz, S., Lachmann, N., Mendel, R.R., Bittner, F., Hetherington and Hedrich, R. (2013). The stomatal Response to reduced relative humidity requires guard cell – autonomous ABA synthesis. Current Biology **23(1)**: 53-57

Bentsink, L., Yuan, K., Koornneef, M., and Vreugdenhil, D. (2003). The genetics of phytate and phosphate accumulation in seeds and leaves of Arabidopsis thaliana, using natural variation. Theor Appl Genet 106, 1234-1243

Bittisnich, D.J., Entwisle, L.O., and Neales, T.F. (1987). Acid-Induced Stomatal Opening in *Vicia faba* L. and the Role of Guard Cell Wall Elasticity. Plant Physiology **85**: 554-557

Blatt, M.R., and Thiel, G. (1994). K+ channels of stomatal guard cells: bimodal control of the K+ inward-rectifier evoked by auxin. The Plant Journal 5 (1): 55-68

Blatt, M.R., Thiel, G. (2003). K+ channels of stomatal guard cells: bimodal control of the K+ inward-rectifier evoked by auxin. Plant Journal 5 (1): 55–68

Bosma, P.J., Seppen, J., Goldhoorn, B., Bakker, C., Elferink, R.O., Chowdhury, J.R., Chowdhury, N.R., and Jansen, P.J. (1994). Bilirubin UDP-glucuronosyltransferase 1 is the only relevant bilirubin glucuronidating isoform in man. The Journal of Biological Chemistry **269**: 17960-17964

Brandt, B., Brodsky, D.E., Xue, S., Negi, J., Iba, K., Kangasjärri, J., Ghassemian, M., Stephan, A.B., Hu, H. and Schroeder, J.I. (2012). Reconsitution of abscisic acid activation of SLAC1 anion channel by CPK6 and OST1 kinases and branched ABI1 PP2C phosphatise action. PNAS **109(26):** 10593-10598

Brearley, J., Venis, M.A., and Blatt, M.R. (1997). The effect of elevated CO_2 concentrations on K^+ and anion channels of *Vicia faba* L. guard cells. Planta **203 (2)**: 145-154

Büchler, M., König, J., Brom, M., Kartenbeck, J., Spring, H., Horie, T., and Keppler, D. (1996). cDNA Cloning of the Hepatocyte Canalicular Isoform of the Multidrug Resistance Protein, cMrp, Reveals a Novel Conjugate Export Pump Deficient in Hyperbilirubinemic Mutant Rats. Journal of Biological Chemistry **271 (25)**: 15091–15098

Burla, B., Klein, M., Martinoia, E. (2006). The multidrug resistance –associated protein (MRP/ABCC) subfamily of ATP-binding cassette transporters in plants. FEBS Letters **580 (4)**: 1112-1122

Casimiro, I., Beeckman, T., Graham, N., Bhalerao, R., Zhang, H., Casero, P., Sandberg, G., and Bennett, M.J. (2003). Dissecting *Arabidopsis* lateral root development. FEBS Letters, **580 (4)**: 1112-1122;

Changcheng, X., Qi, Z. (1993). Effect of drought on lipoxygenase activity, ethylene and ethane production in leaves of soybean plants. Acta Botanica Sinica (China)

Christmann, A., Hoffmann, T., Teplova, I., Grill, E., Müller, A. (2005). Generation of Active Pools of Abscisic Acid Revealed by In Vivo Imaging of Water-Stressed Arabidopsis. Plan Physiology **137**: 209-219

Clint, G.M. and MacRobbie, E.A.C. (1984). Fusicoccin induced Stomatal opening. Journal of Exp. Botany **35 (2)**: 180-192

Clough, S.J. and Bent, A.F. (1998). Floral dip: A simplified method for Agrobacterium-mediated transformation of *Arabisopsis thaliana*. Plant Journal **16(6)**: 735-743

Clowes, F.A.L., and Juniper, B.E. (1964). The Fine Structure of the Quiescent Centre and Neighbouring Tissues. Journal of Exp. Botany, **15 (3)**: 622-623

Cole, S.P., Bhardwaj, G., Gerlach, J.H., Mackie, J.E., Grant, C.E., Almquist, K.C., Stewart, A.J., Kurz, E.U., Duncan, A.M., and Deeley, R.G. (1992). Overexpression of a transporter gene in a multidrug-resistant human lung cancer cell line. Science **258**: 1650 – 1654

Cosloy, S.D., and Oishi, M. (1972). The nature of the transformation process in *E.coli* K12. Molecular and general genetics **124 (1)**: 1-10

Cui, Y., König, J., Buchholz, U., Spring, H., Leier, I., and Keppler, D. (1999). Drug Resistance and ATP-Dependent Conjugate Transport Mediated by the Apical Multidrug Resistance Protein, MRP2, Permanently Expressed in Human and Canine Cells**.** Molecular Pharmacology **55 (5)**: 929-937

Dawson, R.J.P., and Locher, K.P. (2006). Structure of a bacterial multidrug ABC transporter. Nature **443**: 180-185

Dudler, R., and Hertig, D. (1992), Structure of an mdr-like gene from Arabidopsis thaliana. Evolutionary implications. Journal of Biological Chemistry **267**: 5882-5888

Evers, R., Kool, M., van Deemter, L., Janssen, H., Calafat, J., Oomen, L.C., Paulusma, C.C.,Oude Elferink, R.B., Baas, F., Schinkel, A.H., and Borst, P. (1998). Drug export activity of the human canalicular multispecific organic anion transporter in polarized kidney MDCK cells expressing cMOAT (MRP2) cDNA. Journal of Clinical Investigation **101 (7)**: 1310–1319

Gaedeke, N., Klein, M., Kolukisaoglu, U., Forestier, C., Müller, A., Ansorge, M., Becker, D., Mamnun, Y., Kuchler, K., Schulz, B., Mueller-Roeber, B., and Martionia, E. (2001). The Arabidopsis thaliana ABC transporter AtMRP5 controls root development and stomata movement. EMBO Journal **20 (8**): 1875-1887

Gaillard, S., Jacquet, H., Vavasseur, A., Leonhardt, N., and Forestier, C. (2008). *AtMRP6*/*AtABCC6*, an ATP-Binding Cassette transporter gene expressed during early steps of seedling development and up-regulated by cadmium in *Arabidopsis thaliana*. BMC Plant Biology **8:** 22

Geiger, D., Scherzer, S., Mumm, P., Marten, I., Ache, P., Matschi, S., Liese, A, Wellmann, C., Al-Rasheid, K.A.S., Grill, E:, Romeis, T. and Hedrich, R. (2010). Guard cell anion channel SLAC1 is regulated by CDPK protein and kinases with distinct Ca^{2+} affinities. PNAS **107(17)**: 8023-8028

Geiger, D., Scherzer, S., Mumm, P., Stange, A., Marten, I., Bauer, H., Ache, P., Matschi, S., Liese, A., Al-Rasheid, K.A.S., Romeis, T. and Hedrich, R. (2009). Activity of guard cell anion channel SLAC1 is controlled by drought-stress signalling kinase-phosophatase pair. PNAS **106(50)**: 21425-21430

Geiger, D:, Maierhofer, T., Al-Rasheid, K.A.S., Scherzer, S., Mumm, P., Liese, A., Ache, P., Wellmann, C., Marten, I., Grill, E., Romeis, T. and Hedrich, R. (2011). Stomatal closure by fast abscisic acid signalling is mediated by the guard cell anion channel SLAH3 and the receptor RCAR1. Science Signalling **4(173)**: ra32

Geisler, M., Blakslee, J.J., Bouchard, R., Lee, OR., Vincenzetti, V., Bandyopadhyay, A., Titapiwatanakun, B., Peer, WA., Bailly, A., Richards, E.L., Ejendal, K.F.K., Smith, A.P., Baroux, C., Grossniklaus, U., Müller, A., Hrycyna, C.A., Dudler, R., Murphy, A.S., and Martinoia, E. (2005). Cellular efflux of auxin catalyzed by the Arabidopsis MDR/PGP transporter AtPGP1. The Plant Journal **44**: 179-194

Goodman, C.D., Casat, P., and Walbot, V. (2004). A Multidrug Resistance-Associated Protein Involved in Anthocyanin Transport in *Zea mays*. The Plant Cell **16**:1812-1826;

Grabov, A., Leung, J., Giraudat, J., Blatt, M.R. (1997). Alteration of anion channel kinetics in wild-type and abi1-1 transgenic Nicotiana benthamiana guard cells by abscisic acid. Plant Journal **12 (1)**: 203-13

Greenwood, D.J., Gerwitz, A., Stone, D.A., and Barnes, A. (1982). Root development of vegetable crops. Plant and Soil 68 (1): 75-96

Guzmán, P. and Ecker, J.R. (1990). Exploiting the Triple Response of Arabidopsis To Identify Ethylene-Related Mutants. The Plant Cell **2**: 513-523

Hedrich, R., Busch, H., Raschke, K. (1990). Ca^{2+} and nucleotide dependent regulation of voltage dependent anion channels in the plasma membrane of guard cells. EMBO Journal **12**: 3889-3892

Hedrich, R., Neimanis, S., Savchenko, G., Felle, H.H., Kaiser, W.M., Heber, U. (2001). Changes in apoplastic pH and membrane potential in leaves in relation to stomatal responses to CO_2, malate, abscisic acid or interruption of water supply. Planta **213**: 594-601

Henikoff, S., Greene, E.A., Pietrokovski, S., Bork, P., Attwood, T.K., Hood, L. (1997). Gene Families: The Taxonomy of Protein Paralogs and Chimeras. *Science* **278**: 609

Higgins, C.F. (1992). ABC Transporters: From Microorganisms to Man. Annual Review of Cell Biology **8**: 67-113

Higgins, C.F., and Linton, K.J. (2004). The ATP switch model for ABC transporters. Nature structural & molecular biology **11 (10)**: 918-926

Higgins, C.F., Gottesman, M.M. (1992). Is the multidrug transporter a flippase? Trends Biochem. Sci. **17 (1)**:18-21.

Hinder, B., Schellenberg, M., Rodonis, Ginsburg, S., Vogt, E., Martionia, E., Matile, P., Hörtensteiner, S. (1996). How plants dispose of chlororphyll catabolites: transport of linear tetrapyrroles into isolated vacuoles. The Journal of Biological

Chemistry **271**: 27233-27236

Hite, D.R.C., Outlaw, W.H.Jr., and Tarczynski, M.C. (1993). Elevated Levels of Both Sucrose-Phosphate Synthase and Sucrose Synthase in Vicia Guard Cells Indicate Cell-Specific Carbohydrate Interconversions. Plant Physiology **101 (4)**: 1217-1221

Holland,B., Cole,S.P.C., Kuchler,K., Higgins,J&C.F. (2003). ABC Proteins: From Bacteria to Man. Academic Press, pages: 71-78; 107-113; 336-338; 551-566; 589-593

Hollenstein, K., Dawson, R.JP., and Locher, K.P. (2007 b). Structure and mechanism of ABC transporter proteins. Current Opinion in Structural Biology **17 (4)**: 412-418

Hollenstein, K., Frei, D.C., and Locher, K.P. (2007a). Structure of an ABC transporter in complex with its binding protein. Nature **446**: 213-216

Homolya *et al.,* 1993; L Homolya, Z Holló, U A Germann, I Pastan, M M Gottesman, and B Sarkadi; J. Biol. Chem. 1993 268: 21493-21496 ; Fluorescent cellular indicators are extruded by the multidrug resistance protein

Hubbard, K.E., Nishimura, N., Hitomi, K., Getzoff, E.D. and Schroeder, J.I. (2010). Early abscisic acid signal transduction mechanisms: newly discovered components and newly emerging questions. Genes and Development **24**: 1695-1708

Illies, C., Gromada, J., Fiume, R., Leibiger, B., Yu, L., Juhl, K., Yang, S-N., Barma, D. K., Falck, J. R., Saiardi, A., Barker, C. J., and Berggren, P-O. (2007). Requirement of Inositol Pyrophosphates for Full Exocytotic Capacity in Pancreatic β Cells. Science **318 (5854)**:1299-1302

Irving, H.R., Gehring, C.A., and Parish, R.W. (1992). Changes in cytosolic pH and calcium of guard cells precede stomatal movements. PNAS **89 (5)**: 1790-1794

Ishikawa, H., Aizawa, H., Kishira, H., Ogawa, T., and Sakata, M. (1983). Light-Induced Changes of Membrane Potential in Guard Cells of *Vicia faba.* Plant and Cell Physiology **24 (4)**: 769-772

Jaquinod, M., Villiers, F., Kieffer-Jaquinod, S., Hugouvieux, V., Bruley, C., Garin, J., and Bourguinon, J. (2007). A Proteomics Dissection of Arabidopsis thaliana Vacuoles Isolated from Cell Culture. Molecular and Cellular Proteomics **6**: 394-412

Jones, L., Milne, J.L., Ashcroft, D., and McQueen-Mason, S.J. (2003). Cell wall arabinan is essential for guard cell function. PNAS **100 (20)**: 11783-11788

Kang, J., Hwang, J.-U., Lee, M., Kim, Y.-Y., Assmann, S.M., Martinoia, E. and Lee, Y. (2010). PDR-type ABC transporters cellular uptake of the phytohormone abscisic acid. PNAS **107(5)**: 2355-2360

Kang, J., Park, J., Choi, H., Burla, B., Kretzschmar, T., Lee, Y. and Martionia, E. (2011). Plant ABC Transporters. Arabidopsis Book 2009;9;e0153

Kartenbeck, J., Leuschner, U., Mayer, R., and Keppler, D. (1996). Absence of the canalicular isoform of the *MRP* gene-encoded conjugate export pump from the hepatocytes in Dubin-Johnson syndrome. Hepatology **23 (5)**: 1061-1066

Keppler, D., Kartenbeck, J. (1996). The canalicular conjugate export pump encoded by the cMRP/cMOAT gene. Progr. in liver dis. **14**: 55-67

Kessel, R.W. (1989). Perceiving health and experiencing illness. Med Humanit Rev. 3 (2): 64-68.

Kinoshita, T., Doi, M., Suetsugu, N., Kadawa, T., Wada, M., and Shimazaki, K. (2001). phot1 and phot2 mediate blue light regulation of stomatal opening. Nature **414**: 656-660

Klein, C., Kuchler, K. and Valachovic, M. (2011). ABC Proteins in Yeast and Fungal Pathogens. Essays in Biochemistry **50**: 101-120

Klein, M., Geisler, M., Suh, S.J., Kolukisaoglu, Ü., Azevedo, L., Plaza, S., Curtis, M.D., Richter, A., Weder, B., Schulz, B., and Martionia, E. (2004). Disruption of AtMRP4, a guard cell membrane ABCC-type ANC transporter, leads to deregulation of stomatal opening and increased drought susceptibility. The Plant Journal **39 (2)**: 219-236

Klein, M., Martionia, E., Hoffmann-Thoma, G., and Weissenböck, G. (2000). A membrane-potential dependent ABC-like transporter mediates the vacuolar uptake of rye flavone glucuronides: regulation of glucuronide uptake by glutathione and its conjugates. Plant Journal **21 (3)**: 289-304

Klein, M., Perfus-Barbeoch, L., Frelet, A., Gaedeke, N., Reinhardt, D., Mueller-Roeber, B., Martionia, E., and Forestier, C. (2003). The The plant multidrug resistance ABC transporter AtMRP5 is involved in guard cell hormonal signalling and water use. Plant Journal **33**: 119-129

König, J., Nies, A.T., Cui, Y., Leier, I., and Keppler, D. (1999). Conjugate export pumps of the multidrug resistance protein (MRP) family: localization, substrate

specificity, and MRP2-mediated drug resistance. Biochimica et Biophysica Acta 1461 (1999) 377-394

Kreuz, K., Tommasini, R., and Martinoia, E. (1996). Old Enzymes for a New Job (Herbicide Detoxification in Plants). Plant Physiol. **111 (2)**: 349–353

Kwak, J.M., Murata, Y., Baizabal-Aguirre, V.M., Merrill, J., Wang, M., Kemper, A., Hawke, S.D., Tallman, G., and Schroeder, J.I. (2001). Dominant Negative Guard Cell K^+ Channel Mutants Reduce Inward-Rectifying K^+ Currents and Light-Induced Stomatal Opening in Arabidopsis. Plant Physiology **127**: 472-485

Lee, Y.S., Mulugu, S., York, J.D., and O'Shea, E.K. (2007). Regulation of a Cyclin-CDK-CDK Inhibitor Complex by Inositol Pyrophosphates. Science **316**: 109-12

Lehman, A., Black, R., Ecker, J.R. (1996). HOOKLESS1, an ethylene response gene, is required for differential cell elongation in the Arabidopsis hypocotyl. The Cell **85**:183-194

Leier, I., Jedlitschky, G., Buchholzt, U., Cole, S.P.C., Deeley, R.G., and Keppler, D. (1994). The MRP Gene Encodes an ATP-dependent Export Pump for Leukotriene C4 and Structurally Related Conjugate. Journal of Biological Chemistry **269 (45)**: 27807-27810

Lemtiri-Chlieh, F., MacRobbie, E.A.C., and Brearley, C.A. (2000). Inositol hexakisphosphate is a physiological signal regulating the K^+-inward rectifying conductance in guard cells. PNAS **97 (15)**: 8687-8692

Lemtiri-Chlieh, F., MacRobbie, E.A.C., Webb, A.R.R., Manison, N.F., Brownlee, C., Skepper, J.N., Chen, J., Prestwich, G.D., and Brearley, C.A. (2003). Inositol hexakisphosphate mobilizes an endomembrane store of calcium in guard cells. Proc Natl Acad Sci U S A. **100 (17)**: 10091–10095

Leonhardt, N., Marin, E., Vavasseur, A., and Forestier, C. (1997). Evidence for the existence of a sulfonylurea – receptor – like protein in plants: Modulation of stomatal movements and guard cell potassium channels by sulfonylureas and potassium channel openers. PNAS **94 (25)**: 14156-14161

Leonhardt, N., Vavasseur, A., and Forestier, C. (1999). ATP Binding Cassette Modulators Control Abscisic Acid-Regulated Slow Anion Channels in Guard Cells. Plant Cell **11**: 1141-1152

Li, ZS., Lu, YP., Zhen,RG., Szczypka, M., Thiele, D.J., and Rea, P.A. (1997). A new pathway for vacuolar cadmium sequestration in *Sacchormyces cerevisiae*: YCF1-catalyzed transport of bis(glutathionato)cadmium. Proceedings of the National Academy of Sciences of the U.S.A **94 (1)**: 42-47

Li, ZS., Szczypka, M., Lu, YP., Thiele, D.J., and Rea, P.A. (1996). The Yeast Cadmium Factor Protein (YCF1) Is a Vacuolar Glutathione *S*-Conjugate Pump. The Journal of Biological Chemistry **271**: 6509-6517

Liu, G., Sánchez-Fernández, R., Li, ZS., and Rea, P.A. (2001). Enhanced Multispecificity of Arabidopsis Vacuolar Multidrug Resistance-associated Protein-type ATP-binding Cassette Transporter, AtMRP2. Journal of Biological Chemistry **276 (12)**: 8648-8656

Lu, P., Outlaw, W.H.Jr., Smith, B.G., and Freed, G.A. (1997). A New Mechanism for the Regulation of Stomatal Aperture Size in Intact Leaves (Accumulation of Mesophyll-Derived Sucrose in the Guard-Cell Wall of *Vicia faba*). Plant Physiology **114 (1)**: 109-118

Lu, P., Zhang, S.Q., Outlaw, W.H.Jr., and Riddle, K.A. (1995). Sucrose: a solute that accumulates in the guard-cell apoplast and guard-cell symplast of open stomata. FEBS Letters **362 (2)**: 180-184

Lu, YP., Li, ZS., and Rea, P.A. (1997). *AtMRP1* gene of *Arabidopsis* encodes a glutathione *S*-conjugate pump: Isolation and functional definition of a plant ATP-binding cassette transportergene. PNAS **94 (15)**: 8243-8248

Lu, YP., Li, ZS., Drozdowicz, Y.M., Hörtensteiner, S., Martinoia, E., and Rea, P.A. (1998). AtMRP2, an Arabidopsis ATP Binding Cassette Transporter Able to Transport Glutathione *S*-Conjugates and Chlorophyll Catabolites: Functional Comparisons with AtMRP1. Plant Cell **10**: 267-282

Lu, YP., Li, ZS., Drozdowicz, Y.M., Hörtensteiner, S., Martionia, E., and Rea, P.A. (1998). AtMRP2, an Arabidopsis ATP Binding Cassette Transporter Able to Transport Glutathione S-Conjugates and Chlorophyll Catabolites: Functional Comparisons with AtMRP1. Plant Cell **10**: 267-282

Ma, Y., Szostkiewicz, I., Korte, A., Moes, D., Yang, Y., Christmann, A., Grill, E. (2009). Regulators of PP2C Phosphatase Activity Function as Abscisic Acid Sensors. *Science* **324**: 1064–1068

MacRobbie, E.A. (1998). Signal transduction and ion channels in guard cells. Philosophical Transactions of The Royal Society B Biological Science **353 (1374)**: 1475-1488

Martinoia, E., Grill, E., Tommasini, R., Kreuz, K., and Amrhein, N. (1993). ATP-dependent glutathione *S*-conjugate 'export' pump in the vacuolar membrane of plants. Nature **364**: 247-249

Martionia, E., Klein, M., Geisler, M., Bovet, L., Forestier, C., Kolukisaoglu, Ü., Müller-Röber, B., Schulz, B. (2002). Multifunctionality of plant ABC transporters – more than just detoxifiers. Planta **214**: 345-355

Marty, F. (1997). The Plant Vacuole: Ultrastructural Studies of Vacuole Biogenesis New York, Academic Press

Matsuo, M., Ueda, K., Ryder, T. and Ashcroft, F. (2003). The Sulfonylurea Receptor: an ABCC Transporter that acts as an ion channel regulator. ABC Proteins: From Bacteria to Man: 551-576

Merlot, S., Gosti, F., Guerrier, D., Vavasseur, A., and Giraudat, J. (2001). The ABI1 and ABI2 protein phosphatases 2C act in a negative feedback regulatory loop of the abscisic acid signalling pathway. The Plant Journal **25 (3)**: 295–303

Merritt, F., Kemper, A., and Tallman, G. (2001). Inhibitors of Ethylene Synthesis Inhibit Auxin-Induced Stomatal Opening in Epidermis Detached from Leaves of *Vicia Faba* L.**.** Plant and Cell Physiology **42 (2)**: 223-230

Meyer, S., Mumm, P., Imes, D., Endler, A., Weder, B., Al-Rasheid, K.A.S., Geiger, D., Marten, I., Martinoia, E. and Hedrich, R. (2010). AtALMT12 represents an R-type anion channel required for stomatal movement in Arabidopsis guard cells. The Pland Journal **63(6)**: 1054-1062

Mittler, R. (2002). Oxidative Stress, antioxidants and stress tolerance. Trends in plant science **7 (9)**: 405-410

Müller, M., Meuert, C., Zamant, G.J.R., Borst, P., Scheper, R.J., Muldert, N.H., De Vriest, E.G.E., and Jansen, P.L.M. (1994). Overexpression of the gene encoding the multidrug resistance associated protein results in increased ATP-dependent glutathione S-conjugate transport. Proc. Natl. Acad. Sci. USA **91**: 13033-13037

Nagy, R., Grob, H., Weder, B., Green, P., Klein, M., Frelet-Barrand, A., Schjoerring, J.K., Brearley, C., and Martinoia, E. (2009). The *Arabidopsis* ATP-binding Cassette Protein AtMRP5/AtABCC5 Is a High Affinity Inositol Hexa*kis*phosphate Transporter Involved in Guard Cell Signaling and Phytate Storage. Journal of Biological Chemistry **284**: 33614-33622

Negi, J., Matsuda, O., Nagasawa, T., Oba, Y., Takahashi, H., Kawai-Yamada, M., Uchimiya, H., Hashimoto and Iba, K. (2008). CO2 regulator SLAC1 and its homologues are essential for anion homeostastis in plant cells. Nature **452**: 483-486

Nye, P.H., and Tinker, P.B. (1977). Solute Movement in Soil-root System. University of California Press Berkley

Odom, A.R., Stahlberg, A., Wente, S.R., and York, J.D. (2000). A Role for Nuclear

Inositol 1,4,5-Trisphosphate Kinase in Transcriptional Control. Science **287**: 2026-2029

Ortiz, D.F., Ruscitti, T., McCue, K.F., Ow, D.W. (1995): Transport of metal-binding peptides by HMT1, a fission yeast ABC-type vacuolar membrane protein. Journal of biological Chemistry **270(9)**: 4721-4728

Outlaw, W.H.Jr. (2003): Integration of Cellular and Physiological Functions of Guard Cells. Critical Reviews in Plant Sciences **22 (6)**: 503-529

Park, J., Song, W.-Y., Ko, D., Eom, Y., Hausen, T.H., Schiller, M., Lee, T.G., Martinoia, E. and Lee, Y. (2011). The phytochelatin transporters AtABCC1 and AtABCC2 mediate tolerance to cadmium and mercury. The Plant Journal **69(2)**: 278-288

Park, S.-Y., Fung, P., Nishimura, N., Jensen, D. R., Fujii,H., Zhao, Y., Lumba, S., Santiago, J., Rodrigues, A., Chow, T.-F. F., Alfred, S.E., Bonetta, D., Finkelstein, R., Provart, N. J., Desveaux, D., Rodriguez, P. L., McCourt, P., Zhu, J.-K., Schroeder, J.I., Volkman, B.F., and Cutler, S. R. (2009). Abscisic Acid Inhibits Type 2C Protein Phosphatases via the PYR/PYL Family of START Proteins Science 324: 5930**.**

Paulusma, C.C., Bosma, P.J., Zaman, G.J.R, Bakker, C.T.M., Otter, M., Scheffer, G.L., Scheper, R.J., Borst, P., Elferink, R.O. (1996): Congenital Jaundice in Rats with a Mutation in a Multidrug Resistance-Associated Protein Gene**.** Science **271**: 1126 – 1128

Paulusma, C.C., Kool, M., Bosma, P.J., Scheffer, G.L., Borg, F., Scheper, R.J., Tytgat, G.N., Borst, P., Baas, F., Elferink, R.O. (1997). A mutation in the human canalicular multispecific organic anion transporter gene causes the Dubin-Johnson syndrome. Hepatology **25 (6)**: 1539-1542

Pei, Z.M., Kuchitsu, K., Ward, J.M., Schwarz, M., and Schroeder, J.I. (1997). Differential Abscisic Acid Regulation of Guard Cell Slow Anion Channels in Arabidopsis Wild-Type and abi1 and abi2 Mutants. The Plant Cell **9 (3)**: 409-423

Radoy V. (2003). *Myo*-Inositol-1,2,3,4,5,6-hexakisphosphate. Phytochemistry **64**: 1033-1043

Raichaudhuri, A., Peng, M., Naponelli, V., Chen, S., Sánchez-Fernández, R., Gu, H., Gregory III, J.F., Hanson, A.D., and Rea, P.A. (2009). Plant vacuolar ABC transporters that translocate folates and antifolates *in vitro* and contribute to antifolate tolerance *in vivo*. The Journal of Biological Chemistry **284**: 8449-8460

Rea, P.A. (1998a). MRP subfamily ABC transporters from plant to man. Journal of Experimental Botany **50** (Special Issue): 895–913

Rea, P.A., Li, ZS., Lu, YP., Drozdowicz, Y.M. (1998b). From vacuolar GS-X Pumps to multispecific ABC Transporters. Ann. Rev. Plant Physiology and Plant Molecular Biology **49**: 727-760

Reddy, A.R., and Rama Das, V.S. (1986). Stomatal Movements and Sucrose Uptake by Guard Cell Protoplasts of *Commelina benghalensis* L.. Plant and Cell Physiology **27 (8)**: 1565-1570

Ritte, G., Rosenfeld, J., Rohrig, K., and Raschke, K. (1999). Rates of Sugar Uptake by Guard Cell Protoplasts of *Pisum sativum* L. Related to the Solute Requirement for Stomatal Opening. Plant Physiology **121**: 647-656

Rob, M., Roelfsema, G., Hanstein, S., Felle, H.H., and Hedrich, R. (2002). CO_2 provides an intermediate link in the red light response of guard cells. The Plant Journal **32 (1)**: 65-75

Sánchez-Fernández, R., Davies, T.G.E., Coleman, J.O.D., and Rea, P.A. (2001). The *Arabidopsis thaliana* ABC Protein Superfamily, a Complete Inventory. Journal of Biological Chemistry **276 (32)**: 30231–30244

Scheres, B., Wolkenfelt, H., Willemsen, V., Terlouw, M., Lawson, E., Dean, C., and Weisbeek, P. (1994). Embryonic origin of the Arabidopsis primary root and root meristem initials. Development **120 (9)**: 2475-2487

Schneider, E., Hunke, S. (1998). ATP-binding-cassette (ABC) transport systems: functional and structural aspects of the ATP-hydrolyzing subunits/domains. FEMS microbiology review **22 (1)**: 1-20

Schroeder, J.I., and Hagiwara, S. (1990). Repetitive increases in cytosolic Ca2+ of guard cells by abscisic acid activation of nonselective Ca^{2+} permeable channels. PNAS **87 (23)**: 9305-9309

Schroeder, J.I., Raschke, K., and Neher, E. (1987). Voltage dependence of K^+ channels in guard-cell protoplasts. PNAS **84 (12)**: 4108-4112

Schwartz, A., Wu, WH., Tucker, E.B., Assmann, S.M. (1994). Inhibition of inward K^+ channels and stomatal response by abscisic acid: An intracellular locus of phytohormone action. Proc. Natl. Acad. Sci. USA **91**: 4019-4023

Serrano, E.E., Zeiger, E., and Hagiwara, S. (1988): Red light stimulates an electrogenic proton pump in *Vicia* guard cell protoplast. PNAS **85**: 436-440

Sharkey, T.D., and Raschke, K. (1981). Effect of Light Quality on Stomatal Opening in Leaves of *Xanthium strumatium* L.. Plant Physiology **68**: 1170-1174

Sharom, F.J. (2011). The P-glycoprotein multidrug Transporter. Essays in Biochemistry **50**: 161-178

Sidler, M., Hassa, P., Hasan, S., Ringli, C., and Dudler, R. (1998). Involvement of an ABC Transporter in a Developmental Pathway Regulating Hypocotyl Cell Elongation in the Light. Plant Cell **10**: 1623-1636

Slot, A.J., Molinski, S.V. and Cole, S.P.C. (2011). Mammalian multidrug-resistance Proteins (MRPs). Essays in Biochemistry **50**: 179-207

Song, W.-Y., Park, J., Menoza-Cózate, D.G., Suter-Grotemeyer, M., Shim, D., Hörtensteiner, S., Geisler, M., Weder, B., Rea, P.A., Rentsch, D., Schroeder, J.I., Lee, Y. and Martionia, E. (2010). Arsenic tolerance in Arabisopsis is mediated by two ABCC-type phytochelatin transporters. PNAS **107 (49)**: 21187-21192

Song, W.Y., Sohn, E.J., Martionia, E., Lee, Y.J., Yang, Y.-Y., Jasinsky, M., Forestier, C., Hwang, I. and Lee, Y. (2003). Engineering tolerance and accumulation of lead and cadmium in transgenic plants. Nature Biotechnology **21(8)**: 914-919

Stadler, R., Büttner, M., Ache, P., Hedrich, R., Ivashikina, N., Melzer, M., Shearson, S.M., Smith, S.M., and Sauer, N. (2003). Diurnal and Light-Regulated Expression of AtSTP1 in Guard Cells of Arabidopsis. Plant Physiology **133**: 528-537

Stutts, M.J., Canessa, C.M., Olsen, J.C., Hamrick, M., Cohn, J.A., Rossier, B.C. and Boucher, R.C. (1995). CFTR as a cAMP-dependent regulator of sodium channels. Science **269**: 847-850;

Suh, S.J., Wang, JF., Frelet, A., Leonhardt, N., Klein, M., Forestier, C., Mueller-Roeber, B., Cho, M.H., Martinoia, E., and Schroeder, J.I. (2007). The ATP Binding Cassette Transporter AtMRP5 Modulates Anion and Calcium Channel Activities in Arabidopsis Guard Cells. The Journal of Biological Chemistry 282: 1916-1924

Szczypka, M.S., Wemmie, J.A., Moye-Rowley, W.S., and Thiele, D.J. (1994). A Yeast Metal Resistance Protein Similar to Human Cystic Fibrosis Transmembrane Conductance Regulator (CFTR) and Multidrug Resistance-associated Protein. The Journal of Biological Chemistry **269 (36)**: 22853-22857

Taiz, L., and Zeiger, E., Plant Physiology; second edition; Spectrum Verlag

Talbott, L.D., and Zeiger, E. (1998). The role of sucrose in guard cell osmoregulation. Journal of Experimental Botany **49**: 329-337

Tallman, G., and Zeiger, E. (1988) Light Quality and Osmoregulation in *Vicia* Guard Cells. Plant Physiology **88 (3)**: 887-895

Tanaka, Y., Sano, T., Tamaoki, M., Nakajima, N., Kondo, N., and Hasezawa, S. (2005). Ethylene Inhibits Abscisic Acid-Induced Stomatal Closure in Arabidopsis. Plant Physiology **138**: 2337-2343

Taniguchi, K., Wada, M., Kohnno, K., Nakamura, T., Kawabe, T., Kawakami, M., Kagotani, K., Okumura, K., Akiyama, S., and Kuwano, M (1996). A Human Canalicular Multispecific Organic Anion Transporter (cMOAT) Gene Is Overexpressed in Cisplatin-resistant Human Cancer Cell Lines with Decreased Drug Accumulation. Cancer Research **56**: 4124-4129

Thain, S.C., Vandenbussche, F., Laarhoven, L., Dowson-Day, M.J., Wang, ZY., Tobin, E.M., Harren, F., Millar, A.J., and Van Der Straeten, D. (2004). Circadian Rhythms of Ethylene Emission in Arabidopsis. Plant Physiology **136**: 3751-3761

Tommasini, R., Evers, R., Vogt, E., Mornet, C., Zaman, G., Schenkel, A., Borst, P., and Martinoia, E. (1996). The human multidrug resistance-associated protein complements the yeast cadmium resistance factor 1. Proceedings of the National Academy of Sciences of U.S.A. **93**: 6743-6748

Tommasini, R., Vogt, E., Fromenteau, M., Hörtensteiner, S., Matile, P., Amrhein, N., and Martinoia, E. (1998). An ABC-transporter of Arabidopsis thaliana has both glutathione-conjugate and chlorophyll catabolite transport activity. The Plant Journal **13 (6)**: 773-780

Tsujii, H., König, J., Rost, D., Stöckel, B., Leuschner, U., Keppler, D. (1999). Exon-intron organization of the human multidrug-resistance protein 2 (MRP2) gene mutated in Dubin–Johnson syndrome. Gastroenterology **117 (3)**: 653-660

Vahisalu, T., Kollist, H., Wang, Y.-F., Nishimura, N., Chan, W.-Y., Valerio, G., Lamminmäki, A., Brosché, M., Moldau, H., Desikan, R., Schroeder, J.I. and Kangasjärvi, J. (2008). SLAC1 is required for plant cell S-type anion channel function in stomatal signalling. Nature **452**: 487-491

Vavasseur, A., and Raghvendra, A.S. (2005). Guard Cell metabolism and CO_2 sensing. New Phytologist **165 (3)**: 665-682

Verrier, P.J., Bird, D., Burla, B., Dassa, E., Forestier, C., Geisler, M., Klein, M., Kolukisaoglu, Ü., Lee, Y., Martinoia, E., Murphy, A., Rea, P.A., Samuels, L., Schulz, B., Spalding, E.J., Yazaki, K., and Theodoulou, F.L. (2008). Plant ABC proteins – a unified nomenclature and updated inventory. Trends in Plant Science 13 (4): 151-159

Ward, J.M., Pei, Z.M., and Schroeder, J.I. (1995). Roles of Ion Channels in Initiation of Signal Transduction in Higher Plants. Plant Cell **7 (7)**: 833–844;

Xu, C., Zou, Q. (1993). Effect of drought on lipoxygenase activity, ethylene and

ethane production in leaves of soybean plants. Acta Botanica Sinica (China)

York, J.D., Odom, A.R., Murphy, R., Ives, E.B., and Wente, S.R. (1999). A Phospholipase C-Dependent Inositol Polyphosphate Kinase Pathway Required for Efficient Messenger RNA Export. Science **285**: 96-100

Zimmermann, P., Laule, O., Schmitz, J., Hruz, T., Bleuler, S., and Gruissem, W. (2008). Genevestigator Transcriptome Meta-Analysis and Biomarker Search Using Rice and Barley Gene Expressionn Databases. Molecular Plant **1(5)**:851-857

Zolnerciks, J.K., Andress, E.J., Nicolaou, M. and Linton, K.J. (2011). Structures of ABC Transporters. Essays in Biochemistry **50**: 43-61

5 Final Discussion and Conclusion

The aim of my work was the elucidation why *At*MRP5/ABCC5 exhibits the phenotypes described in the preceding publications. This transporter is mainly expressed in two specific parts of the Arabidopsis plant, the seed (Genevestigator Database; Zimmermann *et al.*, 2008) and, most interestingly, in the guard cells (Gaedeke *et al.,* 2001).

The absence of *At*MRP5 affects stomata regulation as well as root growth. Arabidopsis loss-of-function mutants for this transporter exhibited a reduced stomatal aperture in the light compared to the corresponding wild types, This is probably the cause, why *At*MRP5 knock out plants exhibit an increased water-use efficiency, a trait which could be of agronomical interest (Klein *et al.*, 2003). Furthermore stomatal regulation was strongly impaired, since mutant plants did not respond to ABA, Ca^{2+} and auxin (Klein *et al.*, 2003). Using electrophysiological studies, Suh *et al.,* (2007) could show that the activity of the S-type anion channel is reduced in *atmrp5-1*, indicating that *At*MRP5 may not represent an anion channel itself, but could directly or indirectly regulate ion fluxes. At the root level, *At*MRP5 mutants were smaller when grown on ½ MS medium and contained more auxin. However, this phenotype could be reversed when nutrient supply or K^+ concentrations in the medium were raised (Gaedeke *et al.*, 2001)

These results indicated that *At*MRP5 is a transporter important for stomatal function and root development. However, the exact mechanism how *At*MRP5 exerts its role was unknown. Therefore, we posed ourselves two major questions: i) *At*MRP5 was shown to transport glutathione conjugates and glucuronidated compounds. Is there another compound transported by *At*MRP5 that could explain the phenotype of the knock out mutant? ii) Does *At*MRP5 interact with other proteins involved in stomata regulation?

Based on an observation that a close homolog of *At*MRP5 from maize and *Sorghum* affects phytate ($InsP_6$), we investigated whether *At*MRP5 is a phytate transporter or a factor required for phytate transport. We could show that also in *Arabidopsis* phytate contents concomitant with that of several divalent cations were strongly reduced. Transport experiments with yeast vesicles expressing *At*MRP5 allowed demonstrating, that this ABC transporter acts indeed as a highly specific and highly efficient phytate transporter. Inositolpyrophosphates such as $InsP_3$ or $InsP_6$ are involved in many cellular mechanisms, such as exocytosis (Illies *et al.*, 2007), mRNA export (York *et al.*, 1999; Odom *et al.*, 2000) and cell cycle activities (Lee *et al.*, 2007). In plants, $InsP_6$ mobilizes

calcium and negatively regulates the inward rectified potassium ion conductance of guard cells (Lemtiri-Chlieh *et al.*, 2003).

Our findings of *At*MRP5 as an $InsP_6$transporter gave a mechanistic explanation of $InsP_6$ accumulation in storage tissues of plants that differs from the established convention. So far phytate accumulation in membrane-bound protein bodies, for example aleuron bodies, was explained mainly to be due to vesicular trafficking and the source of protein bodies itself (Adams *et al.*, 1985; Marty, 1997).A 99 kb region, coding for an ATPase G-subunit on the tonoplast membrane, was mapped in a natural variation of an $InsP_6$ accumulation trait (Bentsink *et al.*, 2003). Since an exact locus of that trait could not be identified, the accumulation of $InsP_6$ could be dependent on vacuolar transport processes, which could also explain these variations in $InsP_6$ levels.

In chapter 2, it is shown that the disruption of a gene encoding an $InsP_6$ transporter strongly affects stomatal function. Despite the fact that reports in the literature have shown that $InsP_6$ affects several pathways involved in stomata regulation and function (Radoy, 2003), it could not be predicted that $InsP_6$ has such a drastic effect. The observation that the exclusive expression of *At*MRP5in guard cells of *atmrp5*-1 restores the sensitivity to ABA is a strong indication that the *atmrp5*-1 stomata phenotype is indeed due to impaired vacuolar transport of $InsP_6$ in these cells. The physiology of guard cells is dominated by a multitude of ion channels, since opening and closing of the stomata is based on an osmotic system. This is not limited to the plasma membrane, but also involves the vacuole, since this organelle is responsible for the volume changes during stomatal opening and closure (MacRobbie, 1998). It was reported that both the fast and slow Ca^{2+}-permeable conductances of the tonoplast are targets of $InsP_6$ (Lemtiri-Chlieh *et al.*, 2000, Lemtiri-Chlieh *et al.*, 2003). Therefore, it must be postulated that the removal of the signalling molecule $InsP_6$ from the cytosol is a prerequisite for correct stomatal movement.

In conclusion, the identification of a high affinity inositol hexa*kis*phosphate transport amplifies the diversity of functions assigned to ABC transporters, and also answers a long-standing question of how inositol phosphates traverse membranes.

The observation that the SV anion channel activity was reduced but still present in *At*MRP5 mutant guard cells (Suh *et al.*, 2007), raised the question whether

*At*MRP5interacts with other proteins and exerts part of its role through a network. To elucidate this question the yeast two hybrid system approaches was used.

As mentioned in the Introduction of chapter 3, screening a plant cDNA library with a full length ABC-transporter as bait in the membrane-based yeast two hybrid system (split ubiquitin system) causes severe problems. This is why the protein was chopped up and the soluble parts, namely the NBFs used for screening. The amount of positive colonies retrieved in the screen with NBD1 compared to the amount found with NBD2 (for results of the NBD2 screen, see supplementary data) supported our idea, that most of the interactions take place at NBD1. We focused our interest on proteins involved in Ca^{2+}-binding (important 2nd messenger in stomata function), proteins believed to be involved in channel modulation as well as proteins related to phytohormones. To further elucidate the role of those proteins, 16 loss-of-function mutants selected among the putative interacting proteins were compared with the corresponding wild types, as well as with the phenotype of *AtMRP5* mutants.

Surprisingly, the most obvious stomatal phenotype was observed in the *hookless1*mutant. *hls1* was not able to fully close stomatas in the dark and the stomatal aperture was larger than that of the wild type in the light, which is the opposite to the slightly more closed stomata of *atmrp5*. Arabidopsis *Hookless1* (*AtHLS1*) is expressed, similarly to *At*MRP5, in 24h-imbibed seeds and in guard cells (e-FP browser). Until now, the *At*HLS1 loss-of-function mutant was described as an ethylene-insensitive mutant in triple response screens. Etiolated *hls1* seedlings fail to form the apical hook and do not react with the triple response to ethylene treatment (Guzman *et al.*, 1990). *At*HLS1 is a soluble protein with a putative N-acetyltransferase moiety. This putative N-acetyltransferase was proposed to control the differential cell growth in etiolated seedlings via modulating the amount of free auxin (Lehman *et al.*, 1996). It was suggested, that auxin is inactivated via acetylation. These results suggest that *At*HLS1 is acting in the crosstalk between auxin signaling and the ethylene pathway.

To understand the role of *At*MRP5 and its interaction with *At*HLS1 in a general context, it is important to know more about the role of ethylene in stomata regulation. Ethylene is a gaseous plant hormone involved in diverse seasonal, developmental and physiological processes. No general role in guard cells could be established so far, as its function varies among different plant families. In *Arabidopsis thaliana*, ethylene is able to inhibit

ABA-induced stomatal closure (Tanaka *et al.*, 2005). Possible explanations for the physiological function of the antagonistic relationship of ABA and ethylene can be the supply of a minimal amount of carbon dioxide to ensure a minimum level of photosynthesis upon drought stress for a long period (Tanaka *et al.*, 2005). Both hormones are affected by drought stress and increase during desiccation (Xu and Zou, 1993). Ethylene production levels were found to be regulated by the circadian clock and by light (Thain *et al.*, 2004).

Like *atmrp5-1* and *atmrp5-2*, *hls1*was insensitive towards ABA. Since it is known that ethylene is able to inhibit the ABA response we tested AVG, an ethylene biosynthesis inhibitor in our stomata experiments. Surprisingly, stomata of *hls1* plants, which were treated with AVG in the absence of ABA, closed the stomata to a value comparable to the corresponding wild type. Furthermore, as soon as AVG was present, the ABA response was re-established and preceded similarly as in the wild type. This indicates that a pool of ethylene in the stomata of *hls1* inhibits the ABA response, and may also lead to a larger aperture in non-ABA-treated leaves of *hls1* plants. In contrast, the corresponding wild type did not show any alterations when AVG was added. The most important question in this context was whether the interaction between *At*MRP5 and *At*HLS1 circumvented the raise in ethylene concentration. If this is true, it would be expected that also *atmrp5* plants sense ABA when pretreated with AVG. We show that indeed *atmrp5-1* and *atmrp5-2* exhibit ABA-induced stomatal closure when pretreated with AVG. In contrast it cannot be stated that this ethylene pool is the reason for the open state during the dark cycle (results varied strongly from experiment to experiment, data not shown). In this case it might be, that ethylene induces auxin production, which is able to open stomata in the dark. This hypothesis remains to be investigated.

To bring both findings, i.e. transport of $InsP_6$ as well as interaction with HLS1, together we state that HLS1 might modulate the transport activity of *At*MRP5 and hence allows to tightly controll cytosolic $InsP_6$ concentrations. A possibility would be that in contrast to what has been postulated by Lehmann *et al.* (1996), HLS1 does not inactivate auxin but acts as a protein acetyl transferase. By acetylating MRP5 HLS1 may modulate its transport activity. Alternatively, the interaction of MRP5 and HLS1 could be part of a complex network inhibiting ethylene synthesis. However, it maybe that ethylene is not the primary cause of this phenotype, but that ethylene is synthesized in response to

elevated auxin concentrations. It was shown that AVG inhibits the auxin-induced stomatal opening in *Vicia faba*. In contrast, the inhibition of ethylene synthesis in guard cells with AVG did not inhibit the light- or fusicoccin-induced opening of stomata (Clint and MacRobbie, 1984). These findings support the hypothesis that auxin-induced stomatal opening is mediated through auxin-induced ethylene production by guard cells or ethylene-induced auxin synthesis (Merritt *et al.*, 2001).

In conclusion, our results strongly suggest that removing the signalling compound $InsP_6$ from the cytosol is required for correct stomatal function. The yeast two-hybrid data and the similarity of the phenotype of the two *atmrp5* mutants and *hls1* are also strong evidence that these two proteins interact. However, how they affect each other as well as whether ethylene or auxin are the primary cause of the impaired stomata regulation in the two mutants are still open questions. To solve these questions a possibility would be i) to reduce auxin levels by transforming *hls1* and *atmrp5* plants with a stomata-specific construct for an IAA-lysin synthetase, which conjugates lysin to the auxin molecule and thereby inactivates free auxin; ii) to produce recombinant HLS1 protein and see whether it acetylates *At*MRP5 and whether the transport activity of *At*MRP5 is thereby altered and iii) to perform microarray analysis with guard cells to get a closer insight into which pathways are affected in *atmrp5* and *hls1*.

Our results and all findings before concerning the regulation of stomata indicate that the underlying regulatory mechanisms are extremely complex. Yet, the new results show a new level of complexity. Plants as sessile organisms, unlike animals or man, are not able to search appropriate conditions; they had to evolve mechanisms to deal with environmental stresses. Water availability was a critical issue for most plants since they invaded the land and, hence, the complexity of stomata regulation may reflect how much effort plants have invested into this aspect for their survi*al.*

5.1 References

Adams, C., Norby, S. W., and Rinne, R. W. (1985). Production of multiple vacuoles as an early event in the ontogeny of protein bodies in developing soybean seeds. Crop Science 25, 255-262

Bentsink, L., Yuan, K., Koornneef, M., and Vreugdenhil, D. (2003). The genetics of phytate and phosphate accumulation in seeds and leaves of Arabidopsis thaliana, using natural variation. Theor Appl Genet 106, 1234-1243

Clint, G.M., and MacRobbie, E.A.C. (1984). Fusicoccin induced Stomatal opening. Journal of Exp. Botany **35 (2)**: 180-192

Gaedeke, N., Klein, M., Kolukisaoglu, U., Forestier, C., Müller, A., Ansorge, M., Becker, D., Mamnun, Y., Kuchler, K., Schulz, B., Mueller-Roeber, B., and Martionia, E. (2001). The Arabidopsis thaliana ABC transporter AtMRP5 controls root development and stomata movement. EMBO Journal **20 (8**): 1875-1887

Guzmán, P. and Ecker, J.R. (1990). Exploiting the Triple Response of Arabidopsis To Identify Ethylene-Related Mutants. The Plant Cell **2**: 513-523

Illies, C., Gromada, J., Fiume, R., Leibiger, B., Yu, L., Juhl, K., Yang, S-N., Barma, D. K., Falck, J. R., Saiardi, A., Barker, C. J., and Berggren, P-O. (2007). Requirement of Inositol Pyrophosphates for Full Exocytotic Capacity in Pancreatic β Cells. Science **318 (5854)**:1299-1302

Klein, M., Perfus-Barbeoch, L., Frelet, A., Gaedeke, N., Reinhardt, D., Mueller-Roeber, B., Martionia, E., and Forestier, C. (2003). The The plant multidrug resistance ABC transporter AtMRP5 is involved in guard cell hormonal signalling and water use. Plant Journal **33**: 119-129

Lee, Y.S., Mulugu, S., York, J.D., and O'Shea, E.K. (2007). Regulation of a Cyclin-CDK-CDK Inhibitor Complex by Inositol Pyrophosphates. Science **316**: 109-12

Lehman, A., Black, R., Ecker, J.R. (1996). HOOKLESS1, an ethylene response gene, is required for differential cell elongation in the Arabidopsis hypocotyl. The Cell **85**:183-194

Lemtiri-Chlieh, F., MacRobbie, E.A.C., and Brearley, C.A. (2000). Inositol hexakisphosphate is a physiological signal regulating the K^+-inward rectifying conductance in guard cells. PNAS **97 (15)**: 8687-8692

Lemtiri-Chlieh, F., MacRobbie, E.A.C., Webb, A.R.R., Manison, N.F., Brownlee, C., Skepper, J.N., Chen, J., Prestwich, G.D., and Brearley, C.A. (2003). Inositol hexakisphosphate mobilizes an endomembrane store of calcium in guard cells. Proc Natl Acad Sci U S A. **100 (17)**: 10091–10095

MacRobbie, E.A. (1998). Signal transduction and ion channels in guard cells. Philosophical Transactions of The Royal Society B Biological Science **353 (1374)**: 1475-1488

Marty, F. (1997). The Plant Vacuole: Ultrastructural Studies of Vacuole Biogenesis New York, Academic Press

Merritt, F., Kemper, A., and Tallman, G. (2001). Inhibitors of Ethylene Synthesis Inhibit Auxin-Induced Stomatal Opening in Epidermis Detached from Leaves of *Vicia Faba* L.**.** Plant and Cell Physiology **42 (2)**: 223-230

Odom, A.R., Stahlberg, A., Wente, S.R., and York, J.D. (2000). A Role for Nuclear Inositol 1,4,5-Trisphosphate Kinase in Transcriptional Control. Science **287**: 2026-2029

Radoy V. (2003). *Myo*-Inositol-1,2,3,4,5,6-hexakisphosphate. Phytochemistry **64**: 1033-1043

Suh, S.J., Wang, JF., Frelet, A., Leonhardt, N., Klein, M., Forestier, C., Mueller-Roeber, B., Cho, M.H., Martinoia, E., and Schroeder, J.I. (2007). The ATP Binding Cassette Transporter AtMRP5 Modulates Anion and Calcium Channel Activities in Arabidopsis Guard Cells. The Journal of Biological Chemistry **282**: 1916-1924

Tanaka, Y., Sano, T., Tamaoki, M., Nakajima, N., Kondo, N., and Hasezawa, S. (2005). Ethylene Inhibits Abscisic Acid-Induced Stomatal Closure in Arabidopsis. Plant Physiology **138**: 2337-2343

Thain, S.C., Vandenbussche, F., Laarhoven, L., Dowson-Day, M.J., Wang, ZY., Tobin, E.M., Harren, F., Millar, A.J., and Van Der Straeten, D. (2004). Circadian Rhythms of Ethylene Emission in Arabidopsis. Plant Physiology **136**: 3751-3761

Xu, C., Zou, Q. (1993). Effect of drought on lipoxygenase activity, ethylene and ethane production in leaves of soybean plants. Acta Botanica Sinica (China)

York, J.D., Odom, A.R., Murphy, R., Ives, E.B., and Wente, S.R. (1999). A Phospholipase C-Dependent Inositol Polyphosphate Kinase Pathway Required for Efficient Messenger RNA Export. Science **285**: 96-100

Zimmermann, P., Laule, O., Schmitz, J., Hruz, T., Bleuler, S., and Gruissem, W. (2008). Genevestigator Transcriptome Meta-Analysis and Biomarker Search Using Rice and Barley Gene Expressionn Databases. Molecular Plant **1(5)**:851-857

6 Appendix

6.1 Media/Solutions

*6.1.1 Yeast Media**

6.1.1.1 YPAD Medium (liquid)

1%	Bacto Yeast Extract
2%	Bacto Peptone
1.8%	Glucose Anhydrate
0.004%	Adenine Sulphate
	Water

6.1.1.2 YPAD Medium (solid)

1%	Bacto Yeast Extract
2%	Bacto Peptone
1.8%	Glucose Anhydrate
0.004%	Adenine Gulphate
1.5%	Agar Granulated
	Water

6.1.1.3 SD Medium (liquid)

0.17%	Yeast Nitrogen Base w/o amino acids and ammonium sulphate
0.5%	Ammonium Sulphate
1.8%	Glucose Anahydrate
0.06-0.07%	Dropout Mix
	Water

6.1.1.4 SD Medium (solid)

0.17%	Yeast Nitrogen Base w/o amino acids and ammonium sulphate
0.5%	Ammonium Sulphate
1.8%	Glucose Anahydrate
0.06-0.07%	SC Drop Out Mix
1.5%	Agar Granulated
	Water

6.1.2 Synthetic Complete Drop out Medium Mix (SC Drop Out)

All powder Mixes have to be vigorously (best with glass beads) shaken for am hour, to assure the homogeneity of the Mixes.

6.1.2.1 Basic Mix

1g	Arginine
1g	Isoleucine
1g	Lysine HCL
1g	Methionine
1.5g	Phenylalanine
3g	Homoserine
1g	Tyrosine
4.5g	Valine

6.1.2.2 SC Drop out Mix: - Ade

Total	Basic Mix
1g	Histidine HCL
1g	Leucine
1.5g	Tryptophan
0.6g	Uracil

6.1.2.3 SC Drop out Mix: - His

Total	Basic Mix
1g	Adenine Hemisulfate
1g	Leucine
1.5g	Tryptophan
0.6g	Uracil

6.1.2.4 SC Drop out Mix: - Trp

Total	Basic Mix
1g	Adenine Hemisulfate
1g	Histidine HCL
1g	Leucine
0.6g	Uracil

6.1.2.5 SC Drop out Mix: - Trp/ - Leu

Total	Basic Mix
1g	Adenine Hemisulfate
1g	Histidine HCL
0.6g	Uracil

6.1.2.6 SC Drop out Mix: - Trp/ - Leu/ - His

Total	Basic Mix
1g	Adenine Hemisulfate
0.6g	Uracil

*All media have to be autoclaved

6.1.3 Bacteria Media /Antibiotica stocks

6.1.3.1 LB Media (liquid)

1%	Tryptone
0.5%	Yeast Extract
0.5%	NaCl
	ddH_20

6.1.3.2 LB Media (solid)

1%	Tryptone
0.5%	Yeast Extract
0.5%	NaCl
7.5%	Agar
	ddH_20

6.1.3.3 Antibiotics stocks

50 mg/ml	Ampicillin	(Dil. 1:1000)
50 mg/ml	Kanamycin	(Dil. 1:1000)
50 mg/ml	Rifampicin (DMSO)	(Dil. 1:1000)
50 mg/ml	Gentamycin	(Dil. 1:2000)

*All media have to be autoclaved *(except antibiotic stocks)*

6.1.4 WESTERN Blot Media

6.1.4.1 Sample Buffer

0.6 mM	Tris-HCl, pH6.8
15%	SDS
80%	Glycerol
0.1%	Bromphenole blue
6.25%	β-Mercaptoethanole
	ddH_2O

6.1.4.2 Washing Buffer

10mM	Tris-HCl; pH7.5
150mM	NaCl
	ddH_2O

6.1.4.3 Blocking Buffer

1%	BSA
	Washing Buffer
	ddH_2O

6.1.4.4 Transfer Buffer

48mM	Tris, pH8.3
40mM	Glycine
0.0375%	SDS
	ddH_2O and Methanol in a ration 8:2

6.1.4.5 Alkaline Phosphatase Buffer

100mM	Tris
100mM	NaCl
5mM	$MgCl_2$

*6.1.5 Plant Media**

6.1.5.1 Agrobacterium – mediated plant trafo: Infiltration medium

1.14g/l	½ MS salts
5%	sucrose
5mM	$MgCl_2$
	ddH_2O
0.01%	Silwet *(after autoclaving)*

*All media have to be autoclaved

6.2 PCR Programs

6.2.1 Search for homozygous plants within ordered mutant lines (SALK, Gabi)

1.	95°C	2 min
2.	95°C	1 min
	55°C	30 sec
	72°C	1 min
	→ Repeat step 2 29 times	
3.	72°C	2 min
4.	15°C	*forever*

6.3 Chemical List

Chemical:	**Firm**
antibodies/Immunoprecipitation:	
anti-HA monoclonal mouse	Dualsystems
anti-LexA monoclonal mouse	Dualsystems
Dynabeads Protein G	Invitrogen
chemicals:	
ABA	
ACC	
Acetosyringon	Sigma Aldrich
Acrylamide 2K solution (30%)	AppliChem
Adenin hemisulfate	AppliChem
ammonium persulfate (APS)	Fluka
Ammonium sulfate	Fluka
Arginine HCl	AppliChem
AVG	Sigma Aldrich
Bicine	Roth
Bromophenol blue	Fluka
BSA	Applied Bioscience
Calcium chloride	Merck
CTAB	Roth
D-Glucose anhydrat	Fluka
Di-potassiumphosphate	Merck
Di-sodiumphosphate	Merck
DTT	Roth
EDTA	Fluka
glacial acetic acid	Fluka
Glibenclamide	Sigma Aldrich
Glycerol	Fluka
Glycine	Fluka
HEPES	AppliChem
Histidine HCl	Sigma Aldrich
Homoserine	AppliChem
hydrochloric acid	Fluka
Isoleucine	AppliChem
Leucine	AppliChem
Lithium acetate	Fluka
Lysine HCl	AppliChem
Magnesium chloride	AppliChem
Magnesium sulfate	Fluka
MES	AppliChem
Methionine	AppliChem
ONPG	

PEG 3500	Fluka
PEG1000	Fluka
Percoll	GE Healthcare
Phenylalanine	AppliChem
PMSF	Fluka
Potassium acetate	Fluka
Potassium chloride	Fluka
Potassium dihydrogenphosphate	AppliChem
Rapilait	Migros
salmon sperm DNA	Fluka
SDS	AppliChem
Sodium chloride	AppliChem
Sodium dihydrogenphosphate	AppliChem
Sodium hydroxide	Fluka
Sodium hypochlorid	Fluka
Sorbitol	Fluka
Spermidine	Fluka
Sucrose	AppliChem
TEMED	Fluka
Tris	Fluka
Tryptophan	Fluka
Tyrosine	AppliChem
Uracil	Fluka
Valine	AppliChem
X-Gal	
β-Mercaptoethanol	Sigma Aldrich

6.4 Device/Software List

6.4.1 Devices/Instruments

Maschine	Name	Firm
PCR Machine	DNA Engine DYAD	Peltier Thermal Cycler
Incubators 28°C, 37°C	Shaking incubators	Shel Lab
Incubator 30°C	Noctua IH50	Noctua
Centrifuge I	Avanti J-20 XPI	Beckam Coulter
Centrifuge III	Avanti 21R	Beckam Coulter
Centrifuge III	Microfuge 18	Beckam Coulter
Ultracentrifuge	Optima LE-80K	Beckam Coulter
Phytotron	hiromatic g	HIROSS
Western Blot Devices	casting stand and frames, electrophoresis and companion running module, tank, lid buffer dam	Bio-Rad Laboratories AG
Semi Dry Blotting System	iBlot	Invitrogen
Electroporation system	Pulse controler plus/ Capacitance extender Plus/ Gene Pulser II	Bio-Rad Laboratories AG
Spectrophotometer	DU 800	Beckam Coulter
Speed Vac	Univapo 100-ECH / Unicryo MC2L-60°C	Uni Equip
Thermomixer	KTMR-133	HCL
Vortex plus special cap	Vortex Genie 2; TurboMix cap	Scientific Industries
Confocal and Laser	Leica DM IRE2 and Leica TCB SP2	Leica
Epifluorescence microscope	Leica DMR	Leica
→camera that goes with it	Leica DC300F	Leica
Stereomicroscope	Nikon SMZ1500	Nikon
→camera that goes with it	Leica DFC320	Leica
Laptop Computer	Inspirion 510m	DELL
Scanner	Epson perfection 2450PHOTO	Epson
(-80°C) freezer	Hera freeze	Hareus
(-20°C) freezer	Comfort	Liebherr
(+4°C) fridge	Profi Line	Leibherr
Fusion	Fusion α	Packard Bioscience Company

6.4.2 Software / eTools

Software / eTool	Name	Firm
Leica Measuring Software	Leica Qwin	Leica
Microsoft office	Microsoft Office Xp	Microsoft
Graph and Data Analysis	Sigma Plot	Sigma Plot
Expression anylsis	eFP Arabidopsis Browser	University of Toronto
Gene espression analysis	Genevestigator	Nebion
Gene strucure analysis	Tair - Arabidopsis Information ressource center	"Scientific Community"
Plant Membrane Protein Database	Aramemnon	University of Cologne
Arabidopsis gene mapping tool	T-DNA express	SALK Institute
Seed Stocks		NASC: Nottingham arabidopsis seed center
Image managment	Adobe Photoshop	Adobe
Co-regulation studies	Atted	Atted

6.5 Vector Maps

6.5.1 Yeast Two Hybrid System: pLex-kan

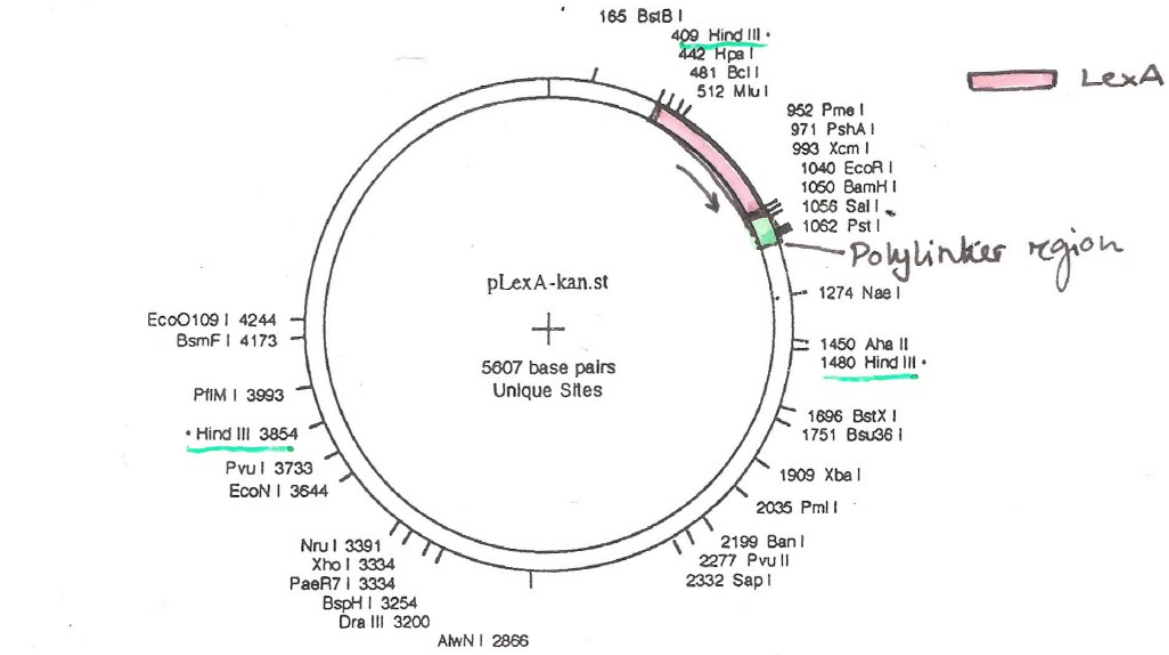

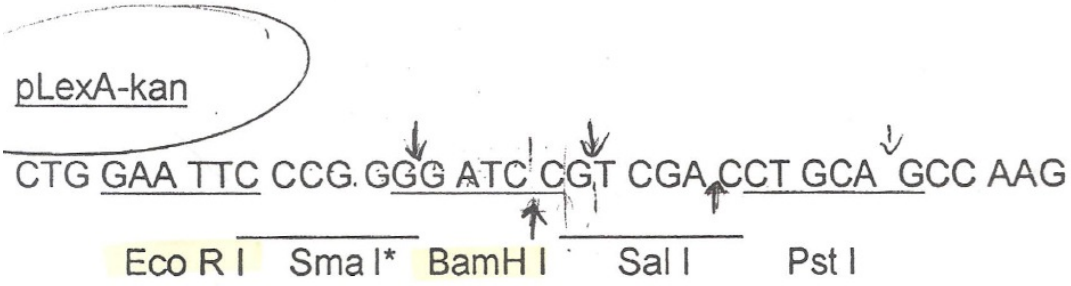

6.5.2 Yeast Two Hybrid System: pACT2

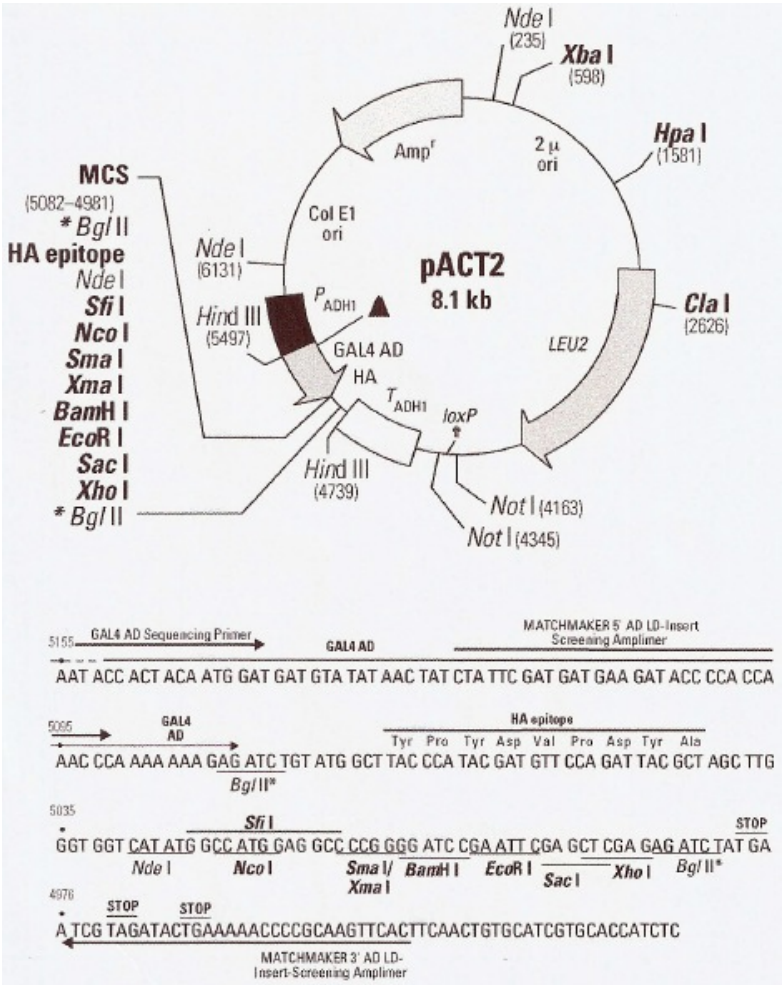

This PhD thesis was just possible to accomplish, because of the kind support, help, and knowledge of many people. Beside of guidance and information supply, I also received a lot of “emotional” support from friends and family.
Here they all should be mentioned:
I want to thank my supervisor Prof. Dr. Enrico Martinoia to whom I am very grateful for his advice, knowledge, calmness and never ending believe, that I - one day - will end that thesis. Special thanks go to Prof. Dr. Felix Keller for his sweet help, Prof. Dr. Stefan Hörtensteiner for all his enlightments during correcting this work, as well as being in my and – not to forget – Dr. Markus Klein, who started with me the ABC journey. I also want to thank Prof. Dr. Leo Eberl for being in my thesis committee and all the interessting discussions, as well I want to thank Prof. Dr. Christoph Ringli, Prof. Dr. Ueli Grossniklaus and Prof. Dr. Beat Keller for giving me all the support needed throughout the years. Furthermore I want to phrenetically thank Dr. Reka Nagy and Barbara Weder for their friendship, ideas, help, and support in every situation and especially for all the funny/silly laughing times. These thanks count also for Reto Schild, Dr. Stefan Meier, Dr. Bo Burla, Dr. Mike Hadorn, Dr. Tobias Kretzschmar, Dr. Krasimira Marinova, Dr. Arco Brunner, Dr. Michael Raissig, Dr. Annie Ferret, Dr. Suh-Jeong Suh and all other former members of the Martinoia group or the institute of plant biology of the University of Zurich.
Last but not least I want to say many, many thanks to my parents, who supported me from day one and gave me all the possiblities in life. My mom I want to thank for her constant nagging to finish up the thesis ☺ and her view to the world and my dad for all his computer support and all our philosophical discussions about society. Not to forget my brother for making me laugh and an aunt and all my friends, who could succesfully distract me from unsuccesful Western blotting and stomata aperture measurements.
Since my practical work in the lab ended 2010, I also want to thank my new employers for giving me the opportunity to enter the business world.

Thank you very much! ☺